2012-06-01

Antagonistic Pleiotropy: The Role of Smurf2 in Cancer and Aging: A Dissertation

Charusheila Ramkumar
University of Massachusetts Medical School

ANTAGONISTIC PLEIOTROPY: THE ROLE OF SMURF2 IN CANCER AND AGING

A Dissertation Presented

By

Charusheila Ramkumar

Submitted to the Faculty of the
University of Massachusetts Graduate School of Biomedical Sciences, Worcester
In partial fulfillment of the requirements for the degree of

DOCTOR OF PHILOSOPHY

June 1st, 2012

Department of Cell Biology

ANTAGONISTIC PLEIOTROPY: THE ROLE OF SMURF2 IN CANCER AND AGING

A Dissertation Presented
By

Charusheila Ramkumar

The signatures of the Dissertation Defense Committee signify completion and approval as to style and content of the Dissertation

Hong Zhang, Ph.D., Thesis Advisor

Stephen Jones, Ph.D., Member of Committee

Janet Stein, Ph.D., Member of Committee

Rachel Gerstein, Ph.D., Member of Committee

John Sedivy, Ph.D., Member of Committee

The signature of the Chair of the Committee signifies that the written dissertation meets the requirements of the Dissertation Committee

Anthony Imbalzano, Ph.D., Chair of Committee

The signature of the Dean of the Graduate School of Biomedical Sciences signifies that the student has met all graduation requirements of the school

Anthony Carruthers, Ph.D.,
Dean of the Graduate School of Biomedical Sciences

Department of Cell Biology

June 1st, 2012

For Amma and Appa

ACKNOWLEDGEMENTS

I would like to thank my advisor Hong Zhang for his support. It has been a privilege to be his first graduate student, and I am deeply grateful for the opportunity he has given me to work on the projects that comprise my thesis. He has been extremely open to discussion and very supportive of my ideas and has encouraged me to follow my interests. I am thankful to him for his patience, support and for teaching me (among a thousand other things) to ‘pay attention to the details’! He has shaped the way I approach Science, and I believe this will stand me in good stead for my career.

I would like to thank all the members of the Zhang Lab, past and present, who have made working here a fun experience. Yahui Kong has been a fabulous friend and colleague. I am grateful to her for her warm friendship and all the helpful discussions over the last 6 years. I would like to thank Hang Cui for collaborating with me on my projects and for all the helpful discussions over the years. Ivan Lebedev was crucial in maintaining the mouse colony for me during 18 very busy months. I would like to thank Ivan for his work, and for changing his mind about medical school and picking grad school instead. May the force be with you!

I would like to thank Rachel Gerstein for collaborating with me on all my projects. She has been generous in sharing both reagents and her time and I am deeply grateful for all the help. She also taught me everything I need to know about FACS, and I’d like to thank her for her patience and support. I would also

like to thank members of the Gerstein Lab, past and present, especially Erin Cloherty for help with experiments involving radiation.

I would like to thank the members of my TRAC committee, Steve Jones, Tony Imbalzano, Janet Stein, Steve Grossman and Rachel Gerstein for their guidance and helpful suggestions over the years.

I would like to thank my family for their love and unswerving support in the face of my wanting to stay in school forever! Thank you Amma and Appa for supporting my career choices, and not insisting I be a computer engineer. (I'd have made a mighty poor engineer!) Thank you for always giving me the right advice, and for cleverly disguising it as soothing conversation. I'd like to thank my brother Vivek for helping me keep it real. It is a truth universally acknowledged that whenever I thought life was crappy he made me feel better, because he was always in more trouble than I! Vivek has been my friend, philosopher and a source of great encouragement in the cesspool that 'following your dreams' can sometimes be.

Life in general, and graduate school in particular would be fairly impossible to navigate without friends. I'd like to thank all the wonderful people who are mine. Special thanks to Deepti Kulkarni for being my 2 am friend. Seema Mittal has been my roommate these last 5 years. She's been a rock of support and I simply couldn't have done it without her friendship. I'd like to thank her for all the good times, and wish her all the best as she begins a new life in India with her husband, Raj.

Finally, I'd like to acknowledge all the wonderful, strong women in my life. Thank you to my grandmother Lakshmi Kunchitapatham, for showing me the meaning of courage under fire. Thank you to my 7-year old cousin Madhurima Premkumar, for teaching me the meaning of true grit. You are an inspiration to me.

Charusheila Ramkumar

11th May 2012

ABSTRACT

In response to telomere shortening, oxidative stress, DNA damage or aberrant activation of oncogenes, normal somatic cells exit the cell cycle and enter an irreversible growth arrest termed senescence. The limited proliferative capacity imposed by senescence on cells impedes the accumulation of mutations necessary for tumorigenesis and prevents proliferation of cells at risk of neoplastic transformation. Opposite to the tumor suppressor function, accumulation of senescent cells in adult organisms is thought to contribute to aging by depleting the renewal capacity of tissues and stem/progenitor cells, and by interfering with tissue homeostasis and functions. The Antagonistic Pleiotropy Theory of senescence proposes that senescence is beneficial early in life by acting as a tumor suppressor, but harmful late in life by contributing to aging. Recent studies have provided evidence strongly supporting the tumor suppressor function of senescence, however, direct evidence supporting the role of senescence in aging remains largely elusive.

In this thesis, I describe studies to test the Antagonistic Pleiotropy Theory of senescence in tumorigenesis and aging. The approach that I have taken is to alter the senescence response *in vivo* by changing the expression of a senescence regulator in mice. The consequence of altered senescence response on tumorigenesis and stem cell self-renewal was investigated. The senescence regulator I studied is Smurf2, which has been shown previously to activate senescence in culture. I hypothesized that the senescence response will be

impaired by Smurf2 deficiency *in vivo*. Consequently, Smurf2-deficient mice will develop tumors at an increased frequency, but also gain enhanced self-renewal capacity of stem/progenitor cells with age.

I generated a Smurf2-deficient mouse model, and found that Smurf2 deficiency attenuated p16 expression and impaired the senescence response in primary cells and tissues. Smurf2-deficient mice exhibited an increased susceptibility to spontaneous tumorigenesis, indicating that Smurf2 is a tumor suppressor. At the premalignant stage of tumorigenesis, a defective senescence response was documented in the Smurf2-deficient mice, providing a mechanistic link between impaired senescence response and increased tumorigenesis. The majority of tumors developed in Smurf2-deficent mice were B-cell lymphomas with an origin in germinal centers of the spleen and a phenotype resembling human diffuse large B-cell lymphoma (DLBCL). I discovered that Smurf2 mediated ubiquitination of YY1, a master regulator of germinal centers. Stabilization of YY1 in the absence of Smurf2 was responsible for increased cell proliferation and drove lymphomagenesis in Smurf2-deficient mice. Consistently, a significant decrease of Smurf2 expression was observed in human primary DLBCL samples, and more importantly, a low level of Smurf2 expression in DLBCL correlated with poor survival prognosis. Moreover, I found that hematopoietic stem cells (HSCs) in Smurf2-deficient mice had enhanced function compared to wild-type controls. This enhanced stem cell function was associated with increased cell proliferation and decreased p16 expression, suggesting that defective senescence response in Smurf2-deficient mice leads to increased self-

renewal capacity of HSCs. My study, for the first time, offers direct genetic evidence of an important tumor suppressor function for Smurf2 as well as its function in contributing to stem cell aging. Collectively, these findings provide strong evidence supporting the Antagonistic Pleiotropy Theory of senescence in tumorigenesis and aging.

TABLE OF CONTENTS

List of Tables

List of Figures

Chapter II

Chapter III

Preface

Portions of Chapter I have appeared in:

Kong Y, Cui H, Ramkumar C, Zhang H (2011) Regulation of senescence in cancer and aging. J Aging Res 2011:963172

Chapter II is a published manuscript.

Ramkumar C, Kong Y, Cui H, Hao S, Jones SN, Gerstein RM, Zhang H (2012) Smurf2 regulates the senescence response and suppresses tumorigenesis in mice. Cancer Res. doi:10.1158/0008-5472.CAN-11-3773

Author contributions

Chapter II

The Southern Blot in Fig.2.1 was done by Yahui Kong

The western Blots in Fig.2.3 were done by Yahui Kong and Hang Cui

Portions of the 3T9 Assay in Fig.2.4 were done by Hong Zhang

Pathology slides in Fig.2.7 were analyzed by Dr.Suyang Hao

The western blot in Fig.2.8 was done by Yahui Kong

Hong Zhang and I wrote the Chapter

Chapter III

FACS data was analyzed with the help of Rachel Gerstein

The bioinformatics analyses in Fig.3.10 and Tables 3.2a,b were done by Hang Cui

Hong Zhang and I wrote the Chapter

Chapter IV

FACS data was analyzed with the help of Rachel Gerstein

Hong Zhang and I wrote the Chapter

CHAPTER I

INTRODUCTION

Since the focus of my thesis is on studying the antagonistic roles played by senescence in regulating varied processes such as tumorigenesis and aging, in the first part of this chapter I will present a general overview of senescence including factors that activate the senescence response, and the pathways regulating senescence. This will be followed by a review of what is currently known about the function of senescence as a tumor suppressor and in aging, with specific emphasis on the functional manifestations and factors regulating HSC aging.

Cellular Senescence

Cellular Senescence is defined as a state of irreversible growth arrest from which cells cannot be stimulated to divide. It was described by Hayflick and Moorhead in normal human fibroblasts in a seminal study which for the first time defined cultured cells as having a finite replicative life span [1]. Senescent cells remain arrested in the G1-G0 phase of the cell cycle and do not respond to growth factors [2,3]. They are also apoptosis resistant [4,5], and associated with changes in morphology including assuming a flat, enlarged shape referred to as ‘fried egg’ appearance [6]. Senescent cells are also characterized by the expression of Senescence-associated β-Galactosidase (SA-β-Gal) activity [7], and unique gene expression signatures [8-12].

Triggers of Senescence:

Telomere dependent senescence-

Telomeres consist of many kilobases of TTAGGG repeats found at the very ends of chromosomes. The telomeric TTAGGG repeats shorten with each cell division due to the end replication problem [13-16]. Telomerase, the enzyme responsible for adding telomere repeats to the ends of chromosomes [17] is not present in somatic cells, and its absence leads to progressive telomere shortening [18,19], which is thought to be the primary cause of replicative senescence [20,21]. Further, the adventitious expression of Telomerase Reverse Transcriptase (TERT) prevents telomere shortening and inhibits the induction of senescence in somatic cells [22-24]. Complementary to this finding, the attenuation of telomerase in immortal cells leads to induction of replicative senescence [25,26]. Telomeres which have reached the critical short length lose the protection of the capping proteins that are usually present at their ends [16]. Further, these uncapped telomeres are recognized as sites of DNA damage and recruit DNA damage response proteins such as 53BP1, γH2AX, MDC1 and MRE11 [27-29].

Telomere independent senescence-

Other stressors can also induce senescence. These include oncogene activation [30-32], DNA damage [33,34], oxidative stress [35-37], and inadequate culture conditions [37-39], and damage to chromatin structure [40-42]. These are referred to as stress-induced premature senescence. These types of senescence are independent of telomere length and cell divisions [43-45].

Stress-induced premature senescence and telomere dependent senescence result in similar final outcomes and share common changes in expression of cell cycle regulators and other morphological properties [31,35,33,34].

In addition to the cell cycle regulatory genes, the expression of DNA damage checkpoint genes, inflammation and stress-associated genes, genes encoding extracellular matrix proteins and extracellular matrix-degrading enzymes, and cytoskeletal genes and metabolic genes is generally altered during replicative and premature senescence. Recent studies suggest that DNA damage could be a common cause for different forms of senescence induced by various stimuli [9,10,12]. Senescence is now considered as a general stress response in normal cells to various types of cellular damage [46].

Molecular pathways regulating senescence:

All the various senescence-inducing stimuli trigger the senescence response through multiple genetic pathways. These pathways finally converge upon the p53 and Rb pathways and inactivation of both pathways is essential to abolish the senescence response.

The p53 pathway-

In senescent cells, p53 is phosphorylated and its transactivation activity is elevated, although its mRNA and protein levels are largely unchanged [29,47-50]. DNA damage response elicited by telomere dysfunction leads to activation of ATM/ATR and Chk1/Chk2, which in turn phosphorylate and stabilize p53

[27,29,28,51]. In addition, p53 is activated and plays an important role in stress-induced premature senescence [30,34,52,53]. This p53 activation is mediated by p14ARF (or p19ARF in mouse) encoded by the INK4a/Arf locus. ARF stabilizes p53 by sequestering Mdm2, an E3 ubiquitin ligase targeting p53 for degradation [54]. The ARF-p53 axis plays an important role during senescence in mouse cells. Inactivation of p53 or ARF in mouse embryo fibroblasts (MEFs) is sufficient to prevent senescence [55-57]. One of the p53 targets is p21 (CIP1/WAF1), whose increased expression transactivated by p53 is responsible for cell cycle arrest [58]. The expression of p21 is upregulated during replicative senescence [59-61]. This p21 up-regulation is dependent on signal(s) initiated by telomere shortening, as expression of TERT blocks this upregulation [62-64]. Overexpression of p21 is able to induce a senescence-like growth arrest in some cells [65,66], while deletion of p21 can postpone senescent arrest [67,68]. Collectively, these studies suggest that p53 regulates senescence at least in part by inducing p21.

The p16-Rb pathway-

In parallel to p21, p16INK4a (p16) is another cyclin dependent kinase inhibitor that leads to pRb hypophosphorylation [58]. The expression of p16 is increased during replicative senescence [69-71], but whether increased p16 expression is regulated by telomere shortening is controversial. As telomere shortening is the major cause of replicative senescence in human fibroblasts [24], and inactivation of both the p53 and pRb pathways is required to prevent replicative senescence

[72], it is reasonable to expect that dysfunctional telomeres may signal into p16-pRb axis. There is indeed an example showing that telomere dysfunction induces p16 expression [73]. However, the dynamics of p16 and p21 elevation in senescent cells are different. The increased expression of p16 occurs after senescence has already been established in culture [69,70,74], in contrast to the rapid increase of p21 expression in cells approaching replicative senescence [62]. Within a senescent population of human cells, some cells express p16, while others express p21 [29,75,74]. DNA damage foci at telomeres are found only in cells expressing p21, but not in p16 positive cells [29], suggesting that p16 elevation is independent of telomere shortening. Consistent with this notion, p16 induction during senescence, unlike p21, is not prevented by ectopic expression of TERT [76].

The expression of p16 is readily increased during premature senescence induced by a variety of stressors [30,32,33,38]. It is not entirely clear how p16 expression is regulated by various senescence signals [77]. Under certain circumstances, p16 is coordinately regulated with Arf, which is also encoded by the INK4a/Arf locus. For example, polycomb complex proteins have been shown to repress the INK4a/Arf locus [74,78,79]. Decreased expression of polycomb complex proteins relieves the repression of the INK4a/Arf locus and is responsible, at least in part, for the elevation of p16 and Arf in senescent cells [74,79].

The expression of p16 varies significantly among different human cell lines [74], and this variable expression seems to hold the key as to whether p53 and

pRb function in a linear or in a parallel manner to regulate senescence. In cells with low or no p16 expression, p53 and pRb may function in a linear pathway, whereas p53 and pRb work in parallel in cells with significant p16 expression. In mouse embryo fibroblasts (MEFs), inactivation of p53 or ARF, but not p16, is sufficient to prevent senescence [56,57,80], indicating that p53-Arf axis is the major regulator of senescence pathway in mouse cells. Human mammary epithelial cells quickly encounter a state of growth arrest that is not associated with telomere shortening but mediated by p16 up-regulation [81]. A subset of cells with p16 inactivation emerge from the arrested population and continue to divide until reaching a second growth arrest that is associated with telomere shortening [81]. Depending on cell types, culture conditions, and the extent of stress, inactivation of either p53-p21-pRb or p16-pRb pathway individually, or both pathways together, is required to prevent senescence.

While senescence was identified as a cell culture phenomenon, its functional significance has been recognized *in vivo*. Senescence is postulated to function as a tumor suppressor mechanism by preventing the accumulation of mutations necessary for neoplastic transformation. The next portion of this Chapter will review what is known about the function of senescence as a tumor suppression mechanism.

Senescence as a barrier to tumorigenesis:

Tumorigenesis is a multistep process, in which a normal cell acquires mutations in a number of cancer-causing genes [82]. By restricting cell proliferation and thereby impeding the accumulation of mutations, senescence acts as an important tumor suppression mechanism. Furthermore, senescence induced by aberrant activation of oncogenes, oxidative stress, or DNA damage prevents cells at risk of malignant transformation from proliferating [44,83]. Senescence represents a physiologic response that cells must overcome in order to divide indefinitely and develop into tumors. Consistent with the notion that senescence is a tumor suppression mechanism, well-established tumor suppressors, including p53, pRb, p16, Arf, and p21, are regulators of senescence [77,83].

In contrast to normal somatic cells, cells derived from tumors divide indefinitely in culture. The ability to escape senescence (i.e., immortality) is a necessary step for cells to become transformed and one of the hallmarks of cancer cells [84]. 80% to 90% of human cancer cells acquire unlimited proliferative potential through reactivation of telomerase [18] while the rest maintain telomere length by a recombination-mediated process termed alternative lengthening of telomeres [85]. These observations in human cancer strongly suggest a connection between the telomere checkpoint and tumor suppression. Supporting this connection, inhibition of telomerase activity in cancer cells limits their growth by triggering telomere shortening and cell death [25,26]. Conversely, ectopic expression of telomerase in normal human cells leads to immortalization and enhances the ability of these cells to be

neoplastically transformed [23,24]. Furthermore, transgenic mice overexpressing TERT show increased propensity to tumorigenesis [86,87].

Genetic studies in mice deficient in telomerase provide further support for telomere shortening as a tumor suppression mechanism. Mice deficient in the telomerase RNA component (mTERC**−/−**) gradually lose telomeres over several generations [88] and tumorigenesis is significantly reduced in late generations of mTERC**−/−** mice with telomere attrition [89-93]. Decreased tumorigenesis is also observed in late generations of mice with a null mutation in telomere catalytic subunit (mTERT**−/−**), and p53 mutation enables tumor progression in these mice [94]. More importantly, two studies provide evidence that senescence induced by telomere shortening is responsible for tumor suppression [95,96]. When apoptosis is blocked by the expression of Bcl-2 or a specific p53 mutant (R172P), shortened telomeres reduce tumorigenesis in mTERC**−/−** mice. Suppression of tumor development requires p53-dependent activation of senescence [96,95], demonstrating that senescence induced by telomere shortening is an effective tumor suppression mechanism *in vivo*.

The discovery that oncogenic Ras protein can induce a senescent arrest after causing an initial hyperproliferation in normal cells suggests that induction of senescence is an intrinsic cellular response that prevents cells at risk from proliferating [30]. In mouse tumor models with oncogenic Ras, senescent cells are found in premalignant lesions in lung [97], spleen [98], breast [99] and pancreas [100]. The observation of senescent cells has been extended to many premalignant lesions or benign tissues induced by activation of different

oncogene or inactivation of tumor suppressor in mouse [101-104] and human [101,105,106]. Importantly, senescent cells are absent in malignant tumors [97-99,103,106] suggesting that oncogene induced senescence is a powerful tumor suppression mechanism by restricting proliferation of cells with oncogenic mutations and this senescence block must be evaded for malignancy to progress. Consistently, deletion of senescence regulators such as p53, Arf, p16, or PRAK abrogates senescence and causes progression of tumors to the malignant stage [98,101,103,104]. These observations point to a causal link between loss of senescence and malignant transformation.

Since the discovery of senescence in cultured cells, it is recognized that cellular senescence and organismal aging may be closely related because of their shared ability to limit lifespan [20]. It is hypothesized that constant tissue regeneration results in accumulation of senescent cells in somatic tissues, which limits tissue renewal, perturbs normal tissue homeostasis and ultimately leads to aging [107,83]. In the next portion of this chapter, I will present an overview of what is known about the role of senescence in aging.

Senescence and Aging:

Cells with characteristics of senescence have been reported to increase with advancing age in mice, primates and humans [7,108-110]. In addition, accumulation of senescent cells is linked with age-associated pathological conditions, such as osteoarthritis [111], atherosclerosis [112,113], and liver cirrhosis [114]. The initial support for the senescence theory of aging comes from the observation of an inverse correlation between the *in vitro* lifespan of cells and the age of donors from which they are derived [115-117], although this correlation has been disputed [118]. Subsequent support comes from studies of cells derived from progeroid patients, such as Werner syndrome, which achieve fewer cell divisions before entering senescence than cells derived from normal individuals of same age [119].

Recent studies suggest that the telomere checkpoint plays an important role in the aging process. It is evident that telomere shortening occurs in aged human tissues [120-125], at sites of age-related pathological conditions [126,114], or associated with stress and obesity [127,128]. Although it remains to be demonstrated whether telomere shortening leads to the accumulation of senescent cells *in vivo*, and more importantly makes a substantial contribution to aging, studies of human premature aging syndromes support a link between telomere attrition and aging. Patients of dyskeratosis congenita and aplastic anemia have mutations in telomerase RNA or catalytic subunit [129-131], and are characterized by accelerated telomere shortening [132,129]. Further evidence for a role of telomere attrition in aging comes from genetic studies of

mice deficient in telomerase. While mice with a null mutation in telomerase RNA (mTERC−/−) are apparently normal in early generations, these mice in later generations gradually lose telomeres [88] and show accelerated aging phenotypes [133,134]. Similarly, premature aging phenotypes are observed in mTERC−/− mice on a CAST/EiJ background, which have shorter and more homogenous telomere length than C576BL/6 strain. Even with the presence of telomerase, shortened telomeres in mTERC+/− mice on CAST/EiJ background are associated with premature aging [135]. A recent study shows that telomerase reactivation can reverse much of the premature aging phenotypes in telomerase-deficient mice [136], indicating that telomere attrition plays a critical role in aging. Furthermore, mutations in WRN or BLM in the telomere dysfunctional background in the mouse cause premature aging phenotypes that are characteristics of Werner or Bloom syndrome in humans Such premature aging phenotypes are absent in mice with WRN or BLM mutation but with long telomeres [137,138]. These studies clearly establish a link between telomere attrition and aging. Whether this link is mediated through senescence triggered by telomere shortening is currently unknown.

Apart from the proliferating cell compartments, the self-renewing stem cell compartments in the body have also been postulated to undergo senescence with age. While the exact role of senescence in stem cell aging is unknown, the functional consequences of stem cell aging have been studied in a number of stem cell compartments. In Chapter 4 of this Thesis I examined the role of Smurf2-deficiency, and consequently, of senescence, in the HSC compartment

of young and aging mice. Therefore, the next portion of this chapter will focus on the consequences and mechanisms of stem cells in aging with an overview of what is known about senescence in stem cell compartments.

Stem cells and Aging:

Stem cells are present in most adult mammalian tissues and they are responsible for maintaining normal tissue homeostasis and regeneration in response to damage [139,140]. As aging is accompanied by a reduced homeostatic and regenerative capacity in all organs, it is a reflection of the declining stem cell activity in the organs with age [141-143]. Stem cell aging is somewhat distinguishable from aging in younger, more proliferative cells. The functional manifestations of stem cell aging include the failure to self-renew, decreased extrinsic signals as well as signal responsiveness and aberrant progenitor differentiation. Each of these processes is reviewed in detail below with particular emphasis on the impact of aging in the HSC compartment, as that is the stem cell compartment I chose to examine in order to study the functional consequences of delayed senescence in aging.

Failure to self-renew-

The inability of stem cells to self-renew with age is associated with a reduction in stem cell number with age. This is especially seen in stem cell compartments such as the brain and skin. The stem cell number that efficiently contributes to generation of neurons and melanocytes decreases with age [144,145]. This

decreased formation of murine Neural Stem cells (NSCs) has been associated with a progressive Parkinsonian disease [91] as well as reduced olfactory discrimination with aging [146].

Similarly, hair graying has been linked to decreased melanocyte stem-cell maintenance, likely associated with melanoblast senescence [147]. These stem cell compartments exhibit formation of progeny that don't maintain the stem cell pool as they age. In flies, oogenesis and spermatogenesis abate gradually with age, and this coincides with a significant drop in the number of germinal stem cells (GSC) as well as reduced stem cell self-renewal capacity of the GSCs that are remaining [148-150].

Aged hematopoietic stem cells (HSCs) are known to be impaired in supporting hematopoiesis. In mice, while there is a strain-dependent increase in hematopoietic stem cell (HSC) number with age [151-154], it is associated with a dose-dependent decrease in self-renewal capacity in serial transplantation experiments *in vivo* [155,156]. This decline in HSC function increases with the number of stem cell transplantations [157-161]. HSCs from aged mice also exhibit a decrease in competitive repopulating ability compared with younger counterparts [162,151,153].

Decreased extrinsic signals as well as signal responsiveness-

The defects in tissue homeostasis or regenerative potential with age may be because of decreased intrinsic responsiveness of the stem cells, or attenuated signals from the external environment to the stem cells. For example, muscle

stem cells (MuSCs) undergo changes in their niche, which leads them to affect a low response to extrinsic stimuli with age, and this leads to the decreased regenerative response [163,164]. This is associated with changes in their niche, which is the myofibre adjacent to the MuSc [165]. Older myofibres express lower levels of the Notch ligand Delta-like 1 that is essential for stem cell activation [166,167]. In older flies, systemic factors such as the *Drosophila* insulin-like peptides (dILPs) also influence GSC proliferation and maintenance. Reduced IIS signaling is seen in the ovary of older females [168-170].

HSCs in the bone marrow are also located in close proximity to the non-hematopoietic cellular elements, and it is hypothesized that the bone marrow niche plays an important role in HSC regulation [171]. The niche evolves and undergoes changes with age and therefore influences HSC function in aging. As the animal ages, DNA damage accumulates within the HSCs and they attempt to cope with this accumulation by activating tumor suppressor pathways. Mice deficient in proteins that are involved in essential DNA repair pathways such as nucleotide excision repair, telomere maintenance and non-homologous end-joining exhibit alterations in number as well as attenuation in HSC function. These phenotypes recapitulate some phenotypes of normal aging [172]. Wild-type HSCs show an accumulation of γ-H2AX foci, a marker of DNA damage, with age [172]. Further, recent studies have shown such accumulation of DNA damage in human hematopoietic stem and progenitor cells [173].

The role of the bone marrow microenvironment on HSC aging has also been studied. When bones from young mice were subcutaneously implanted into

older mice, they exhibited decreased repopulating ability [174]. Also, stromal cells from older mice display attenuated capacity to support primitive hematopoietic bone marrow cells in culture [175]. When time-lapse 2-photon microscopy was performed to quantify the dynamics of young and old hematopoietic cells inside the marrow of long bones of mice in vivo, it was found that the aged early hematopoietic progenitor cells (eHPCs) displayed increased cell protrusion movement *in vivo* and localized more distantly to the endosteum compared with young eHPCs [176]. This further correlated with reduced adhesion to stroma cells as well as reduced cell polarity upon adhesion of aged eHPCs [176]. This result suggests that the changes in eHPC dynamics and cell polarity with age lead to an altered niche biology, which plays an important role in HSC aging. HSCs from older mice are also known to exhibit homing deficiencies when transplanted into older recipients [177], suggesting that the microenvironment is an important determinant of stem cell homing with age.

Aberrant progenitor differentiation-

Stem cells give rise to a number of progenitor cells, which then form effector cells that function to maintain tissue homeostasis and function. As the organism ages, the stem cells may not efficiently function to produce the right type and number of progenitor cells. This might result in skewing of the progenitor cell type to one particular fate, and further aberrant differentiation to abnormal fates.

For example, older MuSCs tend to deviate from the muscle lineage and produce fibrogenic cells. This leads to impaired regeneration and fibrosis. This

has been shown to be due to over activity of the Wnt pathway with age [164]. MuSCs treated with Wnt agonists or aged serum lead to the deviation toward the fibrogenic lineage [164].

The decline in hematopoietic competence with age impacts all the blood cell lineages. Thymic involution with age leads to reduced T-cell production and function as well as a clonal expansion of memory T-cells [178,179]. B-cell function also declines with age, leading to less efficient antibody production, and there is a similar increase in the memory B-cell population [180-182]. However, there is a skewing towards the myeloid lineages with age, which results in the sustenance of a pro-inflammatory environment termed ‘inflammaging’ [180]. The adaptive and humoral immune responses are thus both affected, and this, in combination with the reduced integrity of epithelial barriers, leads to activation of the innate immune responses in response to pathogenic challenge. This results in the emergence of a chronic inflammatory state (inflammaging) that is associated with several age-related diseases [180,183].

HSCs from aging mice display a skewing toward the myeloid lineage. Mice display changes in lineage potential with age, with a decrease in lymphoid output while myeloid potential is maintained [151]. This is associated with a decreased immune response and increased incidence of myeloid leukemias in older populations. Studies in mice have demonstrated that there exist heterogeneous HSC populations within the bone marrow that exhibit different predilections to give rise to different types of progenitor cell populations. They can be either lymphoid-biased, or myeloid-biased or balanced. Single cell transplantations of

purified stem cell populations have demonstrated that the clonal contribution to different blood cell lineages varies significantly and can be maintained in serial passage [184,185].

Further, gene expression profiling of long term HSCs from young and old mice has shown that genes required for myeloid specification are upregulated, but genes mediating lymphoid specification are down regulated in older mice [151]. The cause behind the gene expression changes is currently unclear. However, studies have shown that entire regions of chromosomes that are silenced in young HSCs, are activated in the old HSCs. The converse is also true, that is, regions of chromosomes active in young HSCs are inactive in the old HSCs [162]. Genes regulating chromatin remodeling were among those that changed their expression differentially between young and old HSCs, suggesting that epigenetic alterations may be partially responsible for the wide spread changes in gene expression with age.

Intestinal stem cells (ISCs) from the Drosophila midgut are known to proliferate more with age. This leads to the accumulation of misdifferentiated daughter cells that express markers of both ISCs and terminally differentiated cells [186-188]. Defective misdifferentiation in the midgut leads to deterioration of the midgut epithelium in older flies [187]. Such changes in midgut epithelium are also observed when the gut is exposed to oxidative stress, tissue damaging agents, or bacterial infections of the gut which lead to ISC proliferation and misdifferentiation [186,187,189-191]. Chronic exposure to environmental agents might also be involved in ISC aging in flies.

While the functional consequences of stem cell aging are well known, the role of senescence and its contribution to stem cell aging is less clear. There are some examples of senescence being an important determinant of stem cell aging. The next portion of this chapter will focus on what is currently known about senescence in various stem cell compartments.

Senescence in stem cells:

Thus far, the role of senescence in the changes in stem cell functionality with age is debatable. The pathways that regulate senescence are known to be upregulated in some stem cell compartments with age, but this does not establish a causal link between senescence and aging, but merely provides an association between the two. The expression of senescence markers, such as senescence-associated B-galactosidase, HP-1 (heterochromatin protein-1) foci, and p16INK4a markedly increases with age in many tissues in several mammalian species [171]. Studies of self-renewal in HSCs, NSCs and pancreatic islet cells from $p16^{INK4a}$-deficient and $p16^{INK4a}$-overexpressing mice have suggested that increasing levels of $p16^{INK4a}$ are not only associated with aging, but partly contribute to the age-induced replicative failure of these tissues [192-194]. In all three compartments, $p16^{INK4a}$ deficiency attenuated the age-induced decline in proliferation and function. Likewise, overexpression of $p16^{INK4a}$ attenuated HSC function and islet proliferation in an age-dependent manner. The effects of $p16^{INK4a}$ loss were consistent across these distinct stem cell compartments, suggesting that $p16^{INK4a}$ can promote aging in tissues, however,

the loss of $p16^{INK4a}$ did not completely abrogate the effects of aging in any of the organs studied, suggesting that $p16^{INK4a}$-independent aging also occurs in each of these compartments.

Other mouse models have also provided evidence to support the role of senescence in stem cell aging. The Klotho knockout mouse exhibits a progeroid syndrome that is accompanied by elevated Wnt signaling that potentially causes stem cell senescence in the skin and gut [195,196]. The role of Wnt signaling in stem cell aging has also been demonstrated in the hair follicle stem cells. Normal cycling of hair follicle stem cells is regulated by the induction of Wnt proteins in the niche, and the return of the cells to quiescence is accompanied by a decrease in Wnt activity [197,198]. Transgenic mouse models that constitutively activate the Wnt pathway display persistent proliferation of hair follicle stem cells followed by signs of premature senescence and disappearance of stem cells that correlate with precocious hair loss [196,199]. While this is not a direct demonstration, it suggests that hair follicle stem cells may undergo senescence during normal aging.

Senescence is known to be associated with a critical reduction in telomere length and as I have reviewed earlier in this chapter, it is associated with aging for this reason. Telomere biology also plays a role in stem cell aging and I will now describe briefly what is currently known about the role of telomere length in regulating stem cell compartments, specifically the HSC compartment.

Telomere Biology in HSC aging:

Maintenance of telomere length in HSCs is essential, as the blood cells need to be continuously replenished during the lifespan of a species. The rate of telomere attrition in peripheral blood mononuclear cells (PBMCs) during the first 3 years of life is more than 4-fold higher than in adults during a 3-year period [200]. This high rate of telomere attrition early in life is a reflection of the rapid expansion of the HSCs early in life, which is followed by a replicative decline as adulthood progresses [201]. Longer telomeres have been found in hematopoietic progenitor cells (CD34+) than in mature cells (CD4+, CD8+ cells and granulocytes), providing support to the replicative senescence theory in HSCs [202,203].

Telomere biology has been shown to play an important role in bone marrow related disorders. Dyskeratosis Congenita (DC), a disease that is caused by mutations in the dyskerin (DKC1) gene [204] and results in abnormally short telomeres [205] is associated with high risk of Bone Marrow Failure (BMF), Myelodysplastic Syndrome (MDS) and Acute Myeloid Leukemia (AML). By the age of 30, 80-90% of patients develop aplastic anemia and die due to this [206]. Further patients with DC are known to have extremely short telomeres compared to normal counterparts [207]. Telomere length is also known to be shorter in other bone marrow failure disorders such as Fanconi Anemia, Diamond-Blackfan syndrome, Shwachman-Diamond Syndrome and Paroxysmal Nocturnal Hemoglobinuria [208]. The shorter telomeres in these diseases could be partially

attributed to the genetic defect in DNA damage repair pathways, particularly in Fanconi Anemia and Shwachman-Diamond Syndrome [209].

Further evidence for a role of telomere attrition in aging comes from genetic studies of mice deficient in telomerase. While mice with a null mutation in telomerase RNA (mTERC**−/−**) are apparently normal in early generations, these mice in later generations gradually lose telomeres [88] and show accelerated aging phenotypes [133,134]. Premature aging phenotypes in late generation mTERC**−/−** mice are associated with reduced renewal capacity in highly regenerative tissues such as skin, intestine, bone marrow and reproductive organs [133-136], suggesting that stem cells may be affected by telomere shortening. The self-renewal ability of stem cells is known to decline with advancing age, eventually leading to the accumulation of unrepaired, damaged tissues in old organisms [107,210]. By limiting cell proliferation, senescence in stem cells is hypothesized to contribute to aging by reducing the renewal capacity of these cells [20,107,83].

Taken together, these two functions of senescence, tumor suppression and aging have diametrically opposite effects on the lifespan of a species. While tumor suppression is beneficial, aging is detrimental to survival. While tumor suppression is beneficial, aging is detrimental to survival. A recent study has shown that the accumulation of senescent cells in cutaneous wounds enhances the healing process, thus making it beneficial in wound repair [211]. In light of another study showing that the accumulation of senescent hepatic stellate cells in liver injury limits fibrosis [212], this suggests that senescence may act as a

general wound healing response to limit injury and control fibrosis. This role of senescence as a double-edged sword has led it to be dubbed an Antagonistic Pleiotropic trait. The Antagonistic Pleiotropy Theory is an evolutionary theory of aging. Evolutionary theories of aging argue that aging results from a decline in the force of natural selection. Darwin's theory suggests that evolution occurred primarily to maximize reproductive fitness in an individual. This implies that longevity as a trait would only be selected for if it extended reproductive fitness, which it does not. Several evolutionary theories seek to address this problem, and they base their predictions on Peter Medawar's key observation made in 1952 that beyond a particular age the evolutionary benefit of a longer life span in mammals is negligible [213]. He suggested that the force of natural selection declines as the organism reaches an age beyond which it cannot reproduce efficiently. These evolutionary theories are all in their infancy, and none of them has been conclusively validated. One of the offshoots of Medawar's hypothesis is the Antagonistic Pleiotropy Theory that states that cellular and organismal aging are caused by genes that have opposing effects on the health of an organism at different points in the lifespan of an individual. I have based my thesis work on addressing the role of senescence in fulfilling the criteria posed by this theory. Therefore the next portion of this Chapter will focus on the Antagonistic Pleiotropy Theory and some examples of traits that fit this theory.

The Antagonistic Pleiotropy Theory

The Antagonistic Pleiotropy Theory of aging was proposed by George Williams in 1957 [214] and proposes that cellular damage and organismal aging are caused by pleiotropic genes. Pleiotropic genes are genes that have multiple phenotypic effects.

According to this hypothesis, a gene that functions to have beneficial effects early in life can have detrimental effects as the organism ages. Williams' original example referred to alleles at loci involved in the calcification of bones. Genes that promote efficient calcification would be selected for during early life to promote reproductive fitness. The same genes would cause deleterious calcification in arteries later in life leading to atherosclerosis. Natural selection acts the strongest on traits that manifest during an organism's peak reproductive value, which usually corresponds to the beginning of sexual maturity. This benefits the organism by leading to an overall increase in fitness during the reproductive period. In contrast, natural selection is the weakest on traits manifested after the majority of an organism**'**s reproduction is complete, and impairment to an organism during this time reduce overall fitness less than those manifested at earlier ages. Antagonistically pleiotropic alleles are those that provide a net increase in reproductive fitness during young age while detrimental phenotypes regulated by them are not expressed until post- reproduction [215].

The Antagonistic Pleiotropy Theory has been tested mainly in Drosophila by using artificial selection experiments [216,217]. Young adult flies were mated

with each other and their progeny collected [218,219]. Similarly, progeny derived from older adults that were mated were also collected. The older adults tend to die more frequently before their offspring were collected, therefore leading to stronger selection for longevity in these lines [219-223]. This is demonstrated by an increase in the lifespan of the progeny derived from the older matings compared the younger lines. Conversely, the flies derived from the younger lines demonstrate a reproductive advantage, demonstrating increased fecundity compared to the older lines [218,220,222,223]. It was further demonstrated that the increased fecundity was responsible for the reduced lifespan in the younger lines by experiments in which the reproductive function was abrogated by X-rays or genetic means of sterilization. The flies that could not reproduce exhibited increased life span showing that the aging was a direct consequence of increased fecundity and did not occur because of other effects of aging. There is a considerable time lag between the high fecundity associated with early age of the young lines and the increase in mortality that it led to, further supporting the Antagonistic Pleiotropy Theory.

Some of the seminal work supporting the Antagonistic Pleiotropy Theory has come from studies in the nematode *C.elegans*. Genes that encode components of the insulin signaling pathway when mutated, have been shown to give rise to worms with astonishing differences in lifespan compared with wild-type [224,225]. Worms that are mutant for the gene dauer formation constitutive-2 (DAF-2), a receptor that responds to insulin-like ligands, display 6.4-fold increase in maximum lifespan [226]. Further, reduced insulin signaling in

C.elegans also leads to increased dauer formation [227]. In *C.elegans* aging is accelerated by insulin/IGF signaling, which is hypothesized to function by acting on the neuroendocrine system [228] in response to food levels. The Antagonistic Pleiotropy Theory predicts that the accelerated aging is the trade-off for the increased fecundity caused by insulin signaling early in life. As a proof of principle, caloric restriction, which decreases insulin signaling is known to extend lifespan and reduce fecundity in *C.elegans* [229]. The Drosophila equivalent of DAF-2, is called *Inr,* and when its function is decreased, mean lifespan of the flies increases by 85% [230]. Mouse models deficient in IGF-1 show dwarfism and also exhibit a mean increase in lifespan that is associated with reduced fecundity [231]. Thus, the insulin signaling pathway is one example of an antagonistic pleiotropic trait in species ranging from nematodes to mammals.

One gene that has been postulated to function as an antagonistic pleiotropic trait in mammals is p53. p53 is known to function as a tumor suppressor gene by interrupting aberrant cell proliferation. The effect of p53 on cell proliferation can be detrimental if it influences the proliferation of normal cells such as stem cells that are necessary for self-renewal with aging. The role of p53 in cancer was initially demonstrated in families with Li-Fraumeni Syndrome, an autosomal dominant disorder in which genetic analyses revealed that mutations in p53 co-segregated with the disease phenotype [232]. p53 heterozygous mice (p53+/-) that lack a single allele of p53 exhibit significantly increased risk of cancer [233]. Finally, mice with an additional copy of p53 (super-p53 mice) are

more resistant to cancer compared with wild-type mice with only two copies of p53 [234].

The role of p53 in aging has been explored more recently. Accelerated aging and a reduced life span was seen in mice with seen in mice with a mutant 'm' allele of p53 that has the ability of augment the tumor suppressor function of p53 [235]. The $p53^{m}$ allele lacks the first 6 exons of full-length p53 as well as some uncharacterized upstream sequences. These mice show increased resistance to experimentally induced and spontaneous tumors compared to both p53+/+ and p53+/- animals. Homozygosity of the 'm' allele is lethal [236]. Young $p53^{+/m}$ mice behave just like WT, but the older mice exhibit progeroid symptoms such as weight loss and lordokyphosis that are associated with reduced life spans. Tissues from the $p53^{+/m}$ mice such as skin, fat, spleen, kidney and bone exhibit increased atrophy and decreased repair competency. This loss of regenerative capacity may occur due to the function of p53 in maintaining tissue homeostasis being compromised in the $p53^{+/m}$ mice due to its effect on stem cell activity [237].

Several laboratories have shown that another naturally occurring short isoform of p53 called Δ40p53 also causes premature aging similar to that of $p53^{+/m}$ mice, with a mean lifespan of less than 16 months compared to over 20 months for the non-transgenic controls [238]. The Δ40p53 model is 44kDa in size and identical to full-length p53 except it lacks the first activator domain in the N-terminus of the protein. The Δ40p53 mice and the $p53^{+/m}$ mice show increased tumor suppression in the context of decreased life span. However the Super-p53

mice exhibit a normal aging phenotype. In all three strains increased p53 activation results in increased expression of p21, a p53 target gene [235,239,238].

While there is some evidence to support the Antagonistic Pleiotropy Theory, much has to be done to prove it conclusively true. We are interested in studying the veracity of this theory as it applies to cellular senescence. Therefore we have manipulated the expression of a key senescence regulator, Smurf2, *in vivo* and tested its effects on cancer and aging. The final portion of this chapter will focus on Smurf2 and its role in senescence and other functions.

Smurf2

Smurf2 is a HECT domain E3 ubiquitin ligase. HECT E3 ligases are found across species ranging from yeast to human. They all contain a catalytic HECT (homologous to E6AP C-terminus) domain that comprises of roughly 350 amino acids and is similar to the E6AP C-terminus [240,241]. The HECT domain contains a conserved cysteine residue via which it catalyzes the interaction of the E2 ubiquitin conjugating enzyme with the protein that is targeted for ubiquitination. It mediates the formation of a thioester bond between the target protein and ubiquitin leading to the protein being marked for proteasome-mediated degradation [240,241]. The HECT domain represents the catalytic domain of the E3 ligase [240,241] but substrate specificity is determined by the N-terminus of the protein. HECT E3 ligases are grouped into 3 different sub-types based on distinct N-terminal amino acid motifs. These include, the HECT E3 with RLDs (RCC1-like domains) that are called HERC (HECT and RCC-like domain E3s) [242] and HECT E3s that contain WW domains. (called NEDD4 or NEDD4-like E3s) A third group is composed of E3s that contain neither the RLD nor the WW domains called as SI(ngle) E3s. HECT domain E3 ligases have been associated with several human diseases including cancer [243].

Smurf2 is a WW-domain containing NEDD4-like HECT domain E3 ubiquitin ligase. Smurf2 was identified along with its homolog Smurf1 in a yeast-2-hybrid screen wherein WW domain containing proteins that interact with the PY-containing protein Smad1 which is a component of the TGF-β signaling

pathway [244]. Smurf2 has a N-terminal C2 domain that mediates membrane localization, two WW domains that recognize proline-rich motifs of substrates or adaptor proteins for interactions, and a large C-terminal HECT domain with a catalytic cysteine residue at position 716, which catalyzes the formation of the isopeptide bond with the C-terminus of ubiquitin and the substrate Lysine residue [244].

Work from our lab has shown that apart from functioning as an E3 ligase, Smurf2 also plays an important role in regulating cellular senescence. I will first describe how Smurf2 functions to regulate senescence and then focus on the known targets of Smurf2-mediated ubiquitination.

Smurf2 as a regulator of Cellular Senescence:

Smurf2 was identified as a component of a gene expression signature characteristic of telomere-dependent senescence in human fibroblasts [11]. The up-regulation of Smurf2 in replicatively senescent cells is readily distinguishable its expression in cycling and or quiescent cells. Further the overexpression of Smurf2 in early passage human fibroblast cells resulted in the induction of senescence [245]. This induction of senescence is independent of Smurf2's E3 ligase activity, (the C716A E3 ligase mutant of Smurf2 induces senescence effectively) and is dependent on both the p53 and the Rb pathways [245]. Further, it was shown that Smurf2 regulates p21 independent of its ligase activity. Deletion of the C2 domain does not affect the senescence induction function of Smurf2 [245]. Recently, work from our lab has shown that Smurf2 targets ID1

(Inhibitor of differentiation 1) for ubiquitin-mediated degradation [246]. The inhibitor of differentiation or DNA binding (Id) family of transcription regulators plays an important role in cell proliferation, differentiation, and senescence [247-249]. ID1 is known to inhibit p16 expression by sequestering the bHLH factor E47, and preventing the transactivation of p16 [250,251]. Further, ID1 has been shown to be a key regulator of replicative senescence. Inhibition of ID1 expression activates the senescence response [250,251] and overexpression of ID1 delays senescence [252-256]. Work from our lab has shown that Smurf2 targets ID1 for ubiquitin-mediated degradation and thus regulates p16 expression in senescence [246]. Thus, the ligase-independent regulation of p21 (and the p53 arm of the senescence pathway) and the ligase dependent regulation of p16 (and the pRb arm of the senescence pathway) provide a mechanism for Smurf2's function of inducing senescence by regulating both of the major senescence pathways.

Targets of Smurf2-mediated ubiquitination:

Several targets of Smurf2-mediated ubiquitination play important roles in biologically important processes such as cell-cycle progression, tumor suppression and promotion and cell migration and invasion. These include various components of the TGF-ß signaling pathway, such as Smad1 [257], Smad2 [258], TGF- βR-I [259], TGF-βR-II [260] and SnoN, a transcriptional co-repressor of the TGF-β signaling pathway [261]. Recently, Smurf2 has also been

shown to monoubiquitinate Smad3 and prevent the formation of Smad3 complexes that further inhibit TGF- β signaling [262].

Smurf2 has also been shown to be the E3 ubiquitin ligase for the GTPase Rap1B [263], the RING-H2 protein RNF-11 [264], the Runt domain transcription factors Runx3 [265] and Runx2 [266]. Smurf2 is also known to ubiqutinate components of the Wnt signaling pathway such as β-Catenin [267] and Axin [268].

Smurf1, a homolog of Smurf2 is another known target of Smurf2-mediated ubiquitination, and this ubiquitination leads to migration of breast cancer cells [269]. Smurf2 has also been shown to ubiquitinate the adaptor protein NEDD9 and target it for proteasome-mediated degradation. NEDD9 localizes to the centrosome and is essential for activation of the Aurora-A kinase in mitosis [270]. Aurora-A activation during late G2 is a critical step for commitment to mitosis and Smurf2 depletion leads to delayed entry into mitosis.

The TGF-β signaling pathway is known to play a role in several important processes such as proliferation, differentiation, apoptosis, adhesion, invasion, and cellular micro-environment [271-273]. It has also been shown to play important roles in cancer. Analysis of human tumor samples has shown that immunostaining for TGF-β correlates with metastasis in breast, colon, and prostate cancer [274-276]. Further, the intensity of TGF-β staining was found to be higher in the metastatic lesions than the primary tumors in breast, colon and prostate cancer [277,278]. The TGF-β signaling pathway has both tumor-suppressive and tumor-promoting functions [279]. Runx2 is known to be

abnormally expressed in tumors that metastasize to bone. RNF11 is overexpressed in breast and pancreatic tumors [264]. The Wnt signaling pathway is known to play a role in several important processes ranging from embryonic development to cancer.

Interestingly, Smurf2 has been shown to promote the degradation of p53 by stabilizing MDM2 by enhancing its heterodimerization with MDMX [280]. Further, Smurf2 has also been shown to promote the stabilization of EGFR by ubiquitinating it and protecting it against c-Cbl-mediated degradation [281]. Gene expression microarray data from patients showed a strong correlation of expression between EGFR and Smurf2 suggesting that Smurf2-mediated protective ubiquitination of EGFR may be responsible for EGFR overexpression in tumors [281].

Thus several targets of Smurf2-mediated ubiquitination are known to play an important role in cancer development and progression making it a potentially important player in the regulation of these processes.

CHAPTER II

Smurf2 regulates the senescence response and suppresses tumorigenesis in mice

Abstract

The E3 ubiquitin ligase Smurf2 mediates ubiquitination and degradation of several protein targets involved in tumorigenesis and induces senescence in human cells. However, the functional role of Smurf2 in tumorigenesis has not been fully evaluated. In this study, we generated a mouse model of Smurf2 deficiency to characterize the function of this E3 ligase in tumorigenesis. Smurf2 deficiency attenuated p16 expression and impaired the senescence response of primary mouse embryonic fibroblasts. In support of a functional role in controlling cancer, Smurf2 deficiency increased the susceptibility of mice to spontaneous tumorigenesis, most notably B cell lymphoma. At a premalignant stage of tumorigenesis, we documented a defective senescence response in the spleens of Smurf2-deficient mice, consistent with a mechanistic link between impaired senescence regulation and increased tumorigenesis. Taken together, our findings offer genetic evidence of an important tumor suppressor function for Smurf2.

INTRODUCTION

The E3 ubiquitin ligase Smurf2 has been shown to mediate ubiquitination of several proteins, including components of the TGF-β and Wnt signaling, Runx2, Rap1B, Smurf1 and Id1 [259,258,257,267,266,263,269,282,283,268,246]. These diverse substrates suggest that Smurf2 is involved in many biological processes. We have previously shown that Smurf2 expression increases in response to telomere shortening in senescent cells [11]. Furthermore, we have discovered that Smurf2 recruits both the p53 and pRb pathways to activate senescence [245], suggesting that Smurf2 is a critical regulator of senescence. As an important tumor suppression mechanism, senescence restricts the proliferation of cells at risk of malignant transformation [107,83]. Consistent with this model, we have found that up-regulation of Smurf2 leads to growth arrest in various tumor cells [284].

Despite the advance in our understanding of Smurf2's molecular function, the precise role of Smurf2 in tumorigenesis has not been established. In this study, we generated a mouse model of Smurf2 deficiency, and showed that Smurf2 deficiency leads to an impaired senescence response in primary cells. Consistent with its function in senescence regulation, Smurf2-deficient mice exhibited increased spontaneous tumorigenesis, indicating that Smurf2 functions as a tumor suppressor.

RESULTS

A mouse model of Smurf2 deficiency

We used a mouse embryonic stem (ES) cell line RRA098 with a gene-trapping vector (pGT1lxf) inserted into intron 1 of *Smurf2* (Fig.2.1a) to generate a mouse model of Smurf2 deficiency. A single integration of the trapping vector in RRA098 genome was observed in Southern analysis (Fig.2.1b), and further determined by sequencing analysis (Fig.2.1c and data not shown). *Smurf2* transcripts were increased in ES cells after Cre-mediated excision of *loxP*-flanked splicing acceptor (SA) (Fig.2.1d), indicating that Smurf2 expression is compromised in RRA098 cells, and removal of SA restores its expression.

Mice heterozygous for the trapped allele ($Smurf2^{+/T}$) were viable and developmentally normal. Intercrossing of $Smurf2^{+/T}$ mice generated $Smurf2^{T/T}$ mice with expected Mendelian frequency (36:72:35 for $Smurf2^{+/+}$:$Smurf2^{+/T}$:$Smurf2^{T/T}$) and grossly normal development (Fig.2.2). Smurf2 expression in $Smurf2^{+/T}$ MEFs or embryos was reduced to ~50% of wild-type, whereas Smurf2 (~20%) was still detected in $Smurf2^{T/T}$ MEFs or embryos (Fig.2.3a), suggesting that this trapped allele is hypomorphic. Consistent with this notion, Smurf2 expression was reduced but not absent in many tissues of $Smurf2^{T/T}$ mice compared to wild-type littermates (Fig.2.3b). The $Smurf2^{T/T}$ mouse thus serves as a model of Smurf2 deficiency.

Fig.2.1: Characterization of a mouse model of Smurf2 deficiency. (a) Schematics of the trapped *Smurf2* allele. *En2-1*: mouse *En2* intron 1; *SA*: splicing acceptor; *pA*: SV40 polyadenylation signal. (b) Southern analysis of genomic DNA of RRA098 cells or *Smurf2*$^{+/T}$ mouse tail using *Neo* as a probe. Specific bands are indicated by arrows at left with DNA ladder at right. (c) The integration site of the gene-trapping vector is determined by genomic PCR using primer En2-1 and one of the 12 primers (P1-P12) in the intron 1 of *Smurf2*. (d) Elevated Smurf2 expression in Cre-expressing ES clones, which were identified by genomic PCR with primers P1 and P2 shown in (a).

Fig.2.1

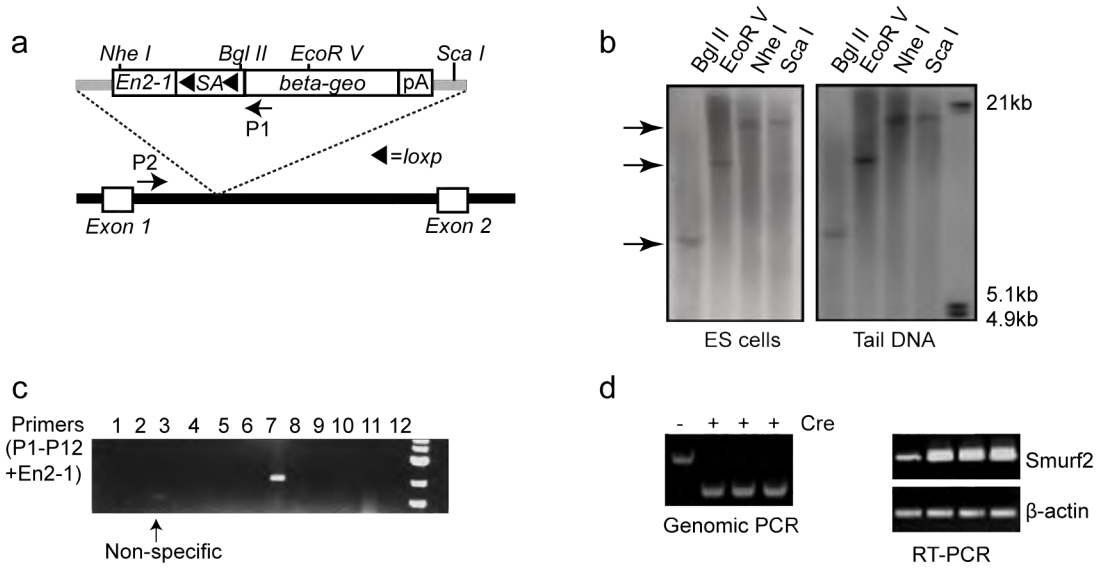
a
Nhe I
Bgl II
EcoR V
Sca I
En2-1
SA
beta-geo
pA
P1
P2
=loxp
Exon 1
Exon 2
b
Bgl II
EcoR V
Nhe I
Sca I
Bgl II
EcoR V
Nhe I
Sca I
21kb
5.1kb
4.9kb
ES cells
Tail DNA
c
Primers
(P1-P12
+En2-1)
1 2 3 4 5 6 7 8 9 10 11 12
Non-specific
d
- + + + Cre
Genomic PCR
Smurf2
β-actin
RT-PCR

Fig.2.2: Smurf2-deficient mice exhibit normal development. H&E staining of tissues from 2-month old wild-type (+/+) and *Smurf2*$^{T/T}$ (T/T) mice shows a normal development of Smurf2-deficient mice. Scale bar is 200 µm for 10X images and 100 µm for 50X images.

Fig.2.2

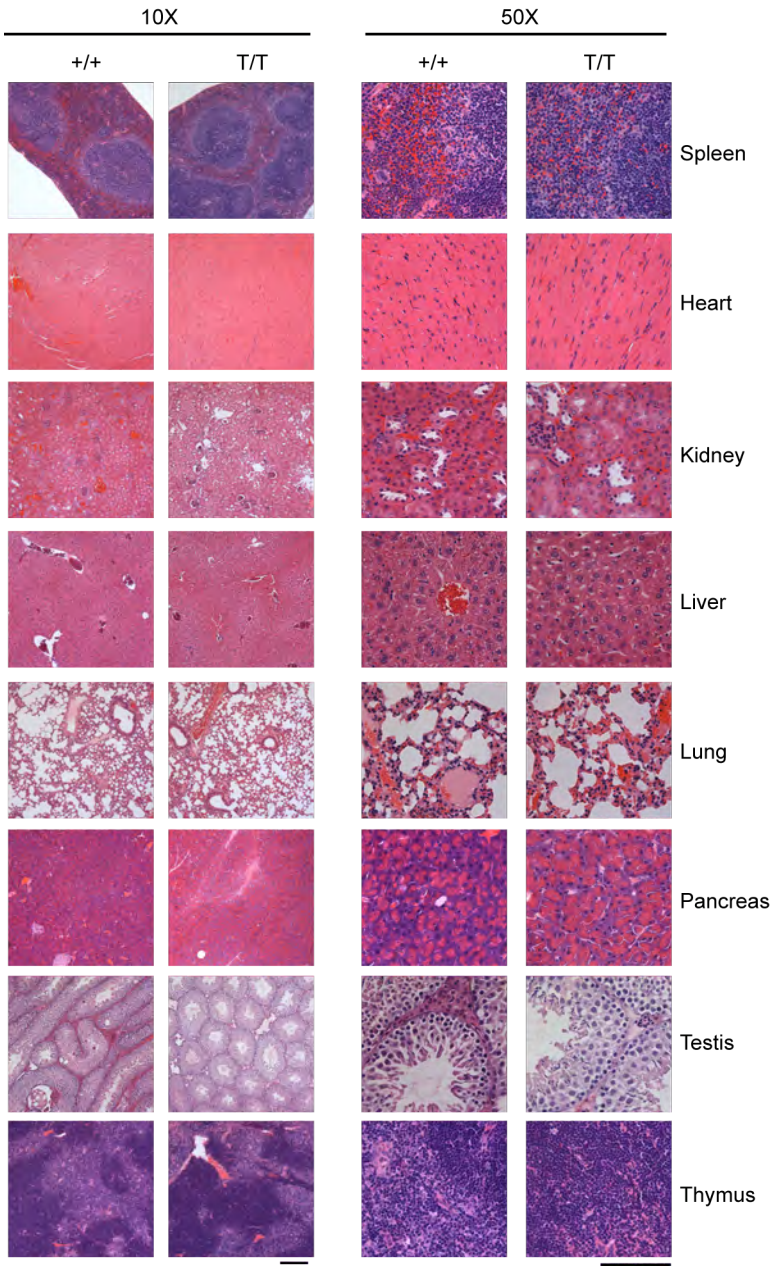
10X
50X
+/+
T/T
+/+
T/T
Spleen
Heart
Kidney
Liver
Lung
Pancreas
Testis
Thymus

Fig.2.3: The Smurf2-deficient mouse model is a hypomorph. (a) Smurf2 expression in wild-type (+/+), *Smurf2*$^{+/T}$ (+/T) and *Smurf2*$^{T/T}$ (T/T) MEFs and embryos analyzed by Western (both) and quantitative RT-PCR (MEFs only). Smurf2 expression in wild-type was set as 100% after normalization with β-actin. Error bars were standard deviations of three independent experiments. (b) Smurf2 expression in tissues of 2-month-old wild-type and *Smurf2*$^{T/T}$ littermates.

Fig.2.3

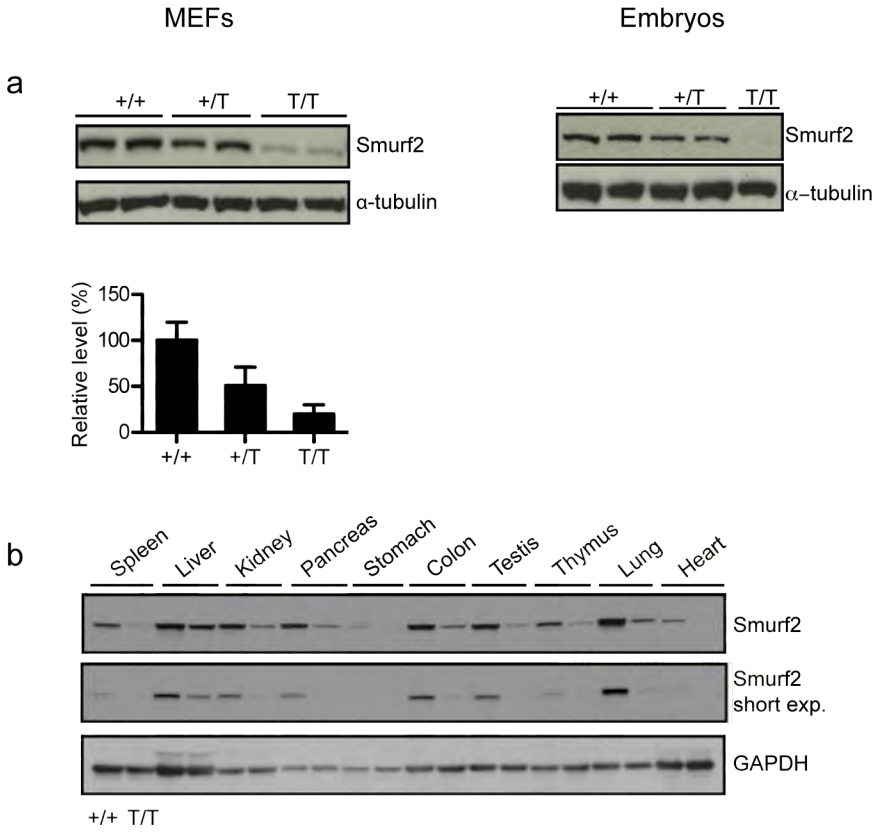
MEFs
Embryos
a
+/+
+/T
T/T
Smurf2
α-tubulin
Relative level (%)
150
100
50
0
b
Spleen
Liver
Kidney
Pancreas
Stomach
Colon
Testis
Thymus
Lung
Heart
Smurf2
Smurf2
short exp.
GAPDH
+/+ T/T

Impaired senescence response in Smurf2-deficient MEFs

At early passage, no obvious difference in cell proliferation was noted among MEFs of different genotypes (Fig.2.4a). However, senescence entry was delayed in *Smurf2*$^{T/T}$ and *Smurf2*$^{+/T}$ MEFs compared to wild-type (Fig.2.4b). We next passaged MEFs with a 3T9 protocol starting from passage 2. Wild-type MEFs entered senescence around passage 7. In contrast, *Smurf2*$^{T/T}$ and even some *Smurf2*$^{+/T}$ MEFs showed a tendency to become immortalized and continued to proliferate beyond passage 20 (Fig.2.4c), indicating that Smurf2 deficiency promotes spontaneous immortalization of primary fibroblasts.

To assess whether immortalization of *Smurf2*$^{T/T}$ MEFs is the result of Smurf2 deficiency or caused by secondary mutations in other genes, we tested whether Smurf2 can induce senescence in these MEFs. Ectopic expression of Smurf2 or a ligase mutant C716A [245] induced senescence in early passage and late passage already immortalized *Smurf2*$^{T/T}$ MEFs (Fig.2.5a), suggesting that Smurf2 is essential for senescence. Furthermore, we found that p53 and p21$^{CIP1/WAF1}$ (p21) increased in early passage and immortalized *Smurf2*$^{T/T}$ MEFs after doxorubicin treatment (Fig.2.5b), indicating that Smurf2-deficient MEFs have a functional DNA damage response, and immortalization of *Smurf2*$^{T/T}$ MEFs is independent of p53 loss.

Fig.2.4: Impaired senescence response in Smurf2-deficient MEFs. (a) Cell proliferation and (b) Senescence analyses in early passage (P2) wild-type (+/+), *Smurf2*$^{+/T}$ (+/T) and *Smurf2*$^{T/T}$ (T/T) MEFs. Student *t*-test was used in pair-wise comparison with statistical significance indicated as: * (P<0.05), ** (P<0.01), and *** (P<0.001). (c) Immortalization assay of MEFs starting from passage 2 with population doubling (PD) set as 0.

Fig.2.4

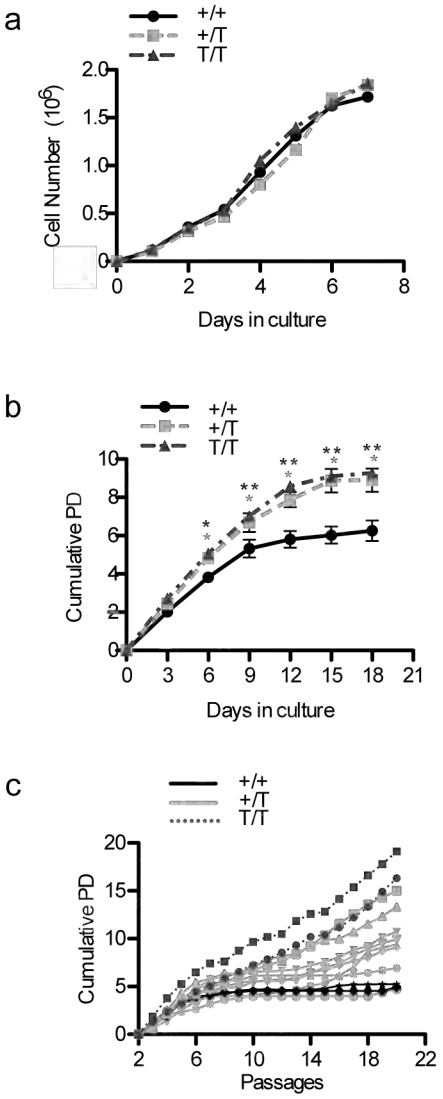
a
+/+
+/T
T/T
Cell Number (10^6)
2.0
1.5
1.0
0.5
0
0
2
4
6
8
Days in culture
b
+/+
+/T
T/T
Cumulative PD
10
8
6
4
2
0
0
3
6
9
12
15
18
21
Days in culture
c
+/+
+/T
T/T
Cumulative PD
20
15
10
5
0
2
6
10
14
18
22
Passages

Fig.2.5: Smurf2-deficient MEFs enter senescence in response to Smurf2 overexpression and have a normal p53 pathway. (a) Early passage (P4) and late passage (P28) already immortalized *Smurf2*$^{T/T}$ (T/T) MEFs were stained with crystal violet and for senescence-associated β-galactosidase (SA-β-gal) activity following ectopic expression of Smurf2, ligase mutant C716A or GFP control. (b) Western analysis of p53 and p21 in MEFs following doxorubicin treatment.

Fig.2.5

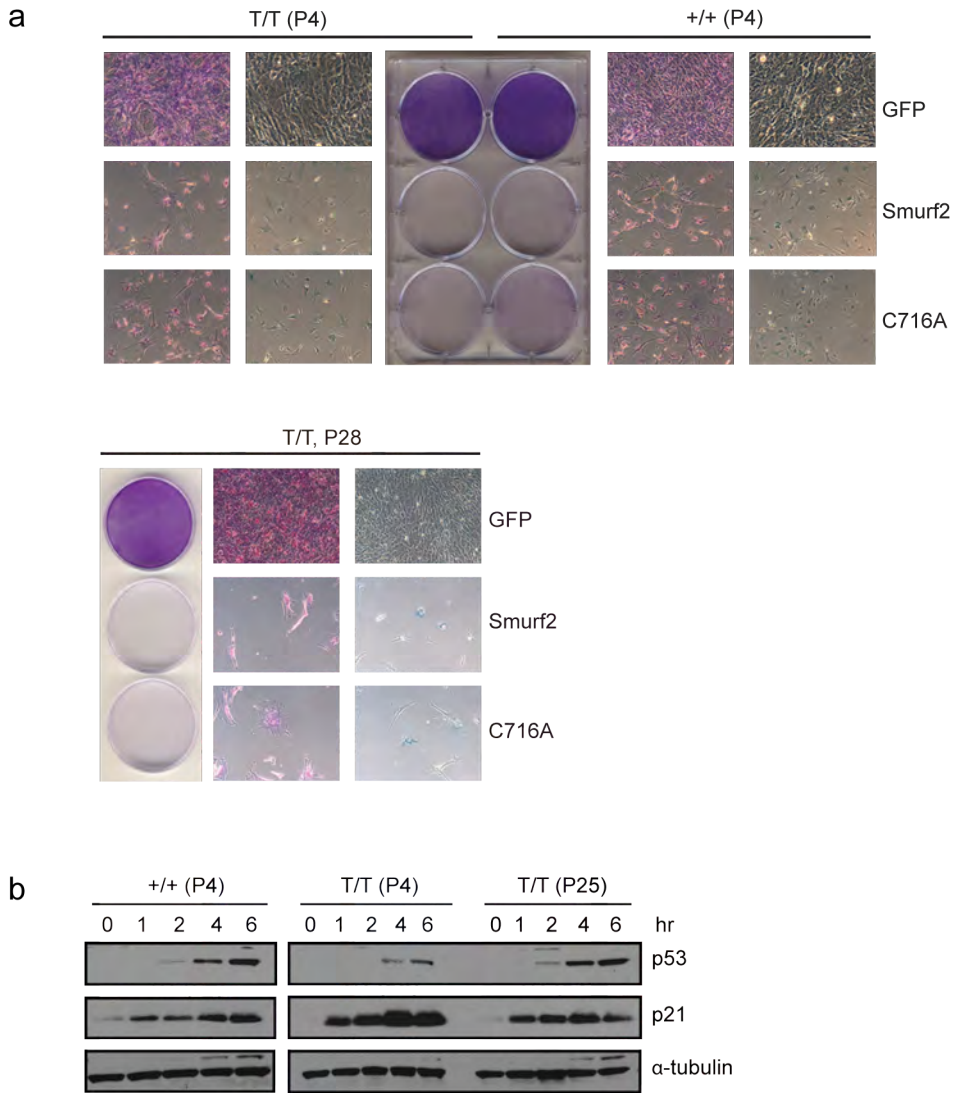
a
T/T (P4)
+/+ (P4)
GFP
Smurf2
C716A
T/T, P28
GFP
Smurf2
C716A
b
+/+ (P4)
T/T (P4)
T/T (P25)
0 1 2 4 6
0 1 2 4 6
0 1 2 4 6
hr
p53
p21
α-tubulin

To further investigate the mechanism underlying the impaired senescence response in Smurf2-deficient MEFs, we examined the expression of known senescence regulators during serial passage. No obvious change in the expression of $p19^{Arf}$ (p19), p21 or p53 was observed between wild-type and *Smurf2*$^{T/T}$ MEFs (Fig.2.6). Consistent with our recent finding that Smurf2 regulates $p16^{INK4a}$ (p16) expression through ubiquitination of Id1 [246], p16 expression in early passage *Smurf2*$^{T/T}$ MEFs was decreased compared to wild-type MEFs. While p16 expression was elevated in late passage wild-type MEFs, this p16 elevation was significantly attenuated in *Smurf2*$^{T/T}$ MEFs (Fig.2.6), suggesting a mechanistic link between inhibition of p16 expression and delayed senescence in Smurf2-deficient MEFs.

Increased spontaneous tumorigenesis in Smurf2-deficient mice

Smurf2$^{T/T}$ (30.6%) and *Smurf2*$^{+/T}$ (23.8%) mice developed tumors spontaneously within 20 months, whereas no tumor was found in wild-type mice within the same period (Fig. 3A). All affected Smurf2-deficient mice had enlarged spleens (Fig.2.7a) and developed lymphomas. A majority of lymphomas (82.4%) stained strongly for B220 (Fig.2.7b), indicating a B-cell origin. The lymphomas often spread to other organs: 47.1% and 23.5% of mice with lymphoma in spleen were found to have lymphoma in kidney and liver, respectively (Fig.2.7b). In addition to lymphoma (72.7% of tumors), we also found other types of tumors, including hepatocellular carcinoma (13.6%), adenocarcinoma in small intestine (4.5%) and sarcoma (9.1%) (Fig.2.7c). Collectively, these results indicate that Smurf2

deficiency leads to increased spontaneous tumorigenesis in mice, and suggest that Smurf2 functions as a tumor suppressor.

Increased spontaneous tumorigenesis was also observed in *Smurf2*$^{+/T}$ mice, which had ~50% of Smurf2 protein. Interestingly, three of the four lymphoma samples from *Smurf2*$^{+/T}$ mice showed lower level of Smurf2 protein than normal spleen of *Smurf2*$^{+/T}$ mice (Fig.2.8a). To test whether loss of heterozygosity occurred during development of these lymphomas, we used quantitative PCR to compare the abundance of the wild-type and trapped *Smurf2* alleles with *GAPDH* in tail and spleen (Fig.2.8b). Three lymphoma samples from *Smurf2*$^{+/T}$ mice with decreased Smurf2 protein levels showed a reduction in the abundance of the wild-type *Smurf2* allele compared to unaffected corresponding tail DNA (Fig.2.8b), whereas the relative abundance of the trapped *Smurf2* allele was either unchanged or increased (Fig.2.8c). These results suggest a loss of the wild-type *Smurf2* allele in these lymphomas, and confirm that loss of Smurf2 results in the formation of tumors in mice.

Fig.2.6: Impaired senescence response in Smurf2-deficient MEFs. Western analysis of senescence regulators in MEFs passaged in Fig.2.4(b).

Fig.2.6

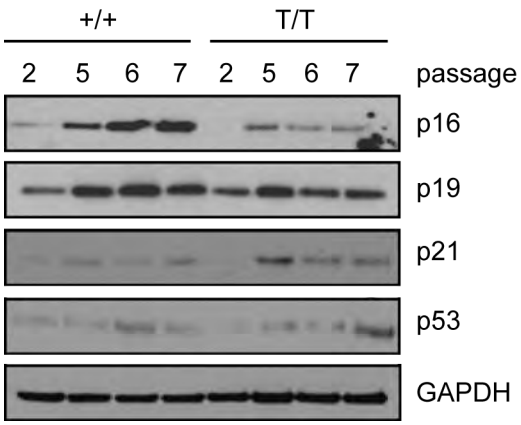

Fig.2.7: Increased spontaneous tumorigenesis in Smurf2-deficient mice. (a) Kaplan-Meier curves of tumor-free survival of wild-type (+/+), *Smurf2*$^{+/T}$ (+/T) and *Smurf2*$^{T/T}$ (T/T) mice. Statistical significance was analyzed by the log-rank test. (b) Representative spleens of a moribund *Smurf2*$^{T/T}$ mouse and an age-matched wild-type mouse. (c) Representative H&E and B220 staining of lymphomas in spleen, liver and kidney of *Smurf2*$^{T/T}$ mice, in comparison to sections of wild-type mice. (d) Representative H&E staining of other types of tumors found in Smurf2-deficient mice. Scale bars for 10x and 50x images are 200 µm and 100 µm, respectively.

Fig.2.7

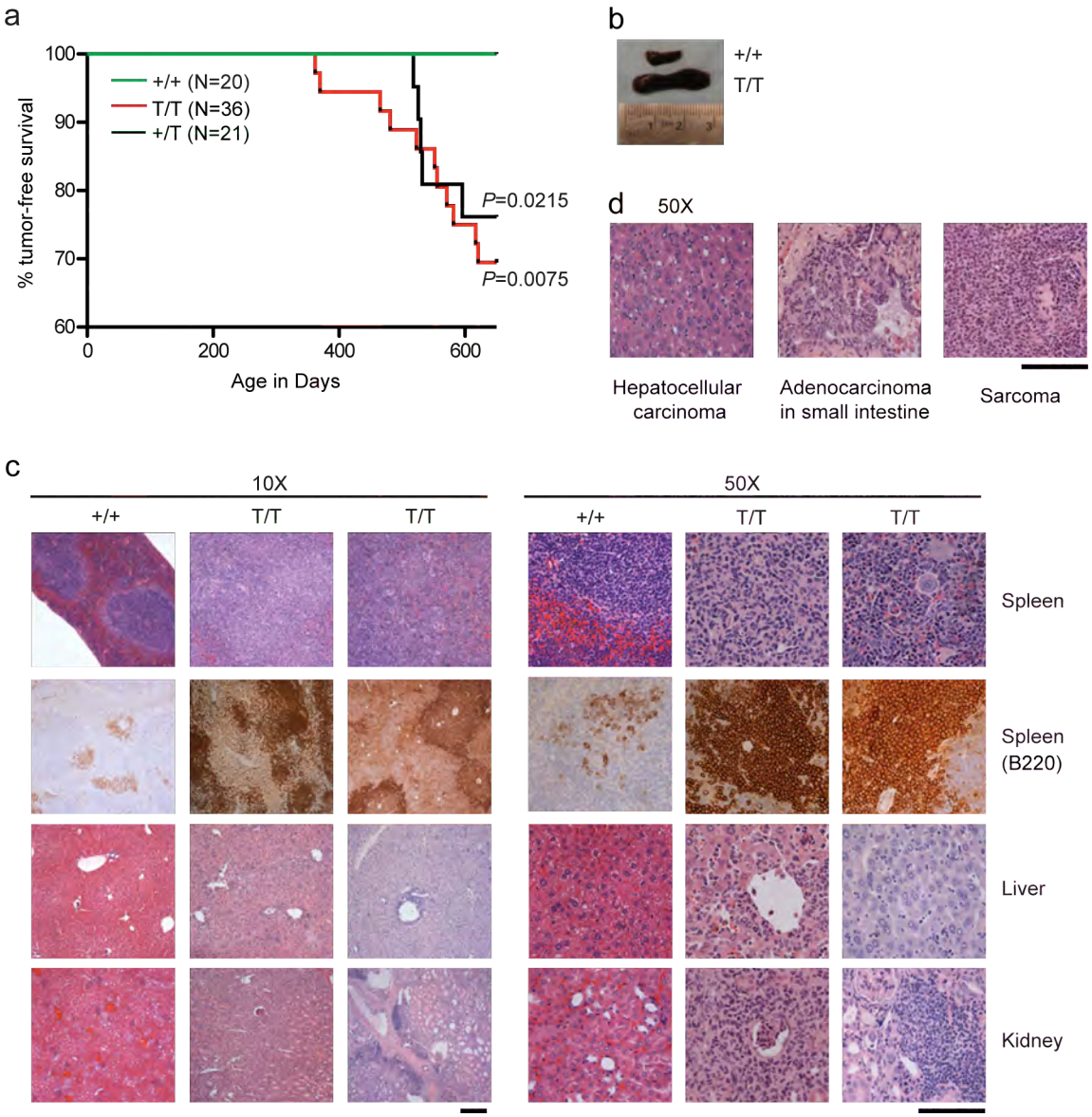
a
100
90
80
70
60
% tumor-free survival
+/+ (N=20)
T/T (N=36)
+/T (N=21)
P=0.0215
P=0.0075
0
200
400
600
Age in Days
b
+/+
T/T
d
50X
Hepatocellular carcinoma
Adenocarcinoma in small intestine
Sarcoma
c
10X
50X
+/+
T/T
T/T
+/+
T/T
T/T
Spleen
Spleen (B220)
Liver
Kidney

Fig.2.8: Analysis of loss of heterozygosity in lymphomas derived from *Smurf2*$^{+/T}$ (+/T) mice. (a) Western blot of Smurf2 expression in lymphomas from *Smurf2*$^{+/T}$ and *Smurf2*$^{T/T}$ mice. Smurf2 expression in spleens of 2-month old wild-type (+/+), *Smurf2*$^{+/T}$ (+/T) and *Smurf2*$^{T/T}$ (T/T) mice is shown for comparison. Quantitation of abundance of (b) the wild-type *Smurf2* allele and (c) the trapped *Smurf2* allele after normalization with the *GAPDH* allele in tail and spleen DNA of 2-month old wild-type (+/+), *Smurf2*$^{+/T}$ (+/T) and *Smurf2*$^{T/T}$ (T/T) littermates. The relative level of the wild-type *Smurf2* allele in +/+ and the relative level of the trapped *Smurf2* allele in T/T mice were set to be 1. Quantitation of abundance of (d) the wild-type *Smurf2* allele and (e) the trapped *Smurf2* allele after normalization with *GAPDH* in DNA from lymphomas of *Smurf2*$^{+/T}$ (+/T) mice and their corresponding tail DNA. The relative level in tail DNA was set to be 1. Lymphoma samples analyzed in (d) and (e) correspond to those shown in (a). Error bars were calculated from standard deviations of three independent experiments.

Fig.2.8

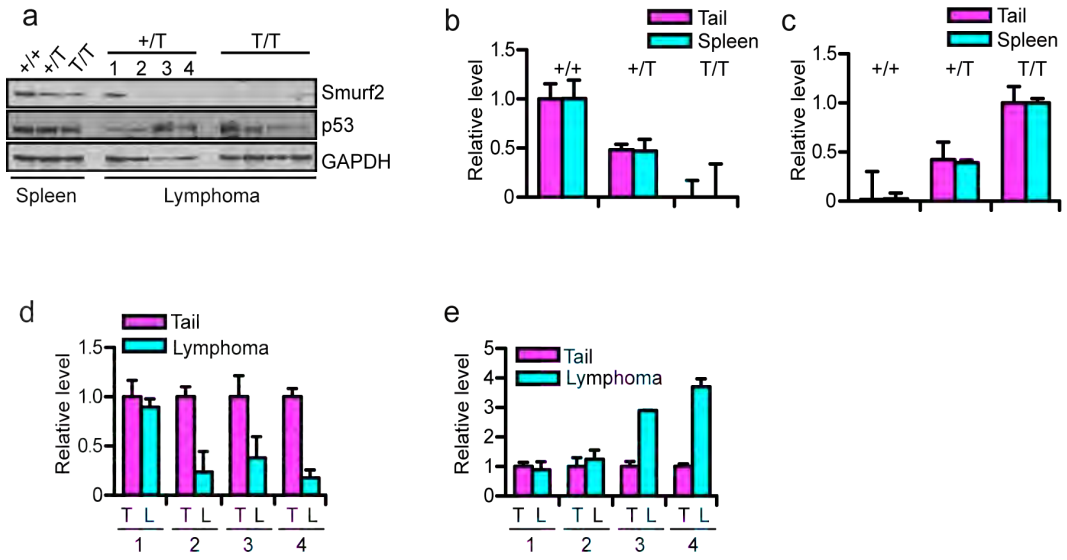
a
+/+
+/T
T/T
+/T
T/T
1 2 3 4
Smurf2
p53
GAPDH
Spleen
Lymphoma
b
Tail
Spleen
Relative level
1.5
1.0
0.5
0
+/+
+/T
T/T
c
Tail
Spleen
Relative level
1.5
1.0
0.5
0
+/+
+/T
T/T
d
Tail
Lymphoma
Relative level
1.5
1.0
0.5
0
T L
T L
T L
T L
1
2
3
4
e
Tail
Lymphoma
Relative level
5
4
3
2
1
0
T L
T L
T L
T L
1
2
3
4

Senescence regulation in spleens of Smurf2-deficient mice

As the majority of tumors found in Smurf2-deficient mice were B-cell lymphomas in spleen, we investigated whether the senescence response was impaired in spleens of Smurf2-deficient mice. In 12-month-old premalignant mice, we found positive staining for SA-β-gal activity in spleens of wild-type mice, whereas such positive staining was largely absent in spleens of *Smurf2*$^{T/T}$ mice (Fig.2.9a), indicating an impaired senescence response in spleens of Smurf2-deficient mice. Consistent with our recent finding that Smurf2 regulates p16 expression through ubiquitination and degradation of Id1 during senescence [246], we found that Id1 was elevated, while p16 expression was decreased in spleens of 12-month-old premalignant *Smurf2*$^{T/T}$ mice compared to age-matched wild-type littermates (Fig.2.9b). These results suggest that the Smurf2-Id1-p16 axis regulates senescence *in vivo*. As senescence acts as an important tumor suppressor to restrict the proliferation of cells at risk of malignant transformation [107,83], an impaired senescence response in Smurf2-deficient cells provides an underlying mechanism of increased spontaneous tumorigenesis in Smurf2-deficient mice.

Fig.2.9: Impaired senescence response in spleens of aged Smurf2-deficient mice. (a) Representative staining for SA-β-gal activity and quantitation (10 randomly selected fields) in spleens of 12-month-old premalignant wild-type (+/+) and *Smurf2*$^{T/T}$ (T/T) mice. (b) Western and quantitative RT-PCR analyses of p16 expression in spleens of 12-month-old mice. The relative expression of p16 in wild-type was set to be 1 after normalization with β-actin. Error bars were standard deviations of three independent experiments. Student *t*-test was used in statistical analysis (*:$P<0.05$, **:$P<0.01$ and ***:$P<0.001$).

Fig.2.9

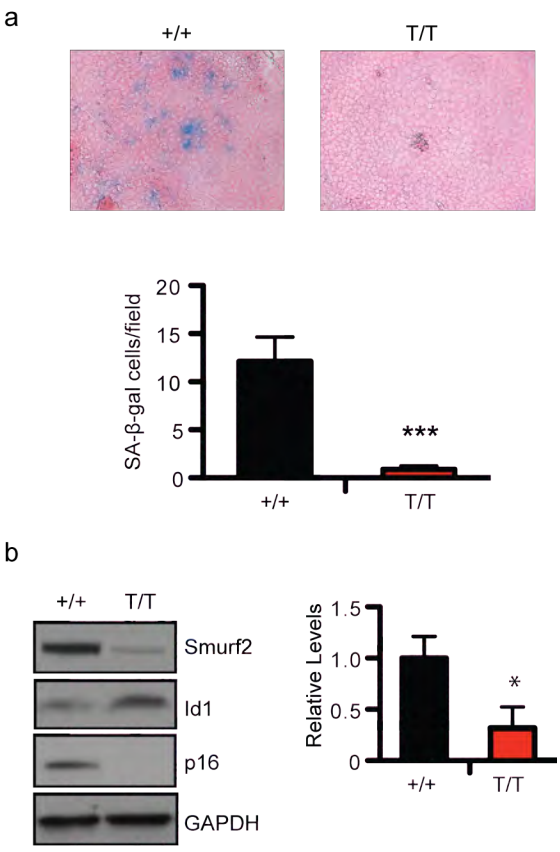
a
+/+
T/T
SA-β-gal cells/field
20
15
10
5
0
***
+/+
T/T
b
+/+
T/T
Smurf2
Id1
p16
GAPDH
Relative Levels
1.5
1.0
0.5
0
*
+/+
T/T

DISCUSSION

In this study, we found that Smurf2-deficient mice exhibited an increased susceptibility to spontaneous tumorigenesis, indicating that Smurf2 has a tumor suppression function. Further support for Smurf2 as a tumor suppressor is the observation of increased spontaneous tumorigenesis in *Smurf2*$^{+/T}$ mice accompanied by frequent loss of the wild-type *Smurf2* allele in these tumors. Another group has also independently reported similar findings using a Smurf2 knockout mouse model [285]. Consistent with the notion that Smurf2 is a tumor suppressor, *Smurf2* mutations have been found in human melanoma (2 out of 8) and lung carcinoma (1 out of 145) samples in COSMIC database (http://www.sanger.ac.uk/genetics/CGP/cosmic). The identified nonsense mutations (1222C>T, R408* or 1774C>T, R592*) would result in truncated Smurf2 proteins lacking a functional HECT domain, thus disrupting its function as an E3 ubiquitin ligase and its ability to induce senescence [245]. Collectively, these observations support the notion that Smurf2 is a tumor suppressor.

Increased tumorigenesis was preceded by an impaired senescence response in spleens and primary fibroblasts of Smurf2-deficient mice. Consistent with our recent finding that Smurf2 ubiquitinates Id1 to regulate p16 expression during senescence in culture [246], we found elevation of Id1 and corresponding decrease in p16 expression in spleens of premalignant Smurf2-deficient mice, suggesting that the Smurf2-Id1-p16 axis regulates senescence response *in vivo*. Emerging evidence indicate that senescence is an important tumor suppression mechanism by restricting proliferation of cells at risk of neoplastic transformation [107,83]. Our current study provides a mechanistic link between Smurf2-

mediated senescence regulation and its role as a tumor suppressor *in vivo*.

Smurf2 is suggested to target Smads and TGF-β receptor for ubiquitination and degradation [259,258,257]. However, these cell culture studies are challenged by recent studies of Smurf2 knockout mice, which indicate that Smurf2 does not regulate protein stability of Smads and TGF-β receptor under physiological conditions *in vivo* [262,283]. Smurf2 has also been implicated to ubiquitinate both negative (Axin and GSK-3β) and positive (β-catenin) regulators of the canonical Wnt signaling pathway [268,267,282]. Studies of Smurf1/2 double knockout mice reveal that Smurf2 instead regulates the non-canonical Wnt signaling through ubiquitination of Prickle1 [283]. We have recently discovered that Smurf2 ubiquitinates Id1 [246], which is involved in diverse cellular processes including proliferation, differentiation and angiogenesis [249]. It will be interesting to determine whether Smurf2-mediated ubiquitination of any of these or other yet unidentified protein substrates, in addition to senescence regulation, plays an important role in its function as a tumor suppressor.

Materials and Methods

Smurf2-deficient mice

Mouse ES cell line RRA098 was purchased from Mutant Mouse Regional Resource Center at University of California-Davis. ES cells were injected into C57BL/6 blastocysts to obtain chimeric mice, which were bred to generate Smurf2-deficient mice. Mouse cohorts on a mixed 129OlaxC57BL/6 background were monitored, and moribund mice were sacrificed for necropsy. Paraffin-embedded tissue sections were stained for Hematoxylin & Eosin and B220 (Abcam). Frozen sections were fixed, stained for senescence-associated β-galactosidase (SA-β-gal) activity [245] and counterstained with Eosin. Mouse studies were approved by the Institutional Animal Care and Use Committee of University of Massachusetts Medical School.

Assays of mouse embryonic fibroblast (MEFs)

MEFs were prepared from E12.5 embryos and cultured as described [286]. To analyze cell proliferation, MEFs were seeded in 6-well plates, harvested in triplicate and counted daily using a Particle Counter (Beckman Coulter). In senescence assay, MEFs were plated in 10-cm dish, and subcultured every 3 days before they reached high cell density. In 3T9 immortalization assay, MEFs were plated at $3x10^6$ per 10-cm dish in triplicate and passaged every 3 days.

MEFs were infected with lentivirus expressing Smurf2 or GFP as previously described [284], and stained with crystal violet or SA-β-gal activity [245] after selection with puromycin. To analyze DNA damage response, MEFs

were treated with 1 μM doxorubicin (Sigma), and cell lysates were collected for Western blotting.

Southern blotting

Genomic DNA was extracted using genomic DNA isolation kit (Lamda Biotech), digested with restriction enzymes (New England Biolabs), electrophoresed in agarose gel and transferred to Hybond nylon membrane (GE Healthcare). Probe labeling, hybridization and detection were carried out using DIG-high prime DNA labeling and detection starter kit (Roche).

Quantitative PCR

Total RNA was isolated using RNeasy Mini kit (Qiagen), and reverse-transcribed using Superscript II (Invitrogen). Real-time PCR was carried out using SYBR Green PCR kit (Bio-Rad) with the following primers: Smurf2 (5'-ATGAAGTCATTCCCCAGCAC-3'; 5'-AACCGTGCTCGTCTCTCTTC-3'), p16 (5'-CGAACTCTTTCGGTCGTACCC-3'; 5'-CGAATCTGCACCGTAGTTGAG-3') or β-actin (5'-GCTCTTTTCCAGCCTTCCTT-3'; 5'-GTGCTAGGAGCCAGAGCAGT-3').

Genomic DNA was used in real-time PCR to determine the relative abundance of the *Smurf2* alleles with the following primers: wild-type *Smurf2* (5'-GAGGGTGTTGGTGAGAGGAA-3'; 5'-TTACACAGCATCTGGCAAGG-3'), trapped *Smurf2* (5'-GAGGGTGTTGGTGAGAGGAA-3'; 5'-GACAAGTAGATCCCGGCGCTC-3') or *GAPDH* (5'-

AGCCTTAAAAGCCCTTGAGC-3'; 5'- CTAGGAAGAGGGGGAGAGGA-3').

Western blotting

Western blotting was carried out as described [246] with the following antibodies: Smurf2 (Epitomics), p53 (Calbiochem), α-tubulin (Sigma), p16, p19, p21 and GAPDH (Santa Cruz Biotechnology).

Statistical analyses

Kaplan-Meier survival curves were plotted and analyzed with the log-rank test. Student *t*-test (two-tailed and unpaired) was used for pair-wise comparisons.

CHAPTER III

Smurf2 mediates ubiquitination of YY1 to regulate c-Myc expression and suppresses B-cell lymphomagenesis in mice

ABSTRACT

We have shown previously that Mice deficient in Smurf2 exhibit increased susceptibility to spontaneous tumorigenesis with the majority of tumors being B-cell lymphomas in spleen. In this chapter, we characterized these lymphomas and determined that they were derived from germinal centers and had a phenotype resembling human diffuse large B-cell lymphoma (DLBCL). We found that these lymphomas were associated with enhanced proliferation and elevated expression of c-Myc in splenic B cells. We discovered that Smurf2 interacted with and mediated ubiquitination of YY1. Stabilization of YY1 in Smurf2-deficient cells up-regulated c-Myc expression and enhanced cell proliferation. The Smurf2-YY1-c-Myc regulatory axis represents a novel mechanism by which Smurf2 suppresses cell proliferation and lymphomagenesis. Furthermore, low level of Smurf2 expression is observed in primary human DLBCL samples and correlates with poor survival prognosis in DLBCL patients, suggesting that Smurf2 is a potential therapeutic target for DLBCL.

INTRODUCTION

We have shown in Chapter 2 that Smurf2 may function as a tumor suppressor *in vivo* by regulating the senescence response. The Smurf2-deficient mice develop tumors spontaneously, and 70% of these tumors are lymphomas. The lymphomas were B-cell derived and were diagnosed as Diffuse Large B-cell Lymphomas (DLBCL), which accounts for 30-40% of newly diagnosed lymphomas and is the most common type of Non-Hodgkin's Lymphoma [287]. Current chemotherapy regimens can cure only 40-50% of patients, and this has been attributed to the fact that DLBCL comprises of a heterogeneous group of cancers [288]. Gene expression profiling has divided DLBCL into 3 molecular subtypes that are histologically tantamount. These include, the Activated B-Cell Like (ABC), the Germinal Center B-Cell like (GCB) and the Primary Mediastinal B-Cell Lymphoma (PMBL) [289-292]. These subtypes differ in gene expression as well as the cell of origin, each of them arising from distinct molecular processes that ultimately lead to neoplastic transformation. Significant progress has been made in our understanding of the various dysregulated pathways and genetic anomalies that govern the development of these lymphomas [293,294], however a sizable fraction of DLBCL are still incurable, suggesting that further understanding in the pathogenesis of this disease is needed in order to develop more specific therapeutic approaches.

A lot of interest in the DLBCL field has focused on the ABC-type of lymphoma and much is known about the molecular pathways deregulated in this sub-type of DLBCL [295-299]. Less is known about the lesions governing the GCB-type DLBCL, and most of the research in this field has focused on the

dysregulated expression of BCL6 and its target genes in these tumors [300-303]. In this chapter we show that the lymphomas in the Smurf2-deficient mice are GCB-type DLBCL, thus providing novel insight into the pathogenesis of these tumors. Further, we have determined that c-Myc is upregulated in the lymphomas as well as normal spleens from the Smurf2-deficient mice. We also show that Smurf2 acts as an E3 ligase for YY1, targeting it for proteasome-mediated degradation. YY1 is a transcription factor that has been previously shown to regulate c-Myc [304,305]. We demonstrate that YY1's regulation of c-Myc is dependent on Smurf2 expression in a lymphoma cell line in culture. We propose that the Smurf2-mediated ubiquitination of YY1 and its regulation of c-Myc is a potential mechanism by which the Smurf2-deficient mice develop GCB-type DLBCL.

RESULTS

Germinal center (GC)-derived lymphomas in Smurf2-deficient mice

Previously we have shown that Smurf2-deficient mice exhibit increased susceptibility to spontaneous tumorigenesis, with the majority of tumors found in spleen. Hematoxylin & Eosin (H&E) staining, B220 staining and histopathological analysis of spleen sections of affected *Smurf2*$^{T/T}$ or *Smurf2*$^{+/T}$ mice indicate that these mice developed lymphomas with a B-cell origin and a phenotype consistent with DLBCL and/or Burkitt's lymphoma [306] (Chapter 2). Further analyses found that these lymphomas stained positively for the GC marker peanut agglutinin (PNA) (Fig.3.1a), suggesting that these lymphomas were likely GC-derived. Consistent with this notion, we observed an expansion of IgD^{neg}IgM^{lo} B cells that were CD23 negative and stained strongly for CD24 in representative lymphomas (Fig.3.1b). Furthermore, these lymphomas underwent class switch recombination to IgG2a (Fig.3.2) and exhibited increased somatic hypermutation in the immunoglobulin heavy chain (*IgH*) locus (Table 3.2). Collectively, these data indicate that lymphomas developed in Smurf2-deficient mice are GC-derived.

When splenic cells from tumor-bearing mice were injected into Recombination Activating Gene 1 knockout (Rag1$^{-/-}$) mice, Rag1$^{-/-}$ recipient mice became moribund 6 weeks after injection. A further expansion of the IgD^{neg}IgM^{lo} B cells was observed in the spleens of Rag1$^{-/-}$ recipients (Fig.3.3). Furthermore, these IgD^{neg}IgM^{lo} B cells stained positively for CD24 and CD95, consistent with a germinal center-derived phenotype (Fig.3.3). Positive staining for IgG2a further confirmed that these tumors underwent class switch recombination (Fig.3.3).

Fig.3.1: **Smurf2-deficient mice develop GCB-type lymphomas.**

(a) Representative H&E and PNA staining of sections of lymphomas in spleen of Smurf2$^{T/T}$ mice. Staining of tissue sections of wild-type mice is shown for comparison. Scale bar for 10x images is 200 µm, and scale bar for 50x images is 100 µm. (b) FACS analyses of splenic B cells from two matched pairs of lymphoma-bearing *Smurf2*$^{T/T}$ (T/T) and age-matched wild-type mice are presented. Live cells are displayed (propidium iodide excluding). CD19 positive cells (left panel) are gated and then displayed in the middle panel. IgM^{lo}IgD^{lo} cells are gated and displayed in the right panel. CD23^{-}CD24^{+} cells, indicated by a gate in the right panel, are activated or previously activated B cells.

Fig.3.1

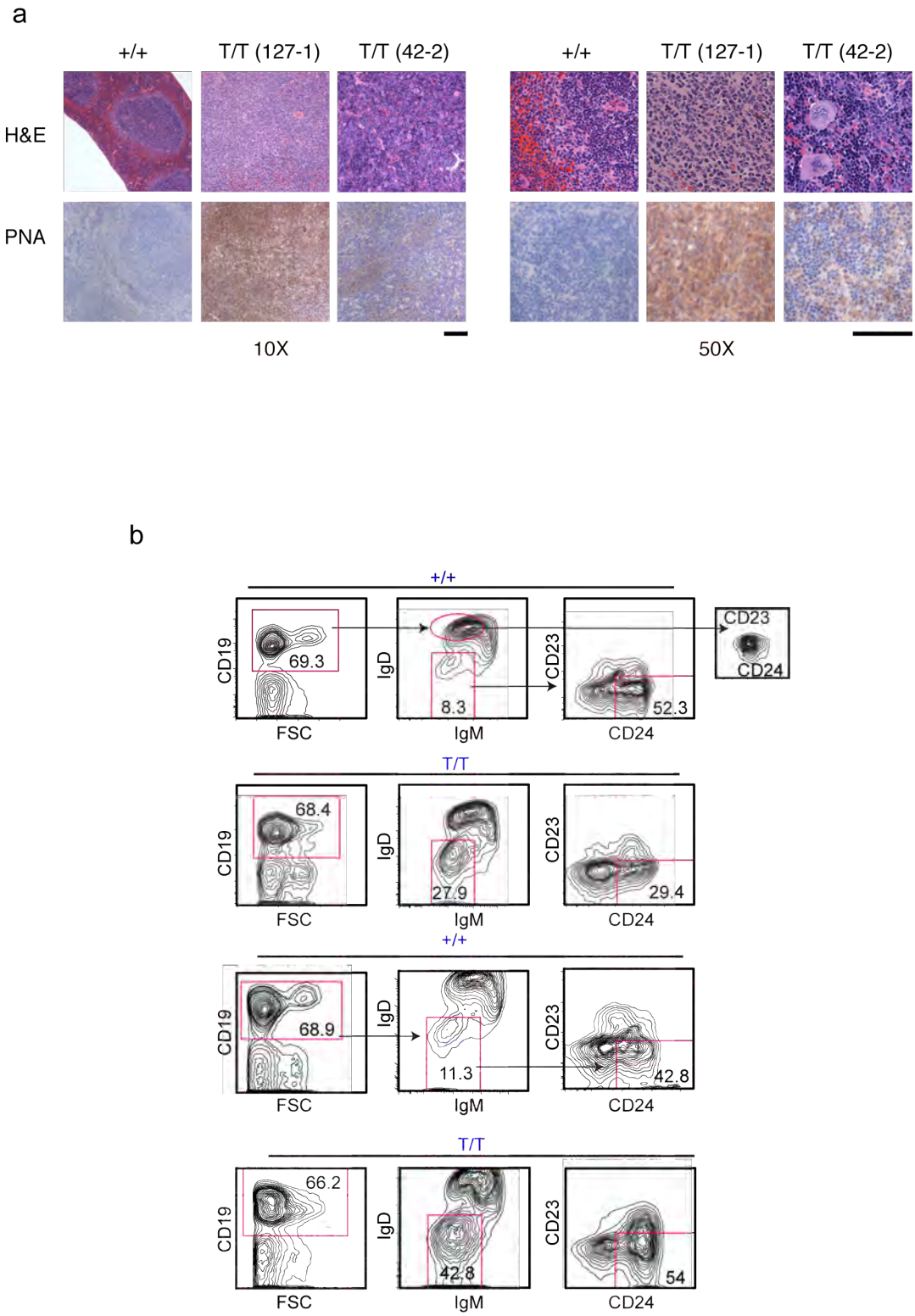
a
+/+
T/T (127-1)
T/T (42-2)
+/+
T/T (127-1)
T/T (42-2)
H&E
PNA
10X
50X
b
+/+
CD19
69.3
FSC
IgD
8.3
IgM
CD23
52.3
CD24
CD23
CD24
T/T
68.4
27.9
29.4
+/+
68.9
11.3
42.8
T/T
66.2
42.8
54

Fig.3.2: Smurf2-deficient lymphomas exhibit features of GCB-type lymphomas. Analysis of class switch recombination in representative lymphomas. Postswitch transcripts (γ1, γ2a, γ2b and γ3) and germline transcripts (μ) of mouse immunoglobulin heavy chain locus were analyzed by quantitative RT-PCR. Splenic cells from wild-type and AID knockout mice were used as controls. Relative expression in wild-type splenic cells was set to be 1 after normalization with β-actin. Error bars were calculated from standard deviations of three independent experiments.

Fig.3.2

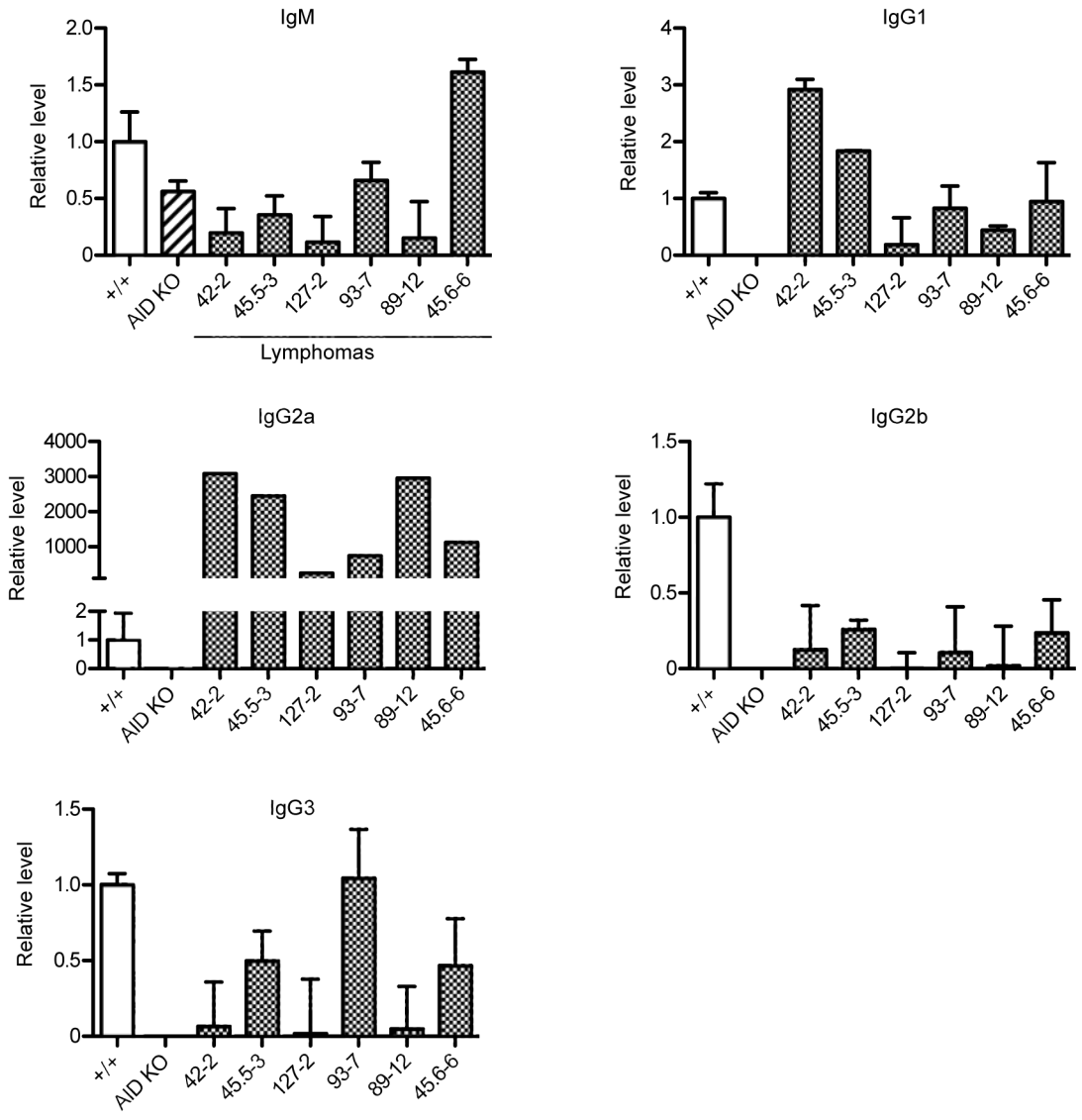
IgM
Relative level
2.0
1.5
1.0
0.5
0
+/+
AID KO
42-2
45.5-3
127-2
93-7
89-12
45.6-6
Lymphomas
IgG1
Relative level
4
3
2
1
0
IgG2a
Relative level
4000
3000
2000
1000
2
1
0
IgG2b
Relative level
1.5
1.0
0.5
0
IgG3
Relative level
1.5
1.0
0.5
0

Table 3.2: Somatic mutations in the rearranged V_H186.2 transcripts of μ isotype in lymphomas derived from spleens of Smurf2-deficent mice[a]

	# chains		Mutations per 10^3 bases[b]										
	Seq	Mut	Total (306 bp)				CDR1+2 (66 bp)				Framework (228 bp)		
			Total	R[c]	S[c]	R/S[c]	Total	R	S	R/S	Total	R	S	R/S
WT Sp[d]	10	8	33.0	23.9	9.1	2.6	62.1	57.6	4.5	12.8	25.9	15.4	10.5	1.5
42-2	6	6	61.5	48.5	13.0	3.7	108.6	103.5	5.1	20.3	50.4	34.4	16.0	2.2
45.6-6[e]	6	6	78.4	56.6	21.8	2.6	184.3	159.1	25.2	6.3	49.7	28.5	21.2	1.3
127-2	3	3	63.2	38.1	25.1	1.5	146.5	111.1	35.4	3.1	39.5	16.1	23.4	0.7
93-7	3	3	73.0	50.1	22.9	2.2	181.8	156.6	25.2	6.2	42.4	19.0	23.4	0.8

[a] The region that was used to determine mutation frequency corresponds to amino acid residues -4 to 98 in V_H186.2 μ transcripts. Nucleotide replacements at the V_HD_H junctions were not scored as mutations.

[b] Mutation frequency was calculated by dividing the accumulated number of mutations in a given region with the total number of nucleotides sequenced for the region, length of which is shown in parentheses.

[c] R and S stand for replacement and silent mutations, respectively. R/S indicates ratio of replacement to silent mutations.

[d] Spleen from wild-type mouse.

[e] A deletion of 128 bp, in addition to point mutations, was found in a clone derived from tumor 45.6-6. This clone was not used in calculation of mutations listed in the table.

Fig.3.3: Tumors from Smurf2-deficient mice can be transplanted into RAG1$^{-/-}$ recipient mice. FACS analyses of splenic B cells from a lymphoma-bearing *Smurf2*$^{T/T}$ (T/T) and a RAG1$^{-/-}$ recipient mouse injected with T/T spleen cells are presented. A wild-type (+/+) panel is provided as a control. Live cells are displayed (propidium iodide excluding). Clonal expansion of the IgM^{lo}IgD^{lo} cells that have been gated out of CD19^{+} cells are displayed in the left panel. These IgM^{lo}IgD^{lo} cells stained positive for CD24 and CD95, both GC markers, as shown in the middle panel. These IgM^{lo}IgD^{lo} cells also stained positive for IgG2a as shown in the right panel. Mice used in this experiment were between 15 and 18 months of age.

Fig.3.3

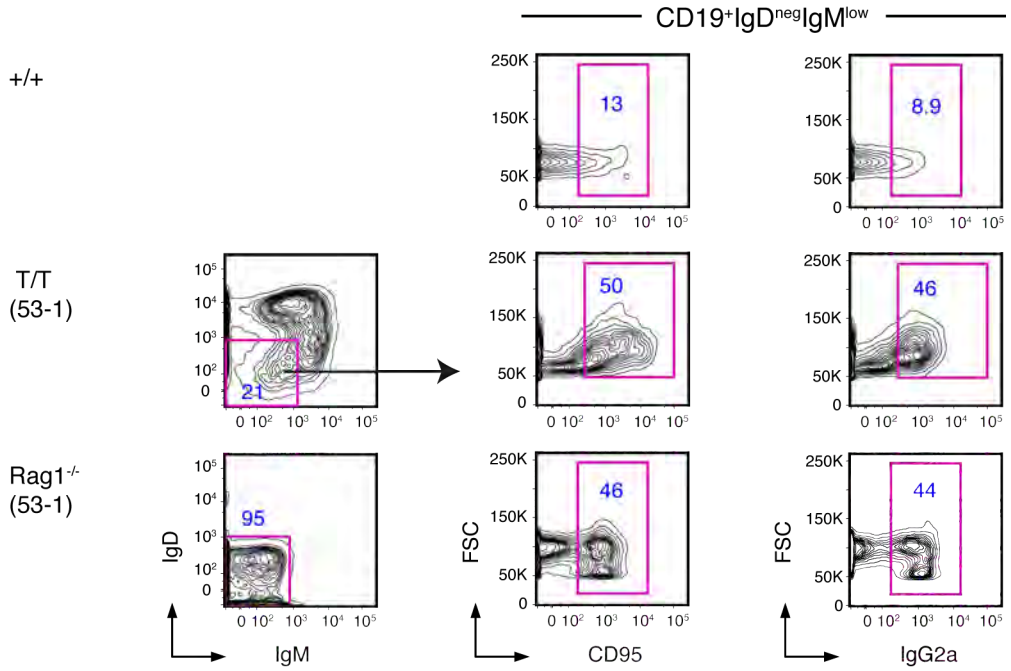
CD19+IgDnegIgMlow
+/+
T/T
(53-1)
Rag1-/-
(53-1)
13
8.9
21
50
46
95
46
44
IgD
IgM
FSC
CD95
FSC
IgG2a

Enhanced proliferation in Smurf2-deficient splenic B cells

All tumor-bearing *Smurf2*$^{T/T}$ mice had enlarged spleens (Fig.2.7), prompting us to examine the spleen in pre-malignant mice. A small but statistically significant increase in spleen weight over body weight was found in the healthy 2-month old *Smurf2*$^{T/T}$ mice compared to wild-type littermates (Fig.3.4a). The frequency of splenic B220+ cells was found to be similar between young *Smurf2*$^{T/T}$ and wild-type littermates (Fig.3.4b). Furthermore, flow cytometric analyses detected no obvious difference in the frequencies of various splenic B-cell sub-populations between these mice (Fig.3.4c), suggesting that B-cell differentiation is normal in Smurf2-deficient mice.

Lymphomas found in *Smurf2*$^{T/T}$ or *Smurf2*$^{+/T}$ mice showed an increase in staining of the cell proliferation-associated antigen Ki-67, but no significant change in TUNEL staining for apoptosis, as compared to spleen sections of age-matched wild-type mice (Fig.3.5a). Interestingly, Ki-67 staining was increased in splenic white pulps of young healthy *Smurf2*$^{T/T}$ mice as compared to wild-type littermates, whereas no significant change in TUNEL staining was observed (Fig.3.5b & c). Furthermore, increased bromodeoxyuridine (BrdU) incorporation was detected in non-cancerous B220^{+} splenic B cells or total splenic cells (Fig.3.5d) of young healthy *Smurf2*$^{T/T}$ mice as compared to wild-type littermates. These results suggest that increased cell proliferation observed in Smurf2-deficient B cell lymphomas or splenic B cells is caused by reduced Smurf2 expression rather than as a consequence of tumorigenesis.

Fig.3.4: Smurf2-deficient mice exhibit normal B-cell development and differentiation (a). Relative gross weight of spleen to body weight (N=12) shows an increase in spleen weights in *Smurf2*$^{T/T}$ (T/T) mice compared with wild-type (+/+). (b).Percent of B220+ cells in spleen (N=3) of 2-month-old wild-type (+/+) and *Smurf2*$^{T/T}$ (T/T) mice are shown. (c). FACS analysis of splenic B cells from 2-month-old wild-type (+/+) and *Smurf2*$^{T/T}$ (T/T) mice indicates that the major splenic B cell populations are present at comparable frequencies. Live cells are displayed (propidium iodide excluding). CD19 positive cells (left panel) are gated, then displayed in the middle panel. The IgD^{++}IgM^{int} population, indicated by a circular gate in the middle panel, are follicular B cells. IgM^{++}IgD^{lo} cells are gated and displayed in the right panel CD93+CD24+ cells, indicated by a circular gate in the right panel, are immature B cells.

Fig.3.4

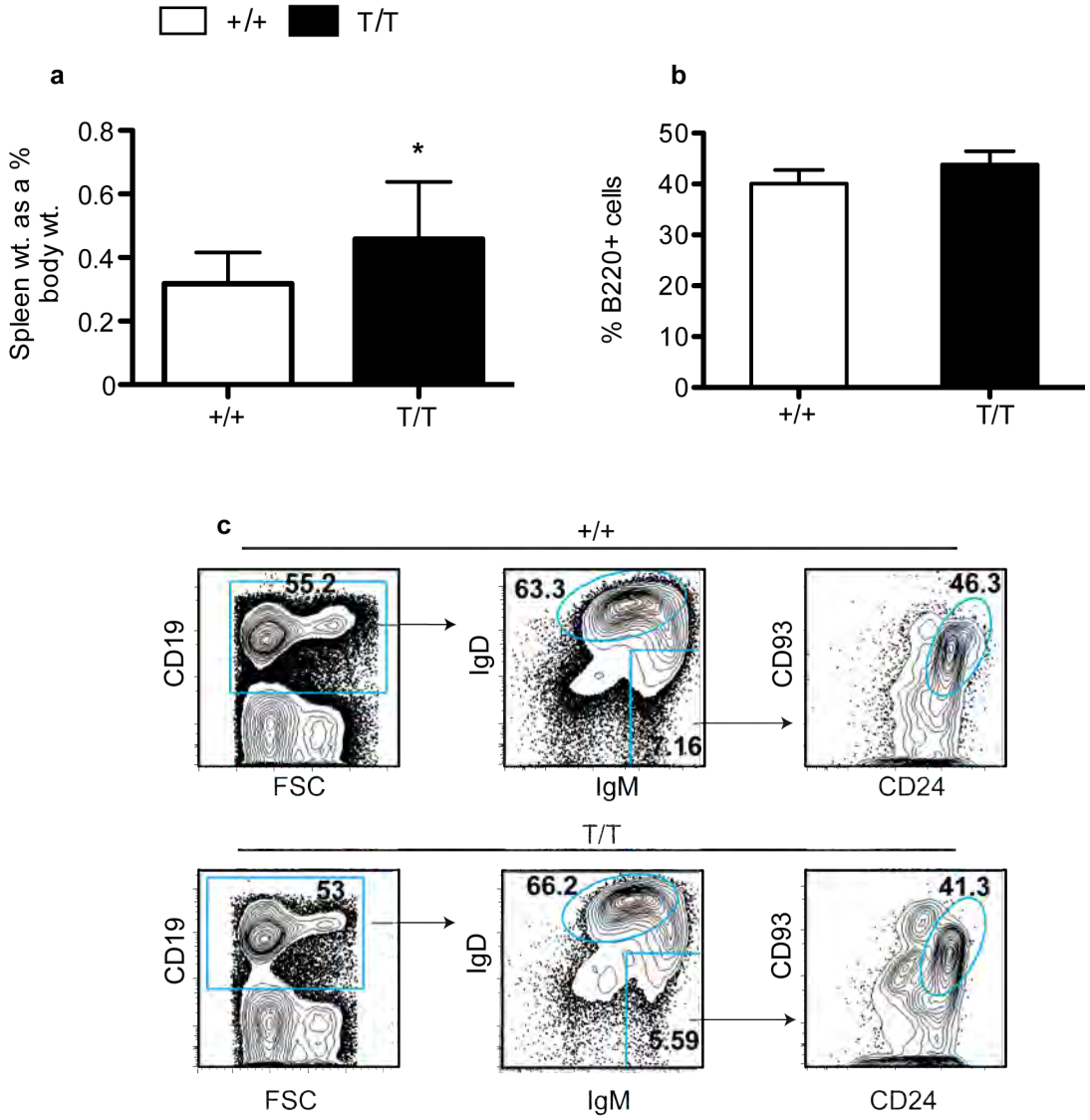
+/+
T/T
a
Spleen wt. as a % body wt.
0.8
0.6
0.4
0.2
0
*
+/+
T/T
b
% B220+ cells
50
40
30
20
10
0
+/+
T/T
c
+/+
CD19
55.2
FSC
IgD
63.3
7.16
IgM
CD93
46.3
CD24
T/T
CD19
53
FSC
IgD
66.2
5.59
IgM
CD93
41.3
CD24

Fig.3.5: Enhanced proliferation in splenic B cells of Smurf2-deficient mice

(a). Representative Ki-67 and TUNEL staining of lymphomas derived from *Smurf2*$^{T/T}$ (T/T) mice. Staining of spleen sections of aged wild-type (+/+) mice and an irradiated (10-Gy) mouse was shown for comparison. (b). Representative Ki-67 and TUNEL staining of spleen sections of 2-month old wild-type and *Smurf2*$^{T/T}$ mice. (c) Quantitation of Ki-67 positive cells in spleen sections of 2-month old wild-type and *Smurf2*$^{T/T}$ mice (average of 10 randomly selected fields). Student *t*-test was used for statistical analysis. (d). Analysis of BrdU incorporation in B220+ splenic cells of 2-month old wild-type and *Smurf2*$^{T/T}$ mice (N=3).

Fig.3.5

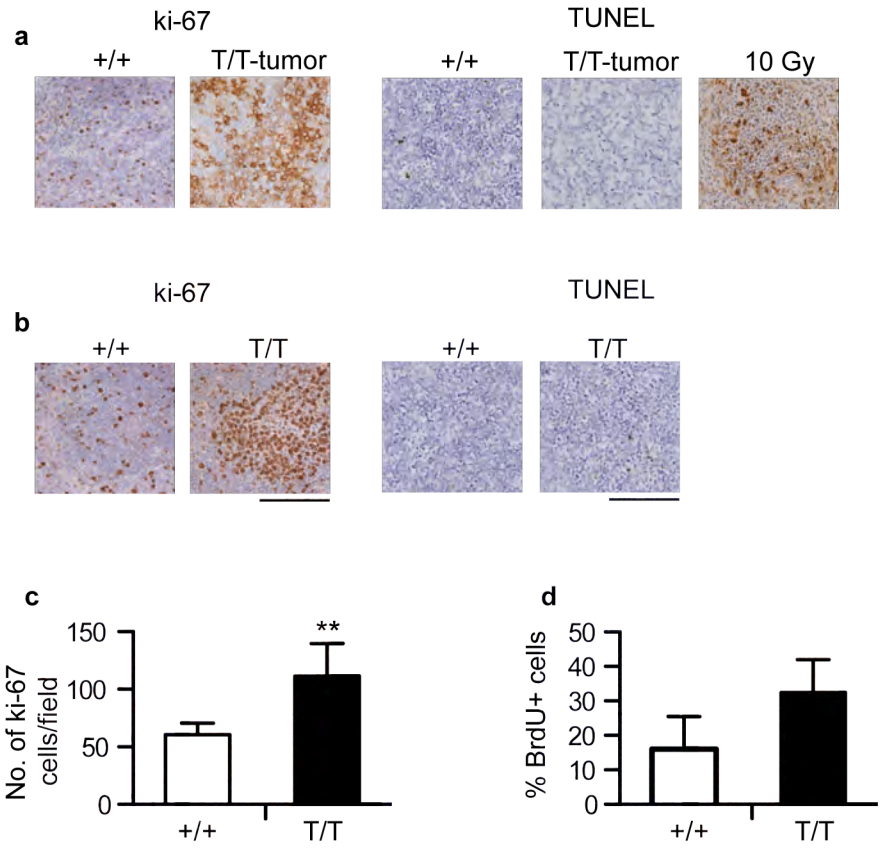
a
ki-67
+/+
T/T-tumor
TUNEL
+/+
T/T-tumor
10 Gy
b
ki-67
+/+
T/T
TUNEL
+/+
T/T
c
No. of ki-67 cells/field
150
100
50
0
**
+/+
T/T
d
% BrdU+ cells
50
40
30
20
10
0
+/+
T/T

To further analyze cell proliferation in splenic B cells, we cultured splenic cells of 2-month old wild-type or *Smurf2*$^{T/T}$ mice with the B-cell mitogen lipopolysaccharide (LPS). In response to LPS, *Smurf2*$^{T/T}$ splenic B cells (B220^{+}) proliferated significantly better than wild-type cells (Fig.3.5e), whereas cell viability was similar between them (Fig.3.5f). Using carboxyfluorescein succinimidyl ester (CFSE) to track cell divisions in cultured splenic B cells, we found that the number of *Smurf2*$^{T/T}$ splenic B cells (B220^{+}) undergoing successive cell divisions was significantly increased as compared to wild-type cells (Fig.3.5g). Cell death was similar between wild-type and *Smurf2*$^{T/T}$ B cells without LPS stimulation (Fig.3.5f), consistent with our observation that apoptosis was unchanged in Smurf2-deficient cells. Collectively, these results indicate that cell proliferation is enhanced in *Smurf2*$^{T/T}$ splenic B cells, suggesting a possible mechanism for increased B-cell lymphomagenesis in Smurf2-deficient mice.

Fig.3.5 (contd): Enhanced proliferation in splenic B cells of Smurf2-deficient mice: (e). Splenic cells from 2-month old wild-type and *Smurf2*$^{T/T}$ mice were cultured with or without LPS. The number of B220+ viable cells (propidium iodide negative) was determined by flow cytometry. Average of 3 independent experiments was shown. Student *t*-test was used for pair-wise comparison.

(f). Viability of splenic B (B220+) cells with or without 5 μM lipopolysaccharide (LPS) treatment. Cell viability was determined as percent of propidium iodide negative B220+ cells in flow cytometry. (g). The number of B220+ cells undergoing different number of cell division was determined by carboxyfluorescein succinimidyl ester (CFSE) staining and flow cytometry. The ratio of the number of B220+ *Smurf2*$^{T/T}$ cells undergoing different cell divisions over that of wild-type cells in one representative experiment is presented. Error bars in (e,f) were calculated from standard deviations of at least three independent experiments. Statistic significance is indicated as: * (P<0.05), ** (P<0.01), and *** (P<0.001).

Fig.3.5

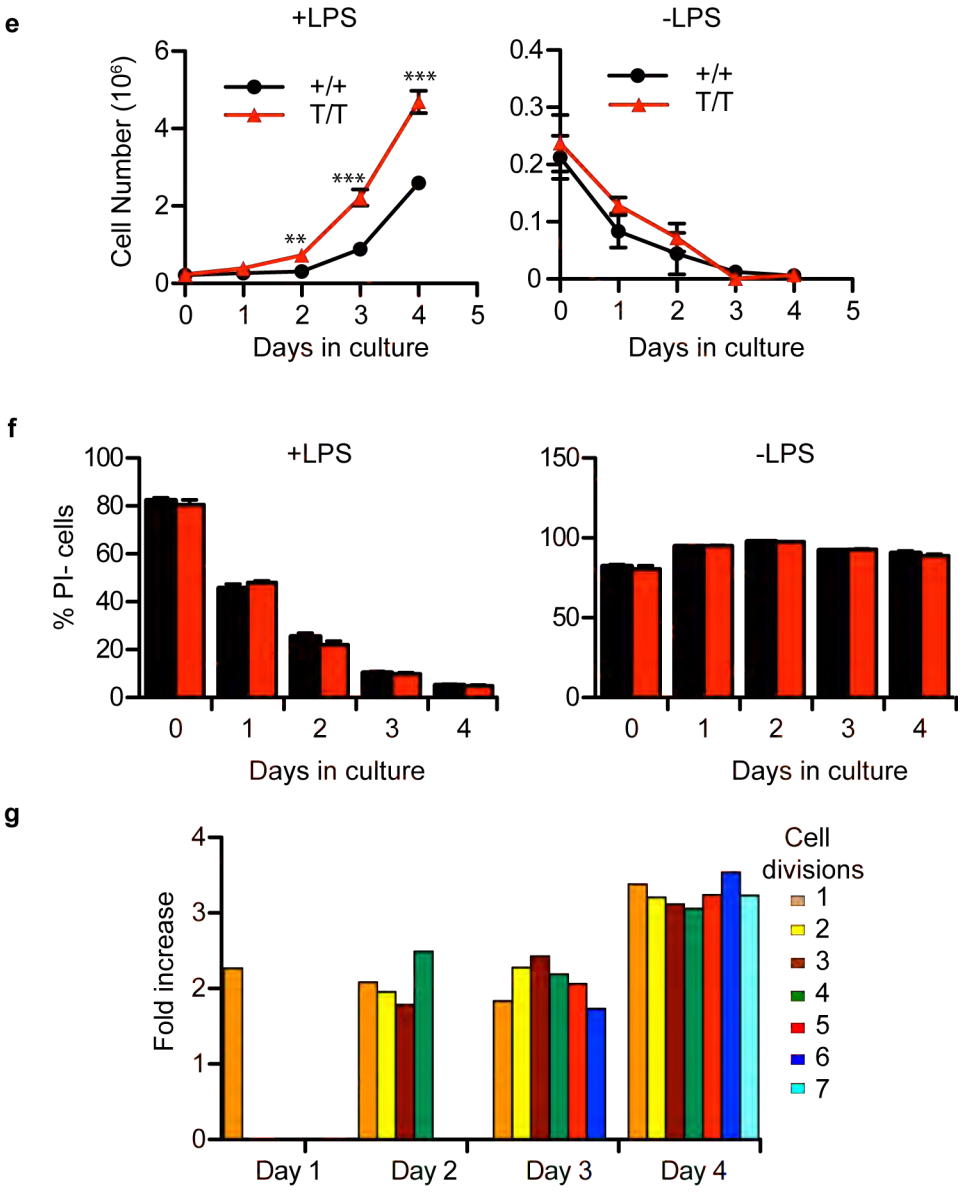
e
+LPS
-LPS
Cell Number (10^6)
+/+
T/T
**
***
***
Days in culture
Days in culture
f
+LPS
-LPS
% PI- cells
Days in culture
Days in culture
g
Fold increase
Cell divisions
1
2
3
4
5
6
7
Day 1
Day 2
Day 3
Day 4

Elevated c-Myc expression in Smurf2-deficient mice

Up-regulation of c-Myc is frequently observed in B-cell lymphoma, and forced expression of c-Myc drives lymphomagenesis in mice [307-310]. To understand the underlying mechanism of increased B-cell proliferation and lymphomagenesis we examined c-Myc expression in Smurf2-deficient mice. The expression of c-Myc in lymphomas of Smurf2-deficient mice was increased as compared to spleen of aged wild-type mice (Fig.3.6a). Moreover, we found an increase in c-Myc expression in spleen (Fig.3.6b) and liver (Fig.3.6c) of 2-month old healthy *Smurf2*$^{T/T}$ mice as compared to age-matched wild-type mice, suggesting that Smurf2 deficiency correlates with increased c-Myc expression.

To further corroborate c-Myc elevation with Smurf2 deficiency, we examined the transcript levels of c-Myc transactivation targets Apex1, Cad and Ncl, which have been validated as c-Myc targets in multiple studies, but are not directly involved in cell proliferation [311]. We found increased transcript levels of these c-Myc targets in lymphomas as well as spleen (Fig.3.6d and e) and liver of young *Smurf2*$^{T/T}$ mice (Fig.3.6f**).**

Fig.3.6: Elevated c-Myc expression in Smurf2-deficient mice.

(a). Quantitative RT-PCR analysis of c-Myc expression in lymphomas from *Smurf2*$^{T/T}$ (T/T) or *Smurf2*$^{+/T}$ (+/T) mice as compared to spleen of aged wild-type (+/+) mice. (b). Quantitative RT-PCR and Western analyses of c-Myc expression in spleen (b) and livers (c) of 2-month old wild-type and *Smurf2*$^{T/T}$ mice.

Fig.3.6

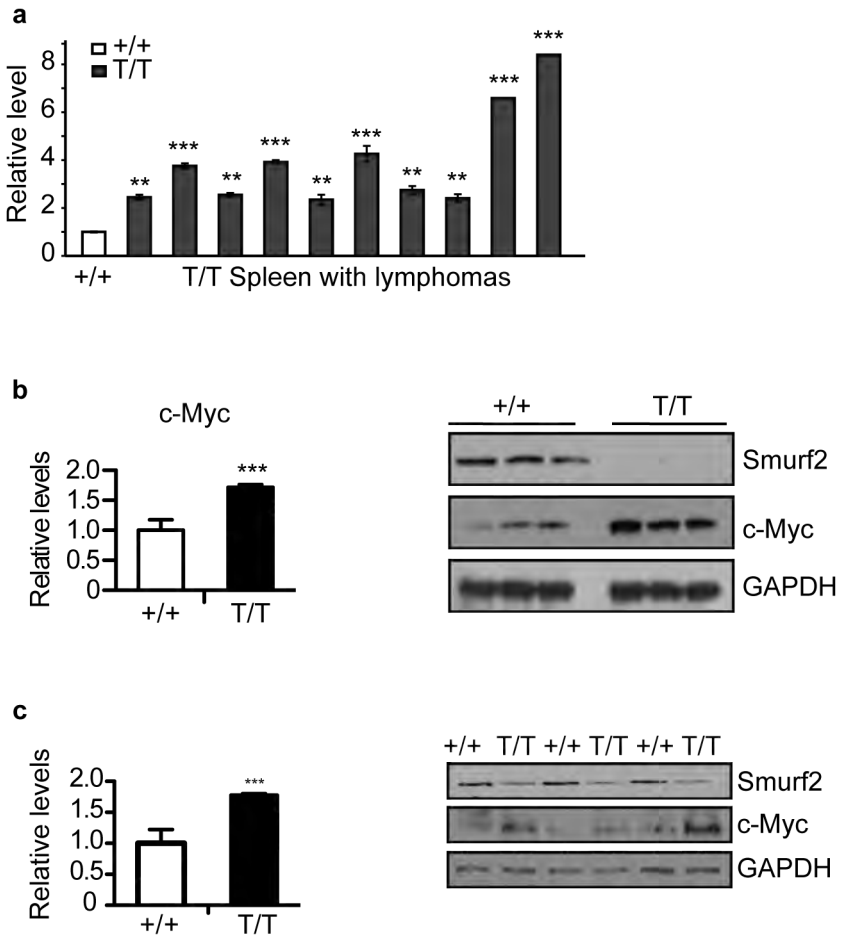
a
+/+
T/T
Relative level
0
2
4
6
8
**
***
**
***
**
***
**
**
***
***
+/+
T/T Spleen with lymphomas
b
c-Myc
Relative levels
2.0
1.5
1.0
0.5
0
***
+/+
T/T
+/+
T/T
Smurf2
c-Myc
GAPDH
c
Relative levels
2.0
1.5
1.0
0.5
0
***
+/+
T/T
+/+ T/T +/+ T/T +/+ T/T
Smurf2
c-Myc
GAPDH

Fig.3.6 (contd): Elevated c-Myc expression in Smurf2-deficient mice.

(d) Quantitative RT-PCR analysis of c-Myc target genes in lymphomas from *Smurf2*$^{T/T}$ mice as compared to spleen of aged wild-type (+/+) mice, and (e) Spleen and (f) Liver of 2-month old wild-type (+/+) and *Smurf2*$^{T/T}$ (T/T) mice. In quantitative RT-PCR analyses, the relative expression in wild-type mice was set to be 1 after normalization with β-actin.

Fig.3.6

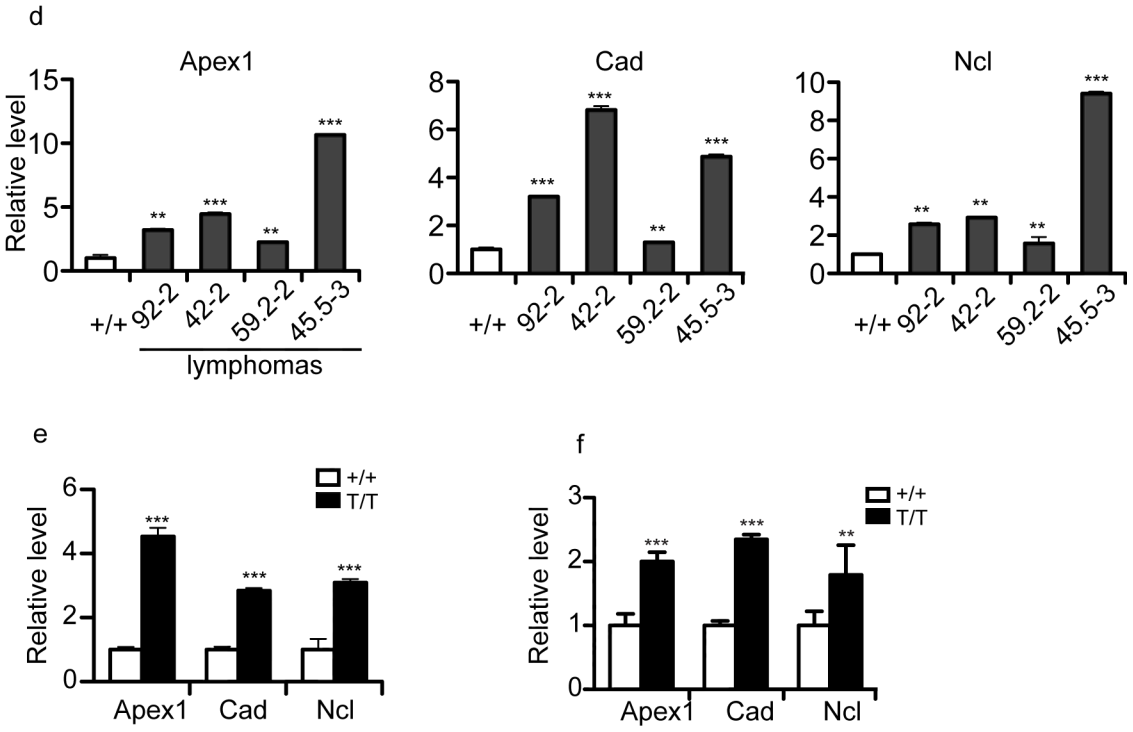
d
Apex1
Cad
Ncl
Relative level
+/+
92-2
42-2
59.2-2
45.5-3
lymphomas
e
f
+/+
T/T
Apex1
Cad
Ncl

Smurf2 mediates ubiquitination of YY1 to regulate c-Myc expression

To investigate the underlying mechanism of Smurf2-mediated regulation of c-Myc expression, we searched for transcriptional regulators that have been shown to transactivate c-Myc and examined their potential as the ubiquitination targets of Smurf2. We reasoned that stabilization of such a transcriptional regulator in Smurf2-deficient mice could be responsible for elevated expression of c-Myc. YY1, which has been previously shown to transactivate c-Myc [304,312], contains a PPDY motif that can potentially interact with WW domains in Smurf2. We found that the protein levels of YY1 were increased in lymphomas derived from Smurf2-deficient mice (Fig.3.7a) as well as in spleens (Fig.3.7b) of young *Smurf2*$^{T/T}$ mice compared to wild-type littermates. In contrast, the transcript level of YY1 was largely unchanged in Smurf2-deficient mice (Fig.3.7b), suggesting a post-transcriptional regulation of YY1 by Smurf2.

To further characterize Smurf2-mediated regulation of YY1, we stably expressed short-hairpin RNA (shRNA) specifically targeting Smurf2 in a human DLBCL cell line SUDHL-6, and found that down-regulation of Smurf2 led to an increase in YY1 protein (Fig.3.8a). Conversely, ectopic expression of Smurf2 resulted in a reduction in the steady-state level of YY1 protein (Fig.3.8b). Consistent with the notion that Smurf2 regulates YY1 at the protein level, YY1 transcripts were largely unchanged when Smurf2 expression was altered (Fig.3.8a and b). These results led us to hypothesize that Smurf2 is the E3 ubiquitin ligase responsible for ubiquitination of YY1.

Fig.3.7: Smurf2-deficient mice exhibit increased YY1 protein

(a). Western analysis of YY1 expression in lymphomas from *Smurf2*$^{T/T}$ (T/T) or *Smurf2*$^{+/T}$ (+/T) mice as compared to spleen of aged wild-type (+/+) mice.

(b). Western and quantitative RT-PCR analyses of YY1 expression in spleen of 2-month old wild-type and *Smurf2*$^{T/T}$ mice.

Fig.3.7

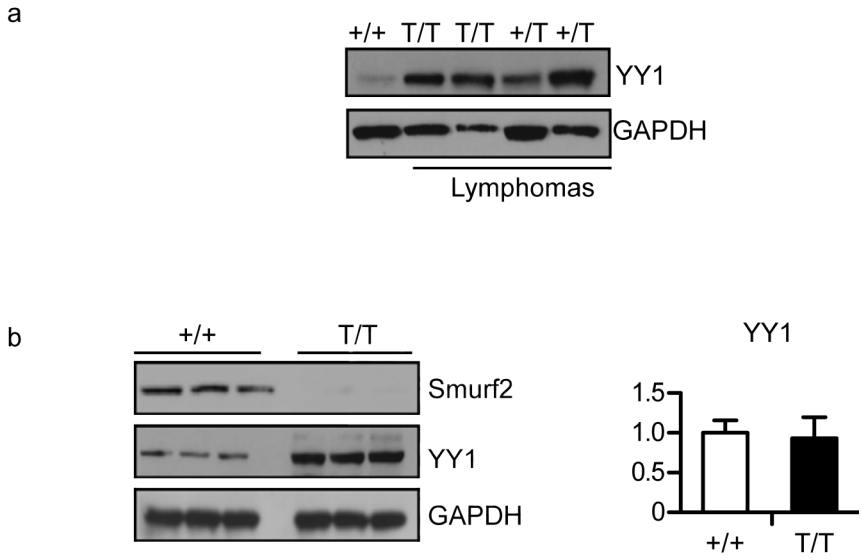
a
+/+ T/T T/T +/T +/T
YY1
GAPDH
Lymphomas
b
+/+
T/T
Smurf2
YY1
GAPDH
YY1
1.5
1.0
0.5
0
+/+
T/T

Fig.3.8: Smurf2 mediates ubiquitination of YY1 to regulate c-Myc expression. (a). Smurf2 expression was knocked down by shRNA or (b) Smurf2 was ectopically expressed in human DLBCL cells SUDHL-6. The expression of YY1 or c-Myc was analyzed in Western and quantitative RT-PCR.

Fig.3.8

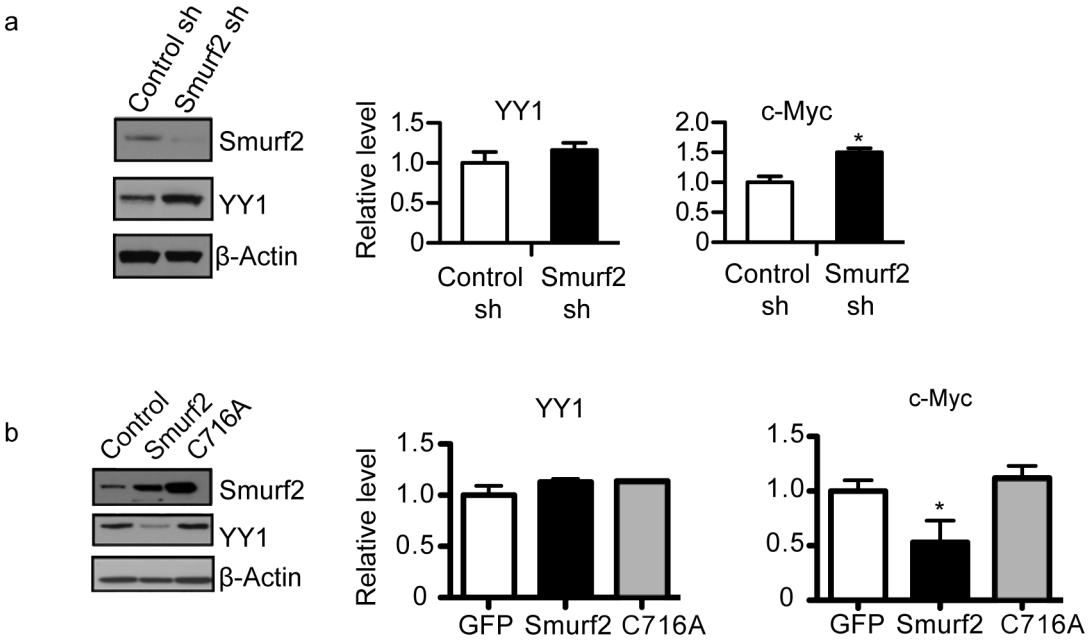
a
Control sh
Smurf2 sh
Smurf2
YY1
β-Actin
YY1
Relative level
1.5
1.0
0.5
0
Control sh
Smurf2 sh
c-Myc
2.0
1.5
1.0
0.5
0
*
Control sh
Smurf2 sh
b
Control
Smurf2
C716A
Smurf2
YY1
β-Actin
YY1
Relative level
1.5
1.0
0.5
0
GFP
Smurf2
C716A
c-Myc
1.5
1.0
0.5
0
*
GFP
Smurf2
C716A

To test this hypothesis, we first investigated whether Smurf2 interacts with YY1, as the C2-WW-HECT class of E3 ligases interacts with their protein substrates to catalyze ubiquitination. To limit potential degradation of YY1 by Smurf2, we used a ligase mutant C716A, in which the conserved cysteine at residue 716 is replaced by alanine to abolish its E3 ligase activity [259,258,257], in co-immunoprecipitation with YY1. Smurf2 and YY1 were found to form a complex in co-immunoprecipitation, whereas deletion of PPDY (ΔPY) completely abolished the Smurf2-YY1 interaction (Fig.3.8c). Furthermore, we found that three WW domains (i.e. WWs), but not C2 or HECT domain of Smurf2, were sufficient to interact with YY1. Deletion of the N-terminal WW domain (ΔWW1) abolished the interaction between Smurf2 and YY1 (Fig.3.8c). Collectively, these results indicate that the Smurf2-YY1 interaction is mediated by the WW domains and the PPDY motif. We next investigated whether Smurf2 induces ubiquitination of YY1. Ubiquitination of YY1, as indicated by a smear of bands, was greatly induced in cells expressing Smurf2 compared to GFP control, whereas catalytically inactive C716A lost the ability to ubiquitinate YY1 (Fig.3.8d). Collectively, these results indicate that Smurf2 is the E3 ubiquitin ligase responsible for ubiquitination of YY1.

YY1 has been previously shown to bind to human c-Myc promoter in chromatin immunoprecipitation assay and up-regulate c-Myc expression [304,312]. We expressed shRNA to specifically knockdown YY1 expression in SUDHL-6 cells, and found that c-Myc transcripts were decreased upon YY1 down-regulation (Fig.3.8e), suggesting that YY1 is required to regulate c-Myc

expression. Furthermore, chromatin immunoprecipitation analysis indicated that YY1 was bound to the c-Myc promoter in mouse spleen, and this binding was increased in spleen of *Smurf2*$^{T/T}$ mice compared to wild-type mice (Fig.3.8f). Collectively, these results suggest that stabilization of YY1 in Smurf2-deficient mice is responsible for the up-regulation of c-Myc.

Fig.3.8 (contd): Smurf2 mediates ubiquitination of YY1 to regulate c-Myc expression. (c). Smurf2 interacts with YY1. 293T cells were transfected with indicated constructs of HA-YY1 and Flag-Smurf2. Immunoprecipitation (IP) with anti-Flag antibody was followed by immunoblotting (IB) with anti-HA antibody. (d). Smurf2 ubiquitinates YY1. 293T cells were transfected with HA-YY1, 3xFlag-Ub and Smurf2. IP with anti-HA antibody was followed by IB with anti-Flag antibody to detect poly-ubiquitinated YY1. (e). Knockdown of YY1 by shRNA leads to down-regulation of c-Myc in SUDHL-6 cells as determined by quantitative RT-PCR. (f). Chromatin immunoprecipitation (ChIP) assay of YY1 binding on c-Myc promoter in spleen of 2-month old wild-type and *Smurf2*$^{T/T}$ mice. Fold enrichment of ChIP with anti-YY1 antibody over IgG control is shown. In quantitative RT-PCR analyses, the relative expression level in controls was set to be 1 after normalization with β-actin. Error bars were calculated from standard deviations of three independent experiments. Student *t*-test was used to calculate statistic significance (*: $P<0.05$, **: $P<0.01$ and ***: $P<0.001$).

Fig.3.8

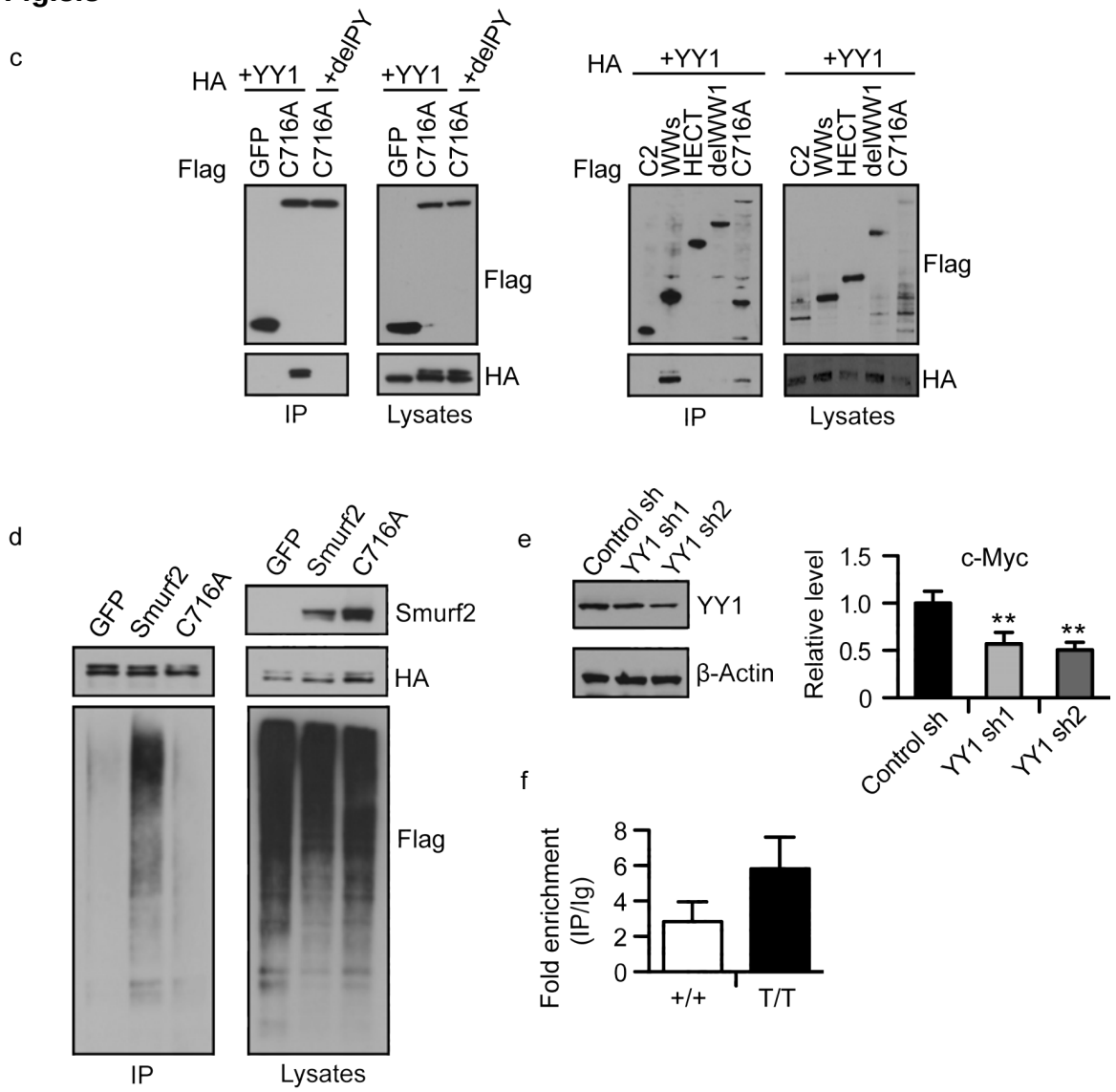
c
HA
+YY1
+delPY
GFP
C716A
C716A
Flag
Flag
HA
IP
Lysates
C2
WWs
HECT
delWW1
C716A
d
GFP
Smurf2
C716A
Smurf2
HA
Flag
IP
Lysates
e
Control sh
YY1 sh1
YY1 sh2
YY1
β-Actin
c-Myc
Relative level
1.5
1.0
0.5
0
**
f
Fold enrichment
(IP/Ig)
8
6
4
2
0
+/+
T/T

Smurf2-mediated regulation of YY1 alters cell proliferation in a lymphoma cell line

To understand the consequence of Smurf2-mediated ubiquitination of YY1 in lymphomagenesis, we investigated the Smurf2-YY1 axis in regulation of cell proliferation in human DLBCL cells. Consistent with our observation of increased cell proliferation in Smurf2-deficent mice, shRNA knockdown of Smurf2 expression in SUDHL-6 cells led to enhanced cell proliferation (Fig.3.9a). Down-regulation of YY1 by shRNA resulted in decreased proliferation in SUDHL-6 cells, suggesting that YY1 is a critical regulator of cell proliferation in DLBCL (Fig.3.9a). Furthermore, down-regulation of YY1 in SUDHL-6 cells that already had shRNA knockdown of Smurf alleviated the increase in cell proliferation mediated by Smurf2 deficiency (Fig.3.9a), suggesting that Smurf2 regulates cell proliferation through YY1. Conversely, when ectopically expressed in SUDHL-6 cells, we found that wild-type Smurf2, but not the ligase mutant C716A, led to significantly decreased cell proliferation (Fig.3.9b). Taken together, these results indicate the Smurf2-YY1 regulatory axis is critical in proliferation of lymphoma cells, and suggest a plausible mechanism underlying increased cell proliferation and lymphomagenesis in Smurf2-deficient mice.

Fig.3.9: Manipulation of Smurf2 expression alters cell proliferation in a YY1 dependent manner. (a). Knockdown of Smurf2 (green bar) and YY1 (blue bar) and double-knockdown of both Smurf2 and YY1 (pink bar) using shRNA in the SuDHl-6 cell line. $5*10^3$ cells were plated in a 6-well plate and counted daily for 5 days. Error bars are calculated from standard deviations of 3 independent experiments. Student *t*-test was used to calculate statistic significance (*: $P<0.05$, **: $P<0.01$ and ***: $P<0.001$). YY1 expression was analyzed in Western Blot. (b). Ectopic expression of Smurf2 and the ligase-dead C716A along with the GFP control in the SuDHL-6 cell line. $5*10^3$ cells were plated in a 6-well plate and counted daily for 5 days. Error bars are calculated from standard deviations of 3 independent experiments. Student *t*-test was used to calculate statistic significance (*: $P<0.05$, **: $P<0.01$ and ***: $P<0.001$).

Fig.3.9

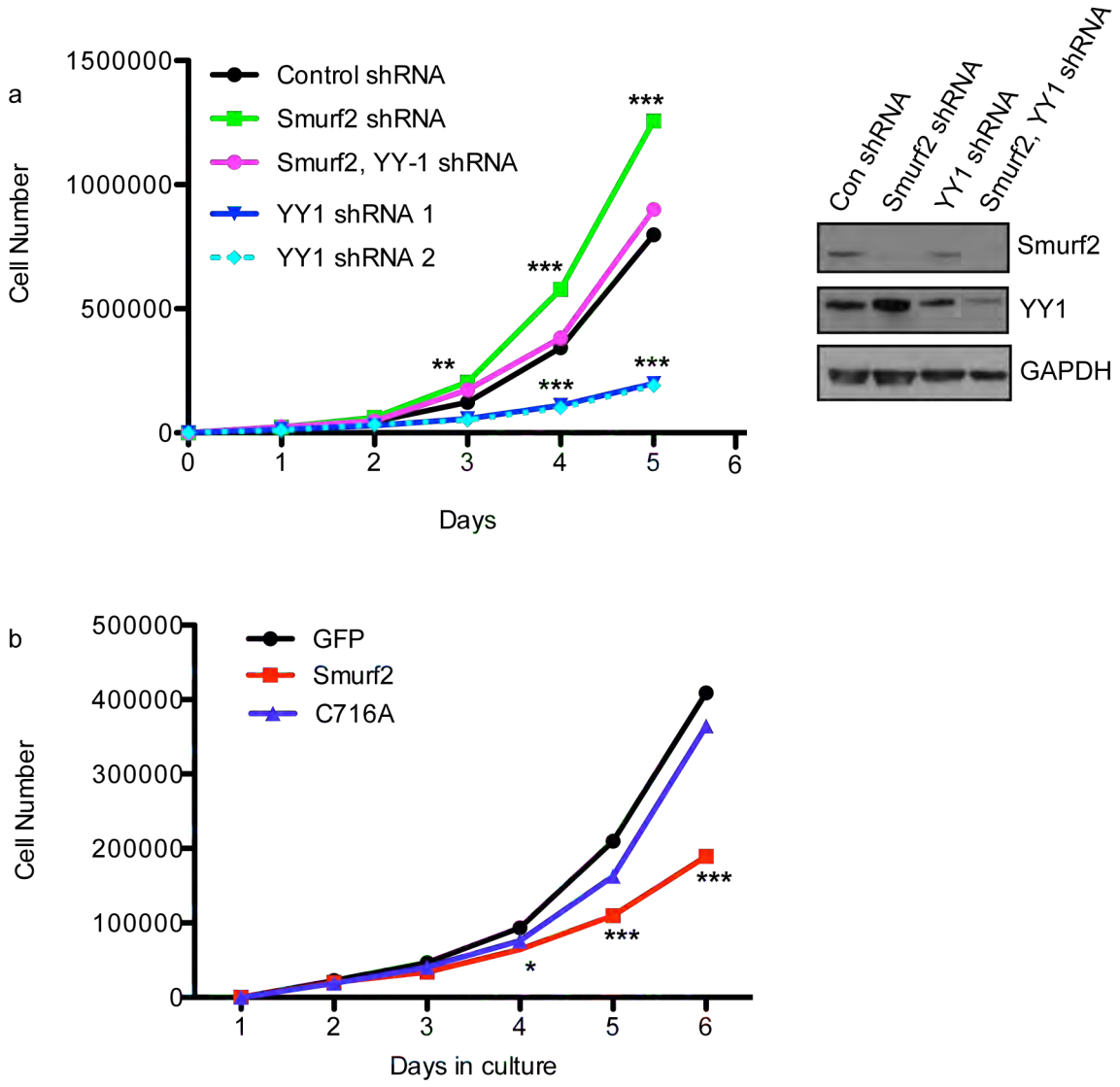
a
Cell Number
1500000
1000000
500000
0
Control shRNA
Smurf2 shRNA
Smurf2, YY-1 shRNA
YY1 shRNA 1
YY1 shRNA 2
***
***
**
***
***
0
1
2
3
4
5
6
Days
Con shRNA
Smurf2 shRNA
YY1 shRNA
Smurf2, YY1 shRNA
Smurf2
YY1
GAPDH
b
Cell Number
500000
400000
300000
200000
100000
0
GFP
Smurf2
C716A
***
***
*
1
2
3
4
5
6
Days in culture

The level of Smurf2 expression correlates with survival prognosis of human DLBCL patients

To investigate whether Smurf2 deficiency has a clinical relevance in human lymphomagenesis, we analyzed Smurf2 expression in human primary lymphoma samples. In a microarray dataset (GSE2350) that contains samples of human B-cell lymphoma and normal B cells [313], we found that the expression of Smurf2 was decreased significantly in DLBCL, Burkitt's lymphoma and follicular lymphoma as compared to normal B cells (Fig.3.10a).

To further understand the relevance of decreased Smurf2 expression in human lymphomagenesis, we next investigated whether the level of Smurf2 expression correlates with clinical outcome. Smurf2 expression was measured in three human B-cell lymphoma microarray datasets, each of which contains survival information of more than 100 patients [314-316]. Within each dataset, we divided lymphoma samples into four groups based on the level of Smurf2 expression, with the 1^{st} quartile having the lowest Smurf2 expression. Survival analysis of dataset GSE4475, which contains both DLBCL and Burkitt's lymphoma patients [314], showed that overall survival of patients with the lowest Smurf2 expression (1^{st} quartile) was significantly worse ($P<0.0001$) than that of patients with higher Smurf2 expression (2^{nd}-4^{th} quartile) (Fig.3.10b). Similarly, a significantly poor survival prognosis ($P=0.0004$) was observed in patients with the low expression of Smurf2 (1^{st} and 2^{nd} quartiles) compared to patients with high Smurf2 expression (3^{rd} and 4^{th} quartiles) in an independent dataset GSE10846 (Fig.3.10c), which contains only DLBCL patients [315]. In contrast, we found no

significant difference in overall survival of patients in a human follicular lymphoma dataset [316] based on Smurf2 expression level (Fig.3.10d), suggesting a specific role of Smurf2 deficiency in human DLBCL and Burkitt's lymphoma.

Certain clinical and molecular parameters have been shown to predict DLBCL patient survival [289,291,317]. Univariate analysis indicated a significant correlation between poor survival prognosis and age, Ann Arbor stage, molecular subtype, or International Prognostic Index (IPI) score. To determine whether Smurf2 expression can predict clinical outcomes independent of other standard parameters, we carried out a multivariate Cox regression analysis, and found that low level of Smurf2 expression was an independent predictor of patient survival in both DLBCL cohorts (P=0.01 for GSE4475 and P=0.027 for GSE10846) (Tables 3.10a and b).

Fig.3.10: Smurf2 expression correlates with overall survival of human DLBCL patients.

(a). Box plot representation of Smurf2 expression in normal B cells, Burkitt's lymphoma (BL), DLBCL and follicular lymphoma (FL). One-way ANOVA was used to compare tumors with normal B cells. Statistic significance is indicated as: ** (P<0.01) and *** (P<0.001). (b) & (c). Kaplan-Meier curves of overall survival of patients in human diffuse large B-cell lymphoma datasets (b) GSE4475 and (c) GSE10846 plotted according to the level of Smurf2 expression. The log-rank test was used for statistical analysis. (d). Kaplan-Meier curves of overall survival of patients in a follicular lymphoma dataset (http://llmpp.nih.gov/FL) [316] plotted according to the level of Smurf2 expression. The log-rank test was used for analysis.

Fig.3.10

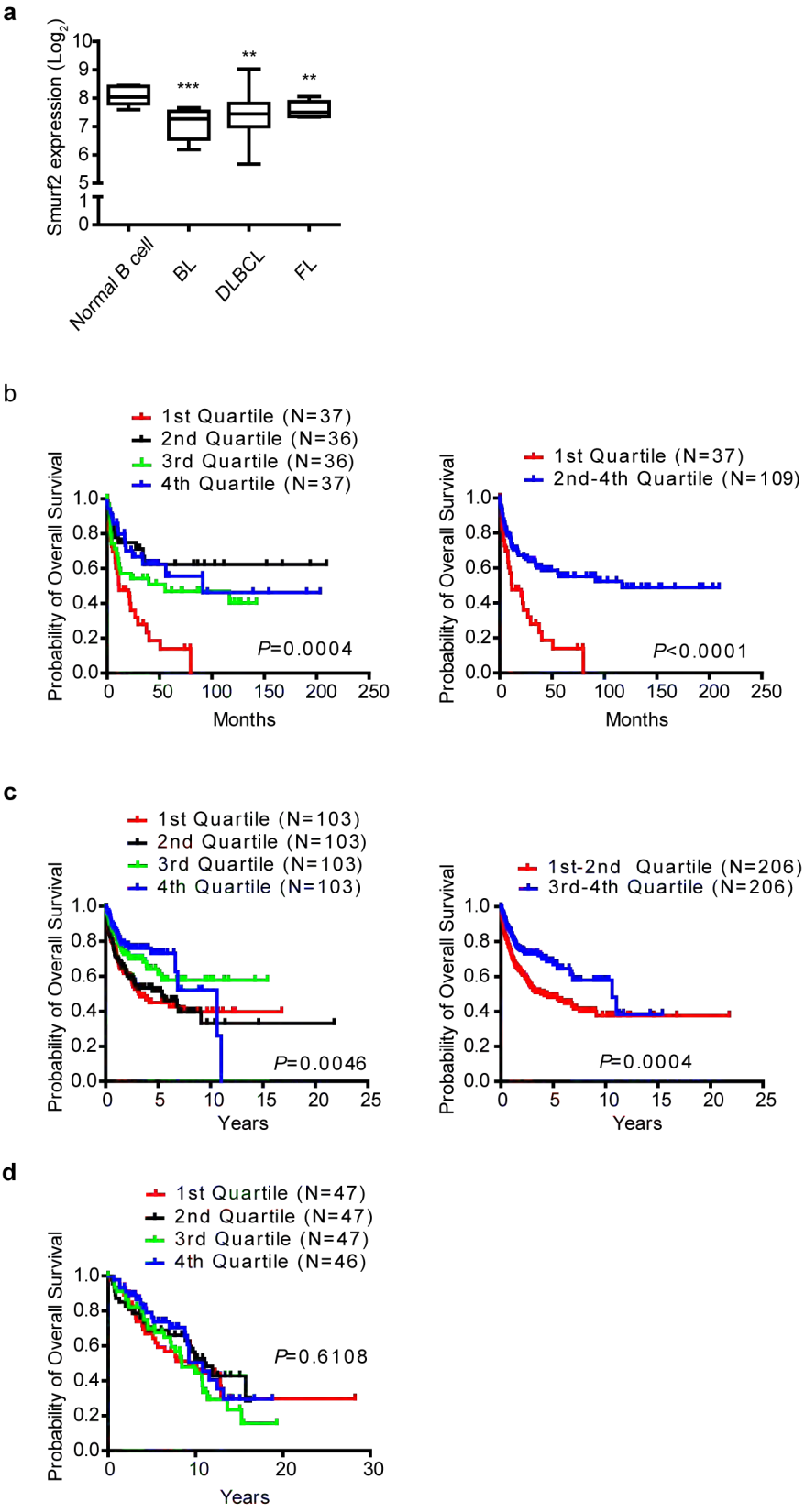
a
Smurf2 expression (Log2)
Normal B cell
BL
DLBCL
FL
b
1st Quartile (N=37)
2nd Quartile (N=36)
3rd Quartile (N=36)
4th Quartile (N=37)
Probability of Overall Survival
P=0.0004
Months
1st Quartile (N=37)
2nd-4th Quartile (N=109)
P<0.0001
c
1st Quartile (N=103)
2nd Quartile (N=103)
3rd Quartile (N=103)
4th Quartile (N=103)
P=0.0046
Years
1st-2nd Quartile (N=206)
3rd-4th Quartile (N=206)
P=0.0004
d
1st Quartile (N=47)
2nd Quartile (N=47)
3rd Quartile (N=47)
4th Quartile (N=46)
P=0.6108

Table 3.10a: Univariate and multivariate analyses of DLBCL prognostic factors associated with patient overall survival in cohorts GSE4475 (N=102) [a].

	Univariate analysis		Multivariate analysis	
Variable	HR (95% CI) [b]	*P*	HR (95% CI) [b]	*P*
Age [c]	2.35 (1.41–3.92)	0.001	1.94 (0.97–3.90)	0.062
Ann Arbor stage [d]	2.16 (1.28–3.65)	0.004	2.60 (1.37–4.94)	0.004
Ki-67 score [e]	0.97 (0.55 –1.72)	0.912	1.26 (0.62–2.56)	0.526
Myc translocation [f]	1.11 (0.68–1.81)	0.68	1.38 (0.68–2.80)	0.379
Subtype [g]	2.26 (1.34–3.82)	0.002	2.12 (1.10–4.07)	0.025
Smurf2 [h]	2.68 (1.64–4.39)	<0.001	2.48 (1.24–4.93)	0.01

[a] Only patients with complete information in all variables were used.

[b] HR: hazard ration; CI: confidence interval

[c] Age: ≥60 vs. <60 years

[d] Ann Arbor stage: III and IV vs. I and II

[e] Ki-67 score: ≥95% vs. <95%

[f] Myc translocation: presence vs. absence

[g] Subtype: ABC vs. GCB

[h] Smurf2: Q1 vs. Q2-Q4

Table 3.10b: Univariate and multivariate analyses of DLBCL prognostic factors associated with patient overall survival in cohorts GSE10846 (N=311) [a].

	Univariate analysis		Multivariate analysis	
Variable	HR (95% CI) [b]	*P*	HR (95% CI) [b]	*P*
Age [c]	2.05 (1.47–2.86)	<0.001	1.41 (0.94–2.11)	0.099
Ann Arbor stage [d]	1.82 (1.31–2.52)	<0.001	0.95 (0.61–1.47)	0.805
Subtype [e]	2.81 (1.98 to 3.99)	<0.001	2.17 (1.49 to 3.16)	<0.001
Revised IPI score [f]	3.20 (2.31 to 4.42)	<0.001	2.90 (1.84 to 4.58)	<0.001
Smurf2 [g]	1.72 (1.28 to 2.42)	<0.001	1.51 (1.05 to 2.18)	0.027

[a] Only patients with complete information in all variables were used.

[b] HR: hazard ration; CI: confidence interval

[c] Age: ≥60 vs. <60 years

[d] Ann Arbor stage: III and IV vs. I and II

[e] Subtype: ABC vs. GCB

[f] Revised IPI score: high (3, 4 and 5) vs. intermediate (1 and 2) and low (0)

[g] Smurf2: Q1+Q2 vs. Q3+Q4

DISCUSSION

In this study, we found that Smurf2-deficient mice displayed an increased rate of forming GCB-type DLBCLs suggesting that Smurf2 has a tumor suppression function in lymphomagenesis. Increased lymphomagenesis in *Smurf2*$^{+/T}$ mice and frequent loss of the wild-type *Smurf2* allele in lymphomas derived from these heterozygous mice (Chapter 2) suggest that the level of Smurf2 expression is important in lymphomagenesis. Consistent with these observations, we found a significant decrease in Smurf2 expression in human DLBCL, Burkitt's lymphoma and follicular lymphoma as compared to normal B cells, indicating a clinical relevance of Smurf2 deficiency in human lymphomagenesis. We did not find evidence that the *Smurf2* locus is deleted in human DLBCL [295,318] or Burkitt's lymphoma [319,320], suggesting that epigenetic regulation probably plays an important role in Smurf2 deficiency in human lymphomagenesis. In addition, decreased Smurf2 expression is observed in other types of human cancer as compared to normal samples, including adult acute and chronic T-cell leukemia, B-cell chronic lymphocytic leukemia, acute myeloid leukemia and lung adenocarcinoma [321-324].

Increased susceptibility to B-cell lymphomagenesis in Smurf2-deficient mice was associated with enhanced proliferation and elevated expression of c-Myc in splenic B cells. An inverse correlation between Smurf2 and c-Myc expression is also noted in human DLBCL samples. As YY1 has been shown to transactivate c-Myc expression [304,312], our discovery of Smurf2-mediated ubiquitination of YY1 provides a novel mechanism by which Smurf2 regulates c-Myc expression and cell proliferation. To our knowledge, Smurf2 is the first E3

ligase identified to ubiquitinate YY1. As a transcriptional regulator, YY1 plays a critical role in many biological processes including development, differentiation and proliferation, and has been implicated in oncogenesis [325,326]. The expression of YY1 is found to be increased in high-grade DLBCL or Burkitt's lymphoma as compared to low grade lymphoma or normal B cells [327]. Furthermore, elevated YY1 expression correlates with poor survival prognosis of DLBCL patients [328], suggesting an oncogenic function for YY1 in human B-cell lymphomagenesis. YY1 is a critical regulator of B-cell development [329], and has been recently identified as a central regulator of the germinal center B-cell-specific transcriptional program [330]. Consistently, our analyses of lymphomas generated in Smurf2-deficient mice indicate that they have a germinal center or post-germinal center phenotype. These results suggest that Smurf2-mediated ubiquitination and degradation of YY1 plays an important role in suppression of lymphomagenesis.

As a master regulator of cell proliferation [331], the oncogenic function of c-Myc in B-cell lymphomagenesis is well documented [310,332,309,307]. Intrinsic tumor suppression mechanisms such as apoptosis and senescence are triggered by activated oncogenes to restrain the oncogenic proliferation. With c-Myc, an additional layer of complexity is provided by the exquisite sensitivity of cells to different levels of c-Myc overexpression. High level of c-Myc overexpression increases cell proliferation and drives lymphomagenesis, but also induces apoptosis [332,309,333]. Suppression of apoptosis exacerbates c-Myc-induced lymphomagenesis, suggesting that apoptosis antagonizes c-Myc's oncogenic

activity [309]. Further, it has been recently found that low level of c-Myc elevation promotes cell proliferation without inducing apoptosis [334]. Consistent with this observation, we found that Smurf2-deficient mice showed low level (~2-fold) of c-Myc elevation and enhanced proliferation in B cells without significant induction of apoptosis. In the absence of apoptosis, senescence likely becomes the critical tumor suppression mechanism to antagonize the oncogenic activity of Myc. A recent study shows that constitutive activation of c-Myc activates senescence [335]. We propose that the impaired senescence response in the Smurf2 deficient mice (Chapter 2), coupled with enhanced cell proliferation induced by low level of c-Myc activation drives lymphomagenesis in these mice. Smurf2 thus plays a dual role in tumor suppression by regulating c-Myc expression as well as the senescence response.

DLBCL shows significant variations in morphology, clinical presentation and response to treatment. Although chemotherapy using a combination of cyclophosphamide, doxorubicin, vincristine, and prednisone (CHOP) or CHOP plus monoclonal antibody rituximab (R-CHOP) successfully induces lengthy remission in 40-50% of DLBCL patients, ~30% of DLBCL patients are resistant to CHOP/R-CHOP treatment or relapse soon after treatment [288], indicating a need for additional therapeutic strategies designed to target specific molecules that are critical for DLBCL pathogenesis. Our finding that low level of Smurf2 expression correlates with poor survival prognosis in DLBCL patients and previous observation that high level of YY1 expression correlates with poor survival prognosis in DLBCL patients [328] suggest that the Smurf2-YY1

regulatory axis is a useful predictor of clinical outcome in DLBCL patients and a potential therapeutic target for treatment of DLBCL.

MATERIALS AND METHODS

Tumor studies:

Mice were generated as described in Chapter 2. A mouse cohort on mixed C57BL/6x129Ola background was monitored until 20-month of age. Moribund mice were sacrificed for necropsy, and selected tissues were harvested for preparation of DNA, RNA and protein. Portions of each tissue were fixed in 10% phosphate-buffered formalin and OCT to make paraffin and frozen sections. Tumor sections (5 μm) were stained for Hematoxylin & Eosin, PNA (Vector Labs), BCL6 (Santa Cruz), Ki-67 (Leica) and TUNEL (Roche). RAG1 knockout mice were a kind gift from Dr. Rachel Gerstein. For the transplantation study $2*10^6$ tumor cells were injected retro-orbitally into sub-lethally (3Gy) irradiated RAG1 knockout mice using a Cesium 137 source. All mouse studies were carried out according to guidelines approved by the Institutional Animal Care and Use Committee of University of Massachusetts Medical School.

Fluorescence-activated cell sorting (FACS) analysis

Mouse spleens were collected and ground between frosted glass slides. After red blood cells were lysed, splenic cells were filtered through 70 μm nylon mesh and incubated with anti-CD16/32 antibody (Bio X Cell) for 10 min on ice to block Fc receptors. Cells were incubated with primary antibodies for 20 min and washed three times. Biotin-stained cells were incubated with streptavidin-pacific blue for 15 min on ice and washed three times. After the final wash, cells were resuspended in 1 μg/ml propidium iodide (PI) to exclude dead cells. Primary

antibodies included CD93-Cy7PE (AA4.1), CD19-PE-TR (6D5), IgD-PE (11-26), IgM-APC, CD23-biotin (B3B4) and CD24-FITC (30F1), CD95-PE and IgG2A-PE. Antibodies and streptavidin were purchased from BD Biosciences, Invitrogen or eBioscience. Flow cytometry was performed on a 3-laser, 12-detector LSR II (BD Biosciences), and data were analyzed using FlowJo software (Treestar).

Class switch recombination analysis

Germline and postswitch transcripts of the mouse immunoglobulin heavy chain (*IgH*) locus were amplified by quantitative RT-PCR with primers as described [336]. Germline transcripts (μ, IgM) were amplified using primers of ImF and CmR. Postswitch transcripts were amplified using the following primers: ImF and Cg1R for γ1 (IgG1), ImF and Cg2aR for γ2a (IgG2a), ImF and Cg2bR for γ2b (IgG2b), ImF and Cg3R for γ3 (IgG3). ImF: 5'-CTCTGGCCCTGCTTATTGTTG-3'; CmR: 5'-GAAGACATTTGGGAAGGACTGACT-3';
Cg1R: 5'-GGATCCAGAGTTCCAGGTCACT-3'; Cg2aR: 5'-GCCACATTGCAGGTGATGGA-3'; Cg2bR: 5'-CACTGAGCTGCTCATAGTGTAGAGTC-3'; Cg3R: 5'-CTCAGGGAAGTAGCCTTTGACA-3'.

Somatic hypermutation assay

The frequency of somatic mutation in mouse immunoglobulin heavy chain (*IgH*) locus was determined as previously described [336]. Briefly, V_H186.2 transcripts of mouse *IgH* μ isotype were amplified in RT-PCR using Phusion hot start high-

fidelity Taq Polymerase (New England Biolabs) with primers V_H186.2 (5'-ttcttggcagcaacagctaca-3') and CmR (5'-GAAGACATTTGGGAAGGACTGACT-3'). PCR products were cloned into pGEM-T-easy vector (Promega), and individual colonies were sequenced to determine the mutation frequency.

Splenic B-cell proliferation assays

Mouse spleen was collected and ground between frosted glass slides. After red blood cells were lysed, cells were filtered through 70 µm nylon mesh and treated with 10 µM carboxyfluorescein succinimidyl ester (CFSE, Invitrogen) at 37ºC for 10 min. Cells were plated at $5x10^5$ per well in 6-well plates and cultured in RPMI-1640 medium supplemented with 10% fetal bovine serum (FBS, Hyclone), 2 mM glutamine, 100 µM MEM non-essential amino acids and 50 µM 2-Mercaptoethanol (Invitrogen) in a humidified chamber containing 5% CO_2 at 37°C. Cells were treated with 5 µM lipopolysaccharide (LPS, Sigma) or left untreated as controls. Cells were collected daily for 4 days, washed with staining media (biotin-, flavin-, and phenol red-deficient RPMI-1640 medium, 10 mM pH7.2 HEPES, 0.02% sodium azide, 1 mM EDTA and 2% FBS), then stained with APC-conjugated anti-B220 antibody (eBioscience). After being washed and re-suspended in 1 µg/ml propidium iodide, cells were analyzed by flow cytometry using a BD FACSCaliber. Data were analyzed using FlowJo software (Treestar). The number of CFSE peaks was determined in order to measure the number of cell divisions.

In Bromodeoxyuridine (BrdU) incorporation assay, mice were injected with 1 mg BrdU (BD Biosciences) intraperitoneally. Spleen was collected 24 hours later and processed as described above. Splenic cells were fixed, and stained with anti-BrdU antibody using a FITC BrdU Flow Kit (BD Biosciences) and APC-conjugated anti-B220 antibody. Data were collected by flow cytometry using a BD FACSCaliber and analyzed using FlowJo software.

Quantitative PCR

Total RNA was isolated from cells or freshly dissected tissues using RNeasy Mini kit (Qiagen). RNA was reverse-transcribed using Superscript II (Invitrogen). Real-time PCR was carried out on a MyiQ iCycler using a SYBR Green PCR kit (Bio-Rad). The following primers were used: c-Myc (F: 5'-GGACAGTGTTCTCTGCC-3'; R: 5'-CGTCGCAGATGAAATAGG-3'), YY1 (F: 5'-TGAGAAAGCATCTGCACACC-3'; R: 5'-CGCAAATTGAAGTCCAGTGA-3'), Apex1 (F: 5'-GCTCCGTCAGACAAAGAAGG-3'; R: 5'-GCATTGGGAACATAGGCTGT-3'), Cad (F: 5'-TGGTCAGTTCATCCTCACTCC-3'; R: 5'-TACATGCCGTTCTCAGCTTG-3'), Ncl (F: 5'-TAAGGGTGAAGGTGGCTTTG-3'; R: 5'-CCTTGTGGCTTGAAGTCTCC-3') and β-actin (F: 5'-GCTCTTTTCCAGCCTTCCTT-3'; R: 5'-GTGCTAGGAGCCAGAGCAGT-3').

Western blot

Total cell lysates were collected using RIPA buffer (50 mM Tris–HCl pH 7.5, 150 mM NaCl, 1% Triton X-100, 0.1% SDS, 0.5% deoxycholic acid, 0.02% sodium azide) with freshly added complete protease inhibitors (Roche). Protein lysates (20 μg) were separated by SDS–PAGE Criterion X-gel (Bio-Rad) and transferred to nitrocellulose membranes (GE Osmonics). Immunoblots were analyzed by Western blotting and visualized by Western lightening chemiluminescence detection (PerkinElmer). Primary antibodies used in this study were Smurf2 (Epitomics), c-Myc (Invitrogen), YY1, β-actin and GAPDH (Santa Cruz Biotechnology).

Co-immunoprecipitation analysis

Cells were lysed in NP40 lysis buffer (20 mM Tris–HCl, 150 mM NaCl, 2 nM EDTA, 1% Nonidet P-40) plus complete protease inhibitors (Roche). Lysates were incubated with anti-Flag M2 affinity gel (Sigma) overnight at 4°C. Immunoprecipitates were washed four times with NP40 lysis buffer, and analyzed in Western blot with anti-HA antibody.

Ubiquitination assay

293T cells were transfected with constructs that express HA-YY1 (a gift of Dr. Yang Shi, Harvard Medical School), 3xFlag-ubiquitin (provided by Dr. Quan Lu, Harvard School of Public Health) and Smurf2. GFP and C716A were used as controls. Cells were treated with MG132 (20 μM, Sigma) for 2 hrs before cell

lysis. Cells were collected in RIPA buffer (50 mM Tris–HCl pH 7.5, 150 mM NaCl, 1% Triton X-100, 0.1% SDS, 0.5% deoxycholic acid, 0.02% sodium azide) plus 10 mM *N*-ethylmaleimide (Fisher Scientific). Cell lysates were incubated with anti-HA affinity gel (Sigma) overnight at 4°C. Immunoprecipitates were washed with RIPA buffer three times, and analyzed in Western blot with anti-Flag antibody to detect ubiquitin conjugation.

Chromatin immunoprecipitation (ChIP) assay

Spleens from 2-month old wild-type and *Smurf2*$^{T/T}$ littermates were harvested and processed as described previously to obtain single cell suspension. Splenic cells were resuspended in RPMI-1640 medium (Invitrogen) with 1% formaldehyde (Sigma) and cross-linking was carried out at room temperature for 10 minutes. After neutralization with glycine (125 nM), cells were lysed in SDS lysis buffer. After sonication, cell extract was used in immunoprecipitation with anti-YY1 antibody (sc-281, Santa Cruz Biotechnology) or matched IgG as a control. ChIP was carried out using a ChromaFlash one step ChIP kit (Epigentek) according to manufacturer's instruction. After reverse of cross-linking at 65°C for 3 hrs, amplification of the specific region of c-Myc promoter containing the YY1 binding site was detected in quantitative PCR with the following primers: F: 5'-tccccagccttagagagacg-3' and R: 5'-ggctccggggtgtaaacagt-3'. Chromatin before ChIP was used as input for comparison.

Cell culture and viral infection

A human DLBCL cell line SUDHL6 (a generous gift of Dr. Subbarao Bondada, University of Kentucky) was cultured in RPMI-1640 medium (Invitrogen) supplemented with 10% fetal bovine serum (Hyclone) in a humidified chamber containing 5% CO_2 at 37°C. Lentiviral vectors expressing Smurf2 or ligase mutant C716A were constructed by insertion of Smurf2 cDNA fragments into pLenti-CMV-MCS-Puro. Lentiviral shRNA constructs targeting Smurf2 (V2LHS_10399), YY1 (V2LHS_219592, V2LHS_389741) and a non-silencing shRNA control (RHS4346) were purchased from Open Biosystems. These Lentiviral shRNA constructs also express GFP. Lentiviral packaging and infection were carried out as described previously [284]. Briefly, lentiviral vectors were co-transfected into 293T cells with a plasmid (pMD2.VSV-G) encoding vesicular stomatitis virus glycoprotein (VSV-G) and a plasmid (pCMVdR8.74) encoding packaging proteins. VSV-G pseudotyped virus were collected 48 hr after transfection and used to infected target cells in the presence of 4 μg/ml polybrene (Sigma). Four days later, infected cells were FACS sorted to obtain GFP positive (shRNA knockdown) cells or selected with Puromycin (1mg/ml) for 1 week to obtain Smurf2 or C716A expressing cells. For growth curves, cells that were sorted or selected were plated at $5*10^3$ cells/well in 6-well plates in triplicate and counted daily for 5 days.

Statistical analyses

Microarray data were retrieved from GEO (http://www.ncbi.nil.nih.gov/geo). Expression values of Smurf2 (log_2 transformed) were analyzed with Box plot. One-way ANOVA was used for statistical analysis. Kaplan-Meier survival curves were plotted and analyzed with the log-rank test. Student *t*-test (two-tailed and unpaired) was used for pairwise comparisons, and data were presented as mean ± standard deviation. Statistical significance was set as $P<0.05$.

CHAPTER IV

Enhanced Long-term HSC activity in the Smurf2-deficient mice

ABSTRACT

Age-dependent decline in the self-renewal ability of stem cells plays a critical role in aging, but the underlying mechanisms of such decline are not well understood. Senescence has been hypothesized as one of the mechanisms to contribute to the decline of stem cell self-renewal with age, although the evidence to support this hypothesis is scant. In this study, we showed that mice deficient in Smurf2, a previously identified regulator of senescence, had an expanded hematopoietic stem cell (HSC) compartment and this was associated with increased proliferation of HSCs. Furthermore, Smurf2-deficient mice exhibited increased short-term and long-term self-renewal activity. Finally, the bone marrow compartment of Smurf2-deficient mice exhibit decreased $p16^{INK4a}$ expression levels. As decreased expression of $p16^{INK4a}$, a key senescence regulator, has been shown to be associated with decreased hematopoietic stem cell function, this provides a plausible mechanism for the phenotype displayed by the Smurf2-deficient mice. Taken together, these data suggest that Smurf2-deficiency regulates HSC activity by delaying senescence through down-regulation of $p16^{INK4a}$.

INTRODUCTION

Age-dependent decline in stem cell function occurs in several tissues and this leads to impairment in tissue homeostasis with age [337,171]. Aging in the hematopoietic system is driven by both intrinsic and extrinsic factors [154,182,152,337,151] and results in decreased immune response [181], increased incidence of myeloid leukemias [338] and anemias [339] and also reduced regenerative capacity [340].

The murine hematopoietic system also exhibits a functional decline with age [341,151-153]. In mice, while there is a strain-dependent increase in hematopoietic stem cell (HSC) number with age [151-154], it is associated with a dose-dependent decrease in self-renewal capacity in serial transplantation experiments *in vivo* [155,156]. This decline in HSC function increases with the number of stem cell transplantations [157-161]. HSCs from aged mice also exhibit a decrease in competitive repopulating ability compared with younger counterparts [162,151,153]. HSCs from mice display a skewing toward the myeloid lineage. Mice display changes in lineage potential with age, with a decrease in lymphoid output while myeloid potential is maintained [151].

While numerous molecular mechanisms have been postulated, the pathways that lead to stem cell aging are not well understood. Senescence is known to be associated with aging. Thus far, the role of senescence in the changes in stem cell functionality with age is debatable. Most of the evidence for senescence in stem cell aging comes from studies showing that senescence markers such as senescence-associated β-galactosidase, HP-1 (heterochromatin protein-1) foci, and p16INK4a markedly increase with age in

many tissues in several mammalian species [171] and from studies of self-renewal in HSCs, from $p16^{INK4a}$-deficient and $p16^{INK4a}$-overexpressing mice that have suggested that increasing levels of $p16^{INK4a}$ are not only associated with aging, but partly contribute to the age-induced replicative failure of HSCs [192].

Work from our lab has previously shown that Smurf2 is a critical regulator of the senescence response [245]. In our Smurf2-deficient mouse-model, we observed a delayed senescence response in MEFs as well as *in vivo* (Chapter 2). We further showed that this delayed senescence response is associated with decreased p16 expression. Work from our lab has also recently shown that Smurf2 can regulate p16 expression in a ligase-dependent manner [246], and this is integral to Smurf2's regulation of senescence. Based on Smurf2's regulation of senescence and p16, we hypothesized that Smurf2 regulates HSC function in an age-dependent manner *in vivo*. In this study, we show that Smurf2-deficiency leads to increased bone marrow and LT-HSC population. Further, young and old Smurf2-deficient mice exhibit better self-renewal capacity in a serial transplantation experiment *in vivo*. We also find that the older Smurf2-deficient HSCs compete better than the young HSCs in a competitive repopulation experiment *in vivo*. This is associated with decreased expression of p16 in the bone marrow compartments of the Smurf2-deficient mice. Our data thus indicate that Smurf2 may regulate LT-HSC function by regulating the senescence response through the downregulation of p16 expression.

RESULTS

Smurf2-deficiency leads to an expansion of the bone marrow compartment and the LT-HSC population

We focused our initial analysis on the whole bone marrow of Smurf2-deficient mice. BM counts from littermates of wild-type and Smurf2-deficient mice showed an expansion of the BM compartment in the young Smurf2-deficient mice (Fig.4.1a) which was maintained as the mice aged (Fig.4.1b). We then extended our study to the BM LT-HSC compartment (Lin^- Sca^+ $c\text{-}kit^+$ $CD135^-$ $CD150^+$) in littermates from wild-type and Smurf2-deficient mice, and found that the Smurf2-deficient mice showed an expansion of the LT-HSC compartment (Fig.4.1c). The Smurf2-deficient mice exhibited a sustained increase in the frequency as well as the absolute number of LT-HSCs in the BM of young (Fig4.1d) as well as old (Fig.4.1e) mice.

To investigate if the increase in LT-HSC count also led to an increase in the other hematopoietic progenitors, we studied the other stem cell and progenitor compartments in the BM. When we examined the other HSC compartments from wild-type and Smurf2-deficient mice, we found no difference in the less immature progenitor compartments including the Lineage depleted BM cells (Lin^-) (Fig.4.2a), the LSK population (Lin^- Sca^+ $c\text{-}kit^+$) (Fig.4.2b), the Short-term HSCs (ST-HSCs: Lin^- Sca^+ $c\text{-}kit^+$, $CD135^-$ $CD150^-$) (Fig.4.2c) or the Multi-potent progenitors (MPPs: Lin^- Sca^+ $c\text{-}kit^+$, $CD135^+$ $CD150^-$) (Fig.4.2d). This indicates that there is a specific increase in the frequency of the LT-HSCs in the Smurf2-deficient mice.

To determine if the effector cells in circulation that arise from the HSCs in the BM are changed by Smurf2-deficiency, we performed complete blood counts on peripheral blood from age-matched wild-type and Smurf2-deficient mice. There was no difference in the various blood cell lineages including WBCs, Lymphocytes, Granulocytes and Monocytes (Fig.4.3) between wild-type and Smurf2-deficient mice. Thus, the increased LT-HSC number has no effect on the resting population of blood cells in circulation.

Fig.4.1: Increased total bone marrow counts in young and aged *Smurf2*$^{T/T}$ mice. (a)Total bone marrow counts from littermates of 2-month old wild-type (+/+) and Smurf2-deficient (*Smurf2*$^{T/T}$) (T/T) mice (n=16) are shown. p=0.0121 (**b)** Increased bone marrow counts in aged *Smurf2*$^{T/T}$ mice. Total bone marrow counts from littermates of 24-month old wild-type (+/+) and Smurf2-deficient (*Smurf2*$^{T/T}$) (T/T) mice (n=4) are shown. p=0.007, Paired Student's *t*-test (2-tailed) was used for statistical analysis. Statistic significance is indicated as: * (*P*<0.05), ** (*P*<0.01), and *** (*P*<0.001).

Fig.4.1

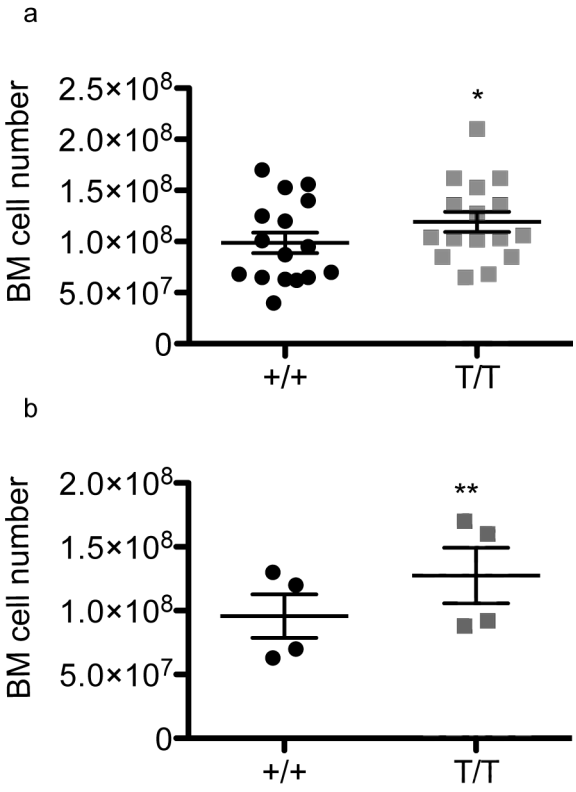
a
BM cell number
2.5×10^8
2.0×10^8
1.5×10^8
1.0×10^8
5.0×10^7
0
*
+/+
T/T
b
BM cell number
2.0×10^8
1.5×10^8
1.0×10^8
5.0×10^7
0
**
+/+
T/T

Fig.4.1c: Expanded LT-HSC population in the Hematopoietic stem cell compartment of *Smurf2*$^{T/T}$ mice. FACS analyses of BM cells stained with the HSC cocktail from wild-type (+/+) (upper panel) and *Smurf2*$^{T/T}$ (T/T) (lower panel) littermates are presented. Live cells are displayed (propidium iodide excluding). LT-HSCs are Lin-, Sca+, c-kit+, CD135-, CD150+. Lineage (Lin) negative cells (left panel) are gated out and Sca1 and c-kit staining on this population is displayed in the middle panel. The Sca+, c-kit+ cells are defined as the LSK (Lin-, sca+, c-kit+) population. LSK cells are further gated out (middle panel) and stained for CD135 and CD150 (right panel). LT-HSCs are CD135-, and CD150+, as displayed in the right panel. ST-HSCs are CD135-, and CD150- and are displayed in the box left of the LT-HSCs. MPPs are CD135+, CD150- and are displayed in the right panel. The *Smurf2*$^{T/T}$ (T/T) mice exhibit an expanded LT-HSC compartment (16% to 9%).

Fig.4.1c

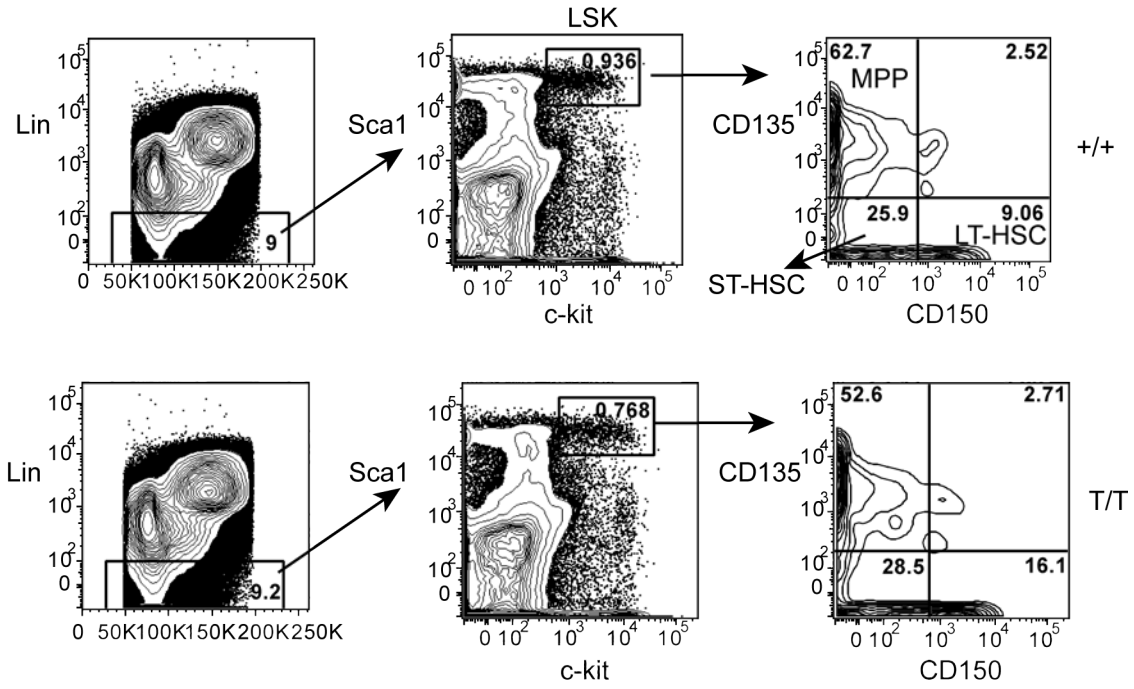
LSK
Lin
Sca1
c-kit
CD135
CD150
9
0.936
62.7
MPP
2.52
25.9
9.06
LT-HSC
ST-HSC
+/+
9.2
0.768
52.6
2.71
28.5
16.1
T/T
0 50K100K150K200K250K

Fig.4.1(contd): Expanded LT-HSC compartment in the bone marrow of *Smurf2*$^{T/T}$ mice. LT-HSCs are Lin-, Sca+, c-kit+, CD135-, CD150+ as determined by FACS analysis. The frequency and absolute numbers of LT-HSCs in the total BM of young **(d)** 2-month old (upper panel, n=10, *p*=0.03) mice and aged **(e)** 24-month old (lower panel, n=4, *p*=0.02) wild-type (+/+) and *Smurf2*$^{T/T}$ (T/T) are displayed. Paired Student's *t*-test (2-tailed) was used for statistical analysis.

Fig.4.1

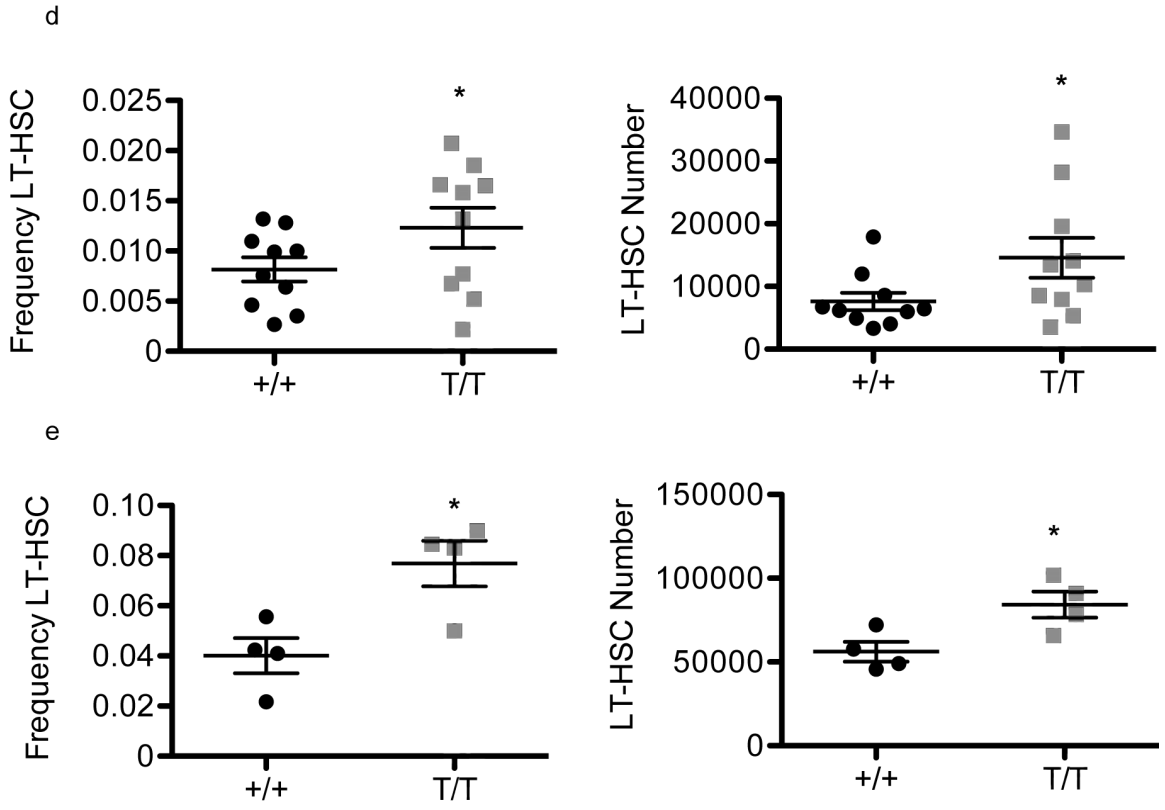
d
Frequency LT-HSC
0.025
0.020
0.015
0.010
0.005
0
*
+/+
T/T
LT-HSC Number
40000
30000
20000
10000
0
*
+/+
T/T
e
Frequency LT-HSC
0.10
0.08
0.06
0.04
0.02
0
*
+/+
T/T
LT-HSC Number
150000
100000
50000
0
*
+/+
T/T

Fig.4.2: The other stem and progenitor cell compartments are unchanged in the BM of *Smurf2*$^{T/T}$ mice. Cells that stain negative for the Lineage cocktail are called Lin-; the LSK population is defined as Lin-, Sca+, c-kit+; ST-HSCs are LSK, CD135-, and CD150-; MPPs are LSK, CD135+, CD150- as determined by FACS analysis. The frequency of Lin- cells **(a)**, LSK cells **(b)**, ST-HSCs **(c)** and MPPs **(d)** in the total BM of young 2-month old (n=10) wild-type (+/+) and *Smurf2*$^{T/T}$ (T/T) are displayed and there is no apparent difference between them.

Fig.4.2

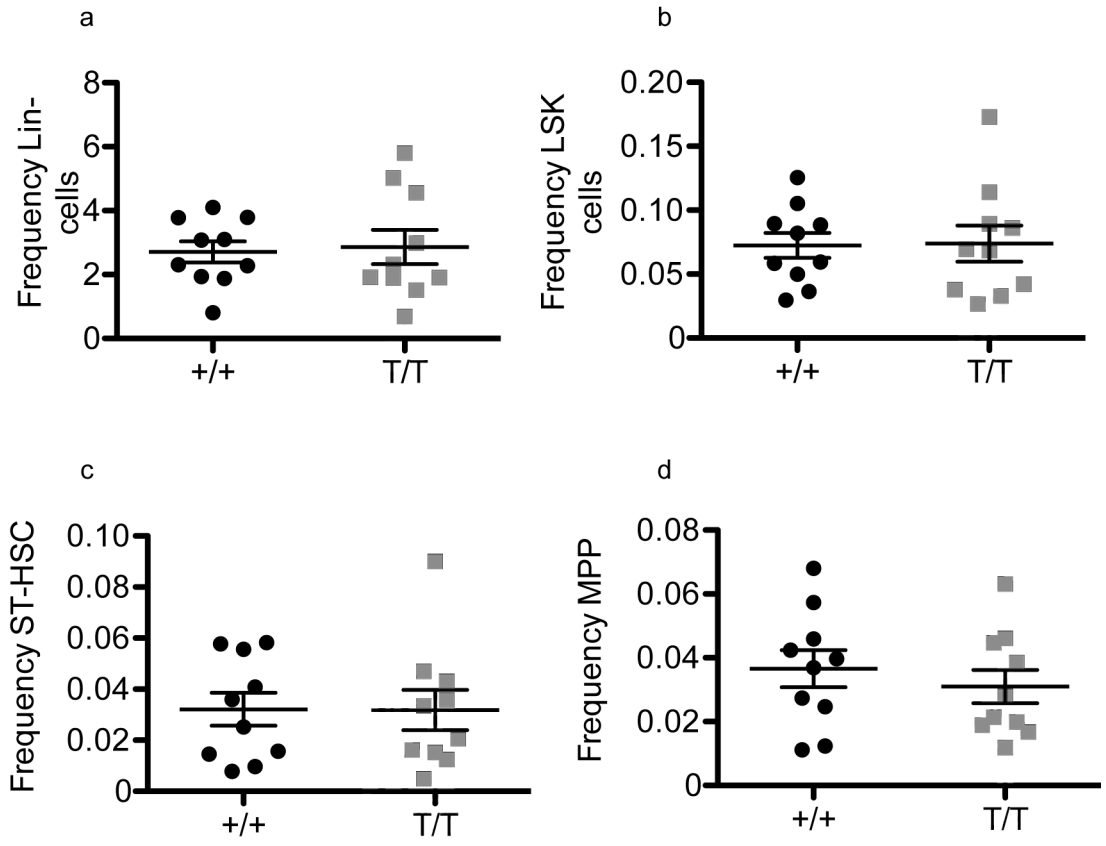
a
Frequency Lin- cells
8
6
4
2
0
+/+
T/T
b
Frequency LSK cells
0.20
0.15
0.10
0.05
0
+/+
T/T
c
Frequency ST-HSC
0.10
0.08
0.06
0.04
0.02
0
+/+
T/T
d
Frequency MPP
0.08
0.06
0.04
0.02
0
+/+
T/T

Fig.4.3: Peripheral blood counts in the *Smurf2*$^{T/T}$ mice are unchanged. Complete blood counts on peripheral blood from 2 month old WT (+/+) and *Smurf2*$^{T/T}$ (T/T) littermates (n=6) are displayed. The White Blood Cell (WBC) count, Lymphocyte count, Monocyte count and Granulocyte count are similar between the WT (+/+) and *Smurf2*$^{T/T}$ (T/T) mice.

Fig.4.3

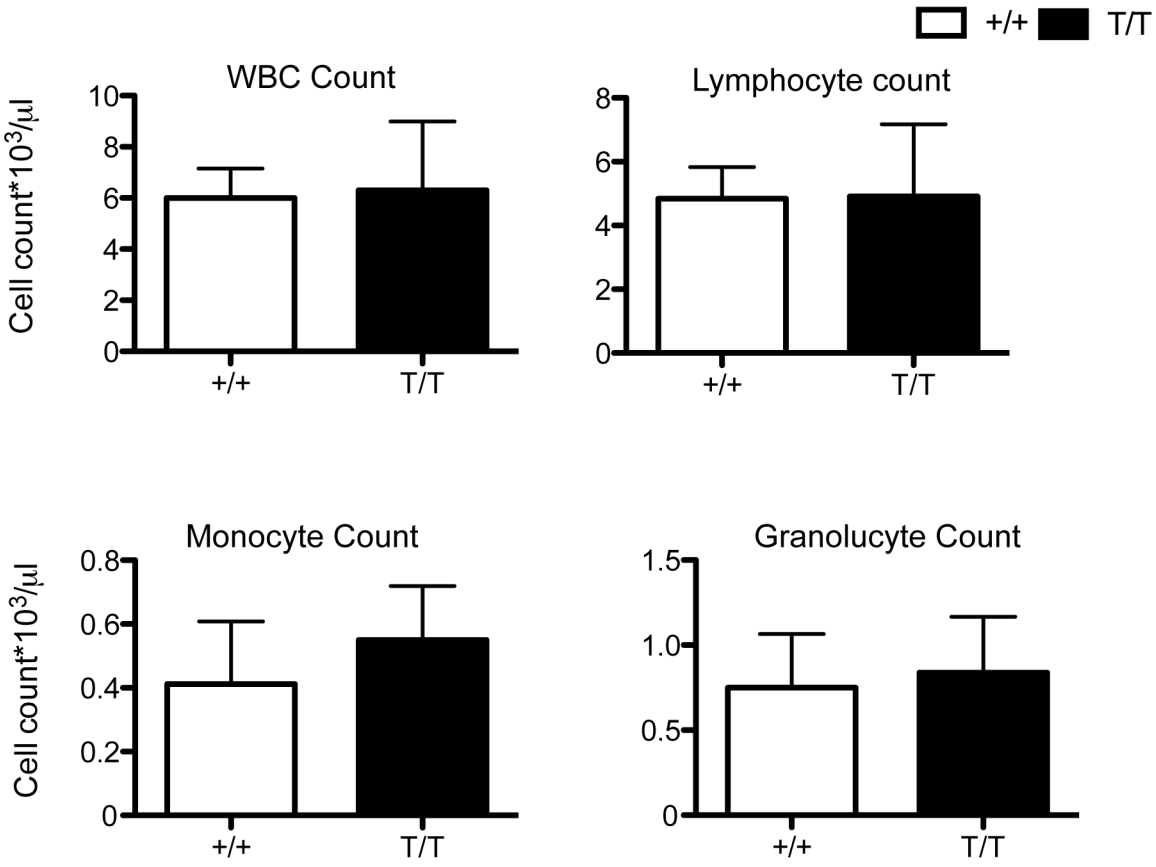
+/+
T/T
WBC Count
Cell count*10^3/µl
10
8
6
4
2
0
+/+
T/T
Lymphocyte count
8
6
4
2
0
+/+
T/T
Monocyte Count
Cell count*10^3/µl
0.8
0.6
0.4
0.2
0
+/+
T/T
Granolucyte Count
1.5
1.0
0.5
0
+/+
T/T

Smurf2-deficient LT-HSCs exhibit better self-renewal capacity *in vivo*

To evaluate the functional capacity of the Smurf2-deficient LT-HSCs we performed a serial transplantation experiment. As a gold standard test for long-term self-renewal and multi-lineage potential of HSCs, serial transplantation of bone marrow cells is able to reconstitute lethally-irradiated recipients in successive but limited transplants, reflecting the finite potential of HSC self-renewal [159,161,342]. It has been shown that serial transplantation leads to a dose-dependent decrease in self-renewal capacity of HSCs [155,156].

Total BM cells ($5*10^6$) from young wild-type or Smurf2-deficient mice were injected into lethally irradiated (10Gy) recipients. In order to distinguish the relative contributions of the donors from the recipients we used recipient mice of a congenic strain bearing the allelic variant CD45.1 that can be distinguished from the donors (CD45.2) by flow cytometric analysis. We were able to rescue 100% of the recipients from wild-type and Smurf2-deficient mice for the first 3 cycles of transplantations (Fig.4.4a). In the 4^{th} cycle, 100% of the recipients of wild-type BM died within 3 weeks of being transplanted, but up to 70% of the recipients of Smurf2-deficient BM survived (Fig.4.4a). When we carried recipients of the Smurf2-deficient BM forward for the 5^{th} transplantation, 60% of the injected mice survived (Fig.4.4a). Further, staining of the BM from the recipient mice with the CD45.2 anitbody in conjunction with the HSC cocktail 2 months after transplantation revealed that ˜ 95% of the LT-HSC population had been reconstituted by the donor BM (Fig.4.4b) with almost no residual recipient HSCs surviving irradiation. To determine if the newly reconstituted HSCs in the bone

marrows of the recipient mice were able to form the various blood cell lineages, we bled the mice and performed CBC counts at 2 months after reconstitution. We found that both wild-type and Smurf2-deficient HSCs were able to successfully reconstitute all the blood cell lineages (Fig.4.4c). These data indicate that the young Smurf2-deficient LT-HSCs may have better self-renewal capacity *in vivo*, allowing them to reconstitute bone marrow for more number of transplantation cycles than wild-type. When we examined the bone marrows of the recipients from successive transplantations we found that the increase in total BM count and LT-HSC count was maintained by the recipients of the Smurf2-deficient BM (Fig.4.4d). This indicates that the better functional capacity of the Smurf2-deficient LT-HSCs is likely a cell-intrinsic phenomenon and independent of the microenvironment.

Fig.4.4a: *Smurf2$^{T/T}$* (T/T) deficient mice exhibit increased self-renewal capacity *in vivo.* Kaplan-Meier curves from the serial transplantation experiment showing survival of recipients of wild-type (+/+) and *Smurf2$^{T/T}$* (T/T) BM over successive transplants are displayed. 5*10^6 BM cells from a healthy 2 month-old WT (+/+) and *Smurf2$^{T/T}$* (T/T) donor CD45.2+ mice are injected into lethally irradiated (10Gy) CD45.1+ recipient mice (n=5) for the 1st 3 transplantations. The experiment was repeated twice (upper panel 1st set, lower panel 2nd repeat). For the 4th transplantation, BMs from 3° transplant recipients (n=22 for the 1st set $p<0.0001$, n=8 for the 2nd repeat $p< 0.0004$) were injected. Recipients of *Smurf2$^{T/T}$* (T/T) BM were able to reconstitute mice for up to 5 transplants, compared to 3 for wild-type. For the 1st set, the 4th transplant T/T survivors were carried forward for the 5th transplant. Curve comparison was performed using the log-rank test.

Fig.4.4a

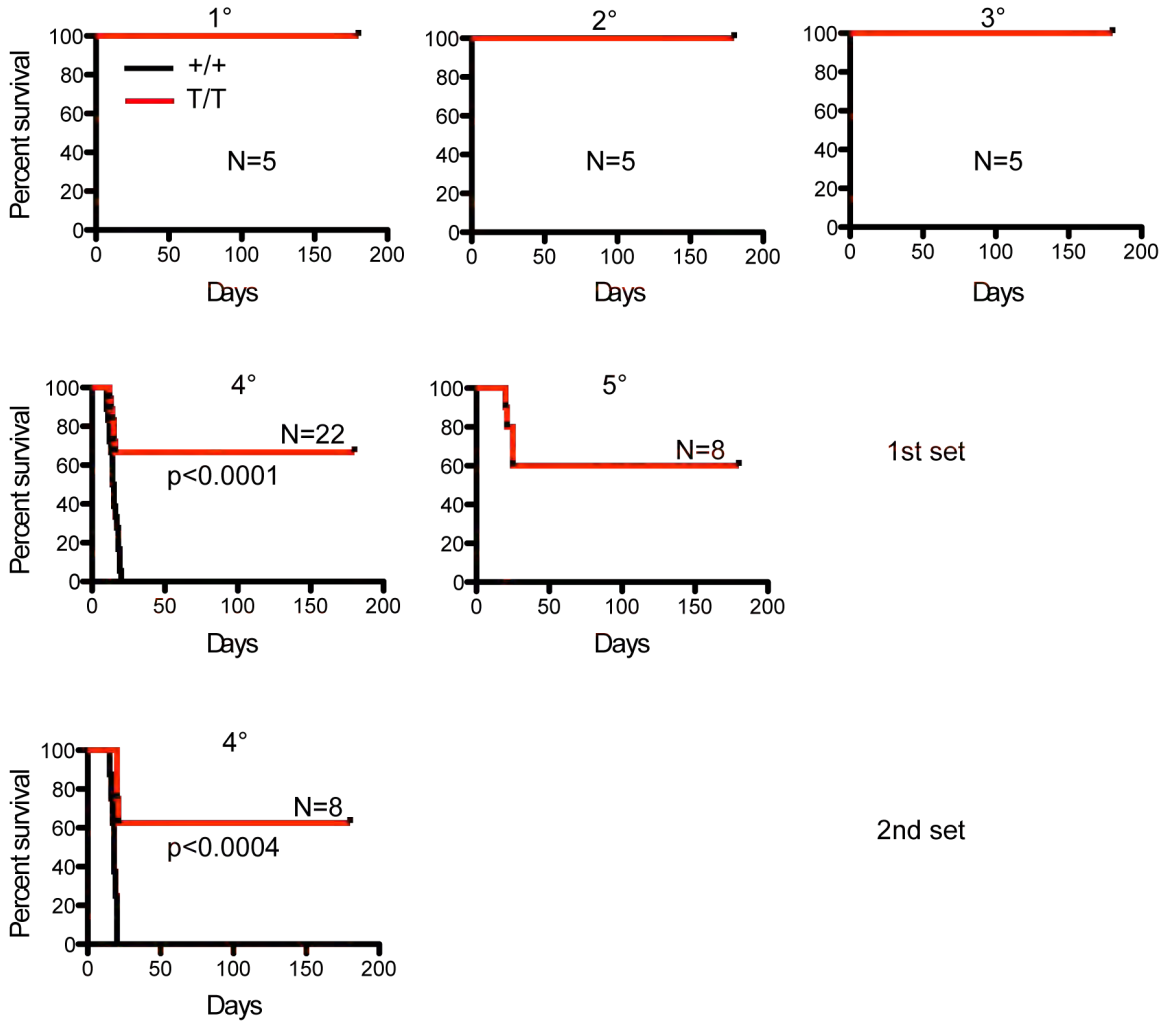
1°
2°
3°
4°
5°
+/+
T/T
N=5
N=5
N=5
N=22
p<0.0001
N=8
1st set
N=8
p<0.0004
2nd set
Percent survival
Days
0
20
40
60
80
100
0
50
100
150
200

Fig.4.4b: HSCs in the transplant recipients are derived from donor bone marrow. FACS analyses of BM cells stained with the CD45.2+ antibody along with the HSC cocktail from wild-type (+/+) (upper panel) and *Smurf2*$^{T/T}$ (T/T) (lower panel) littermates are presented. Live cells are displayed (propidium iodide excluding). Lin- cells are gated out (left panel) and stained for CD45.2 (middle left panel). The CD45.2+ (donor) cells are gated (middle left panel) and then further stained for Sca1 and c-kit (middle right panel). The LSK population (Lin- Sca+ c-kit+) cells are gated (middle right panel) and stained for CD135 and CD150 (right panel) to determine the LT-HSC population (Lin-, Sca+, c-kit+, CD135-, CD150+).

Fig.4.4b

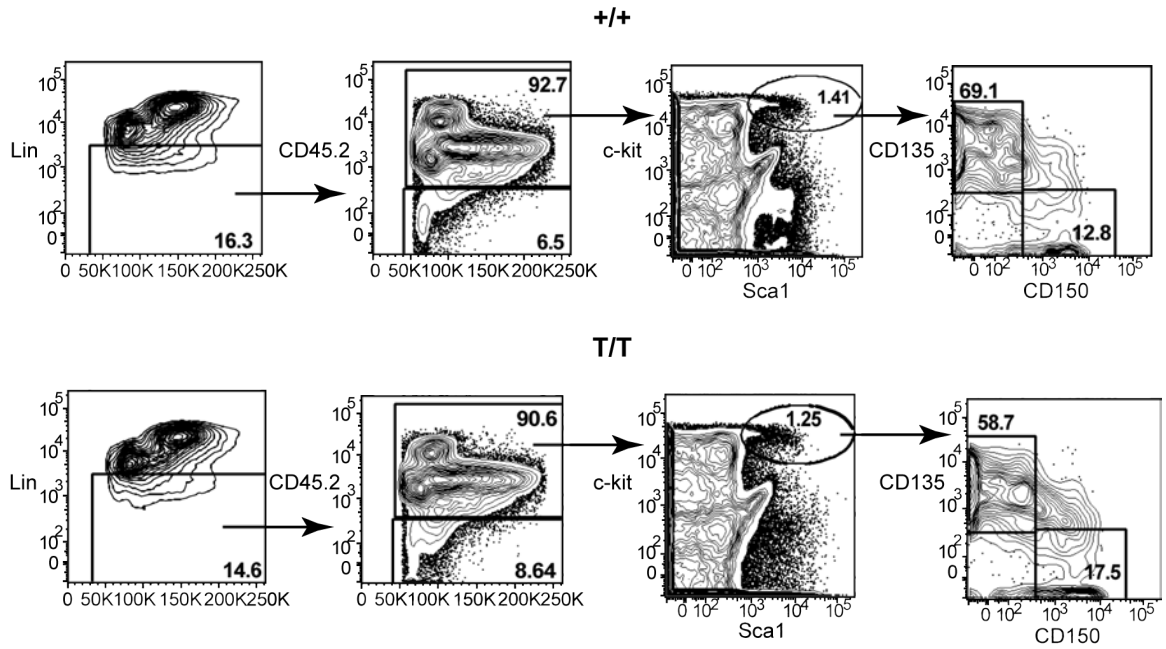
+/+
Lin
16.3
CD45.2
92.7
6.5
c-kit
1.41
Sca1
CD135
69.1
12.8
CD150
T/T
Lin
14.6
CD45.2
90.6
8.64
c-kit
1.25
Sca1
CD135
58.7
17.5
CD150

Fig.4.4c: HSCs from reconstituted transplant recipients can form all the blood cell lineages effectively. Recipients of each transplantation from both wild-type (+/+) and *Smurf2*$^{T/T}$ (T/T) mice (n=3) were bled 4 months after transplantation and complete blood counts were performed. Recipients of both wild-type (+/+) and *Smurf2*$^{T/T}$ (T/T) BM were able to form WBCs, Lymphocytes, Granulocytes and Monocytes effectively.

Fig.4.4c

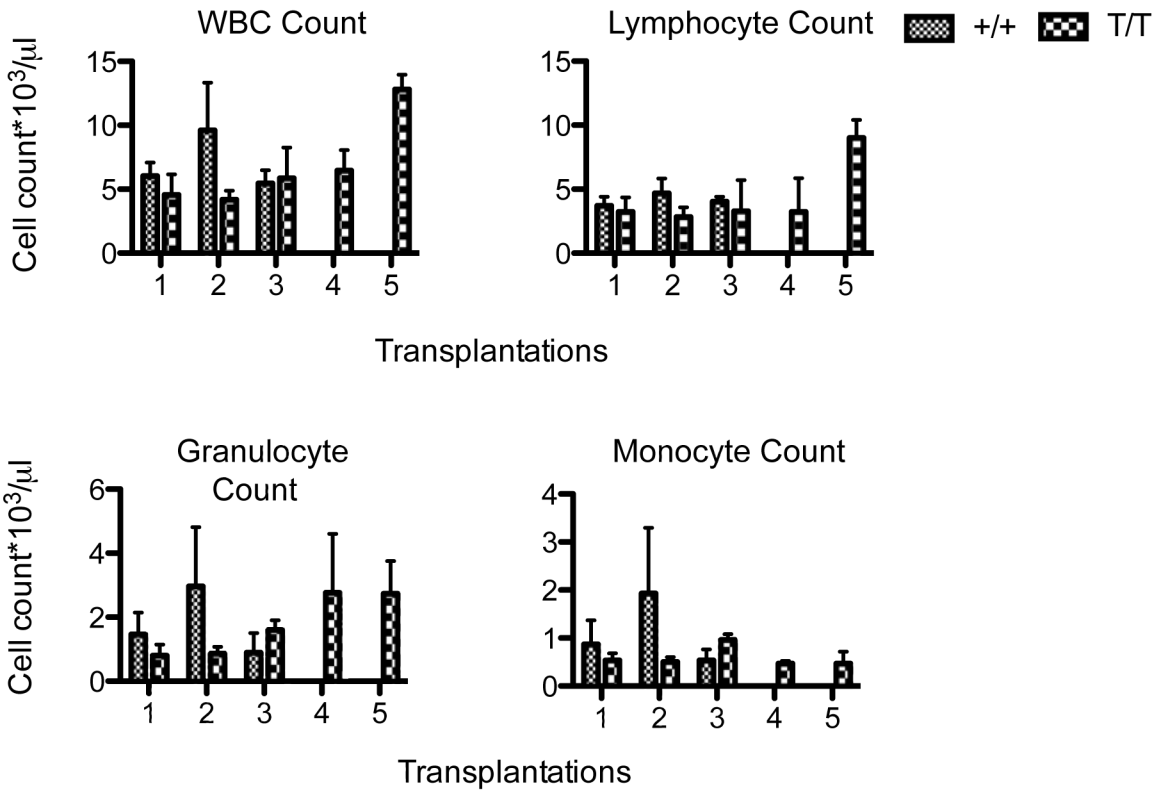
WBC Count
Lymphocyte Count
+/+
T/T
Cell count*10^3/µl
15
10
5
0
1 2 3 4 5
Transplantations
Granulocyte Count
Monocyte Count
6
4
2
0
4
3
2
1
0

Fig.4.4d: Recipients of *Smurf2*$^{T/T}$ (T/T) BM display increased total BM and LT-HSC number in the serial transplantation experiment. BM counts from recipients of successive transplants from wild-type (+/+) (open bars) and *Smurf2*$^{T/T}$ (T/T) (black bars) donors (left panels) are shown. LT-HSC counts from the same animals as determined by FACS analysis are displayed in the right panels. Upper panel is the 1st set of transplantations. Lower panel is the 2nd repeat. Since WT (+/+) recipients were not available after the 3rd transplantation, a 3rd transplant WT (+/+) recipient was sacrificed as a control for the 4th and 5th transplantation experiments. In each case, the *Smurf2*$^{T/T}$ (T/T) mice exhibited increased total BM and LT-HSC populations compared to WT (+/+).

Fig.4.4d

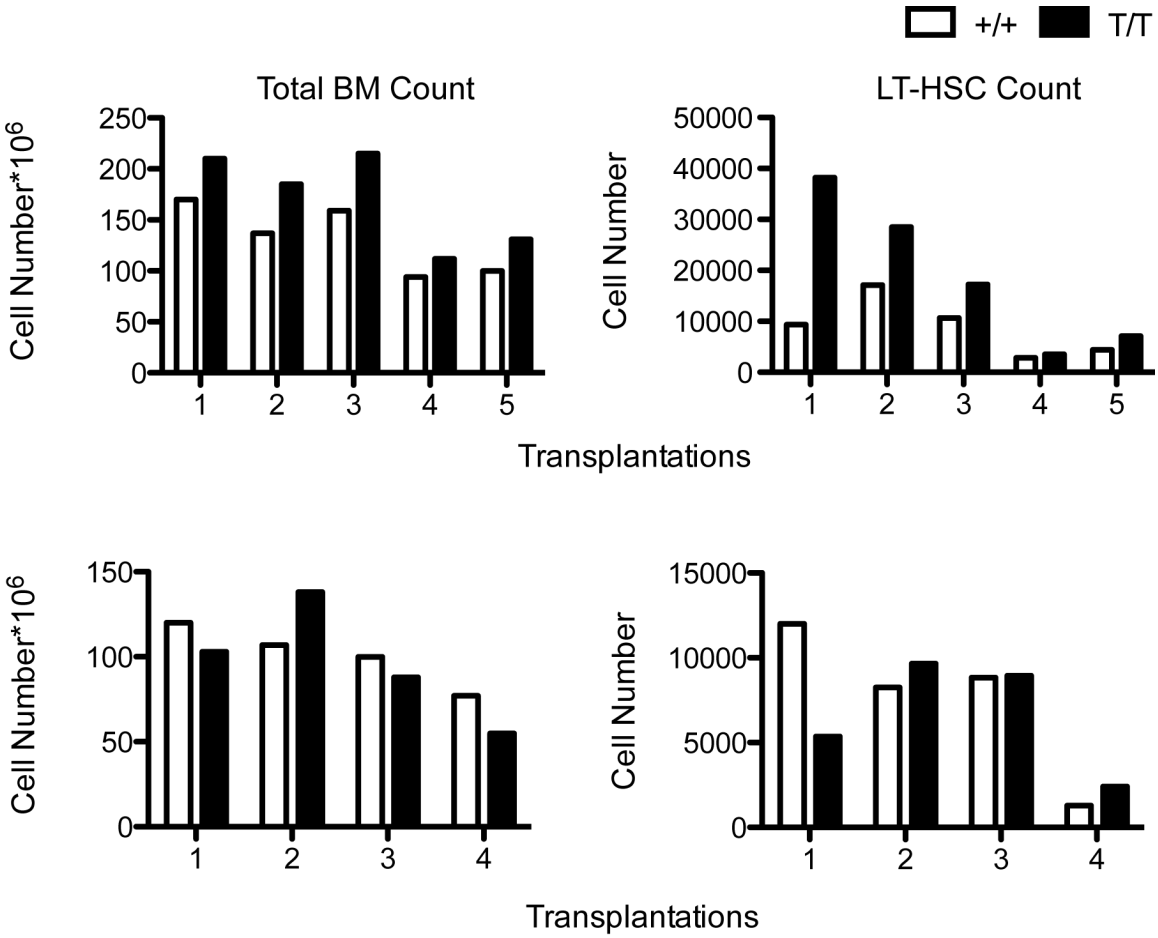
+/+
T/T
Total BM Count
LT-HSC Count
Cell Number*10^6
Cell Number
250
200
150
100
50
0
50000
40000
30000
20000
10000
0
1
2
3
4
5
Transplantations
150
100
50
0
15000
10000
5000
0
1
2
3
4
Transplantations

Aged Smurf2-deficient LT-HSCs exhibit better self-renewal capacity *in vivo*

To investigate if the old Smurf2-deficient LT-HSCs also exhibited better self-renewal capacity compared to their wild-type counterparts we performed serial transplantation experiments using 24-month old wild-type and Smurf2-deficient littermates as donors. The old Smurf2-deficient mice were able to carry forward the transplantations to the 4^{th} cycle with 100% of the recipients surviving the 4^{th} transplant, while the recipients of wild-type marrow died within 20 days of the 4^{th} transplantation (Fig.4.5a). CBC counts from the bloods of the reconstituted recipients revealed that the HSCs from both wild-type and Smurf2-deficient mice were able to effectively form the various blood cell lineages (Fig.4.5b). Similar to the recipients of young Smurf2-deficient marrow, the old recipients also maintained the increase in total BM count as well as LT-HSC numbers over successive transplants (Fig.4.5c). Thus, the increased self-renewal capacity of the Smurf2-deficient mice was sustained as the mice aged. This indicates that the increased self-renewal capacity of the young Smurf2-deficient LT-HSCs did not lead these mice to exhaust sooner.

Fig.4.5a: Aged *Smurf2*$^{T/T}$ (T/T) deficient mice exhibit increased self-renewal capacity *in vivo.* Kaplan-Meier curves from the serial transplantation experiment showing survival of recipients of wild-type (+/+) and *Smurf2*$^{T/T}$ (T/T) BM over successive transplants are displayed. 5*10^6 BM cells from a healthy 24 month-old WT (+/+) and *Smurf2*$^{T/T}$ (T/T) donor mice (mixed background) are injected into lethally irradiated (10Gy) recipient mice *(mixed BL/6:129/Sv,* n=5*)* for the 1st 3 transplantations. For the 4th transplantation, BMs from 3° transplant recipients were injected into 10 recipient mice each. Recipients of *Smurf2*$^{T/T}$ (T/T) BM were able to reconstitute mice over 4 transplants, compared to 3 for wild-type, $p<0.0001$. Curve comparison was performed using the log-rank test.

Fig.4.5a

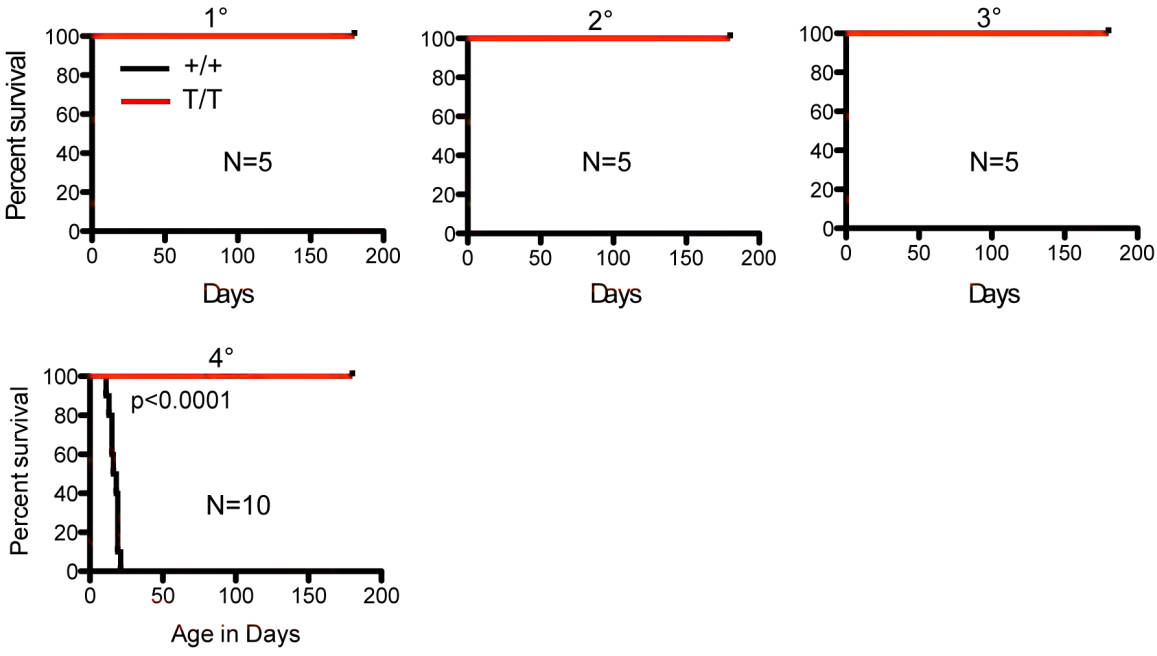
1°
2°
3°
4°
Percent survival
+/+
T/T
N=5
N=5
N=5
p<0.0001
N=10
Days
Days
Days
Age in Days
0
20
40
60
80
100
0
50
100
150
200

Fig.4.5b: HSCs from reconstituted transplant recipients can reconstitute all the blood cell lineages effectively. Recipients of each transplantation from aged wild-type (+/+) and *Smurf2*$^{T/T}$ (T/T) (n=3) mice were bled 4 months after transplantation and complete blood counts were performed. Recipients of both aged wild-type (+/+) and *Smurf2*$^{T/T}$ (T/T) BM were able to form WBCs, Lymphocytes, Granulocytes and Monocytes effectively and with no apparent difference.

Fig.4.5b

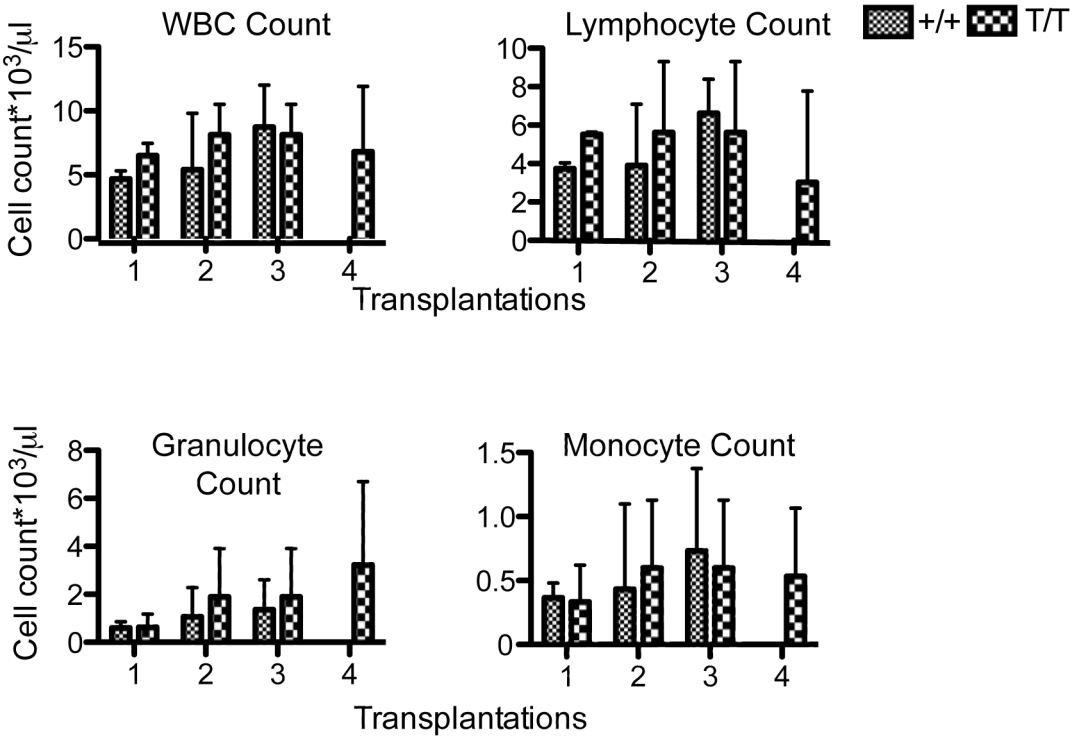
WBC Count
Lymphocyte Count
+/+
T/T
Cell count*10^3/µl
15
10
5
0
10
8
6
4
2
0
1
2
3
4
Transplantations
Granulocyte Count
Monocyte Count
8
6
4
2
0
1.5
1.0
0.5
0
1
2
3
4
Transplantations

Fig.4.5c: Recipients of aged *Smurf2*$^{T/T}$ (T/T) BM display increased total BM and LT-HSC number in the serial transplantation experiment. BM counts from recipients of successive transplants from aged wild-type (+/+) (black bars) and *Smurf2*$^{T/T}$ (T/T) (grey bars) donors (upper panel) are shown. LT-HSC counts from the same animals as determined by FACS analysis are displayed in the lower panels. The recipients of *Smurf2*$^{T/T}$ BM display a consistent increase in the total BM and LT-HSC count over several transplantations compared with wild-type.

Fig.4.5c

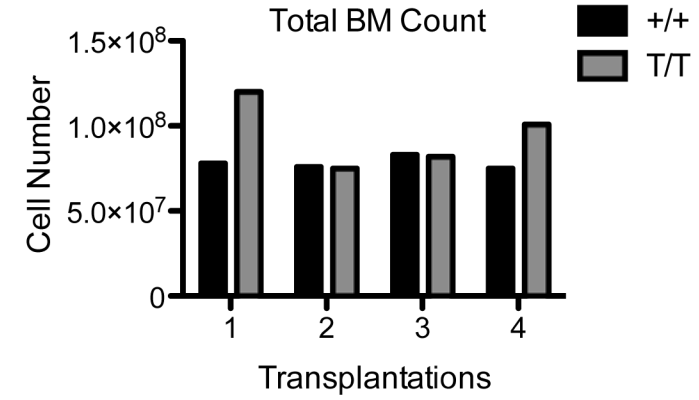
Total BM Count
+/+
T/T
Cell Number
1.5×10^8
1.0×10^8
5.0×10^7
0
1
2
3
4
Transplantations

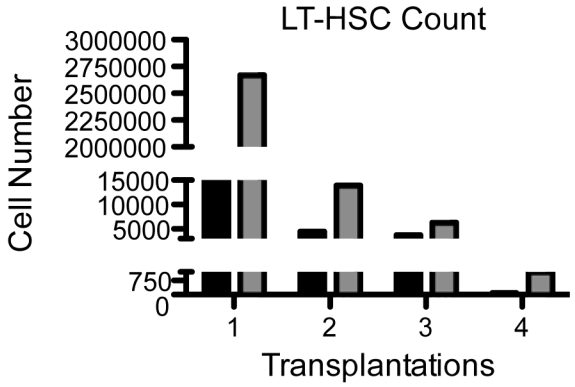
LT-HSC Count
Cell Number
3000000
2750000
2500000
2250000
2000000
15000
10000
5000
750
0
1
2
3
4
Transplantations

Old Smurf2-deficient LT-HSCs compete more robustly than wild-type in a Competitive Repopulation Assay

To test the ability of the Smurf2-deficient LT-HSCs to repopulate the BM of stem-cell depleted mice relative to wild-type LT-HSCs, we performed a competitive repopulation experiment. In this experiment we injected either wild-type or Smurf2-deficient (both CD45.2) BM mixed in a 1:1 ratio with competitor BM (CD45.1/2) into lethally irradiated CD45.1 recipient mice. We performed this experiment using young (2 month old) or old (24 month old) donors and competitors of corresponding ages. We assayed for B-cells, T-cells and Myeloid cells in the blood of the recipient mice every month, starting 2 months after transplantation. To determine the relative contribution of the donor HSCs to the reconstituted cells we calculated the Repopulating Unit (RU) of the donor towards each lineage of cells. The RUs from young wild-type and Smurf2-deficient LT-HSCs were similar (Fig.4.6) in all the 3 lineages we tested. However, the old Smurf2-deficient LT-HSCs exhibited at least ~2-fold better RU activity than their wild-type counterparts (Fig.4.6). These data suggest that the LT-HSCs from aged Smurf2-deficient mice have better short-term repopulating activity than wild-type LT-HSCs.

Fig.4.6: Aged *Smurf2*$^{T/T}$ LT-HSCs display better short-term repopulating ability than wild-type. The competitive repopulation experiment was performed using young (2-month old) and aged (24 month old) wild-type (+/+) and *Smurf2*$^{T/T}$ (T/T) donors with BM from a young CD45.1/2 as a competitor. Recipient mice (n=5) were bled monthly and FACS analysis was performed to determine the percentage of B220+, CD3+ and CD11b+ cells along with CD45.1+ and CD45.2+ cells to estimate the relative contributions from donor and competitive BMs. RUs for each lineage (B-cell, T-cell and Myeloid) are shown for recipients of both genotypes on the Y-axis. The upper panel shows the RUs at 2 months and the lower panel for 3 months after transplantation. Recipients of young BM showed no difference between the wild-type and *Smurf2*$^{T/T}$ donors. But the recipients of BM from aged wild-type and *Smurf2*$^{T/T}$ BM showed a significant increase in the RUs for all 3 lineages tested. Paired Student's *t*-test (2-tailed) was used for statistical analysis. Statistic significance is indicated as: * (P<0.05), ** (P<0.01), and *** (P<0.001).

Fig.4.6

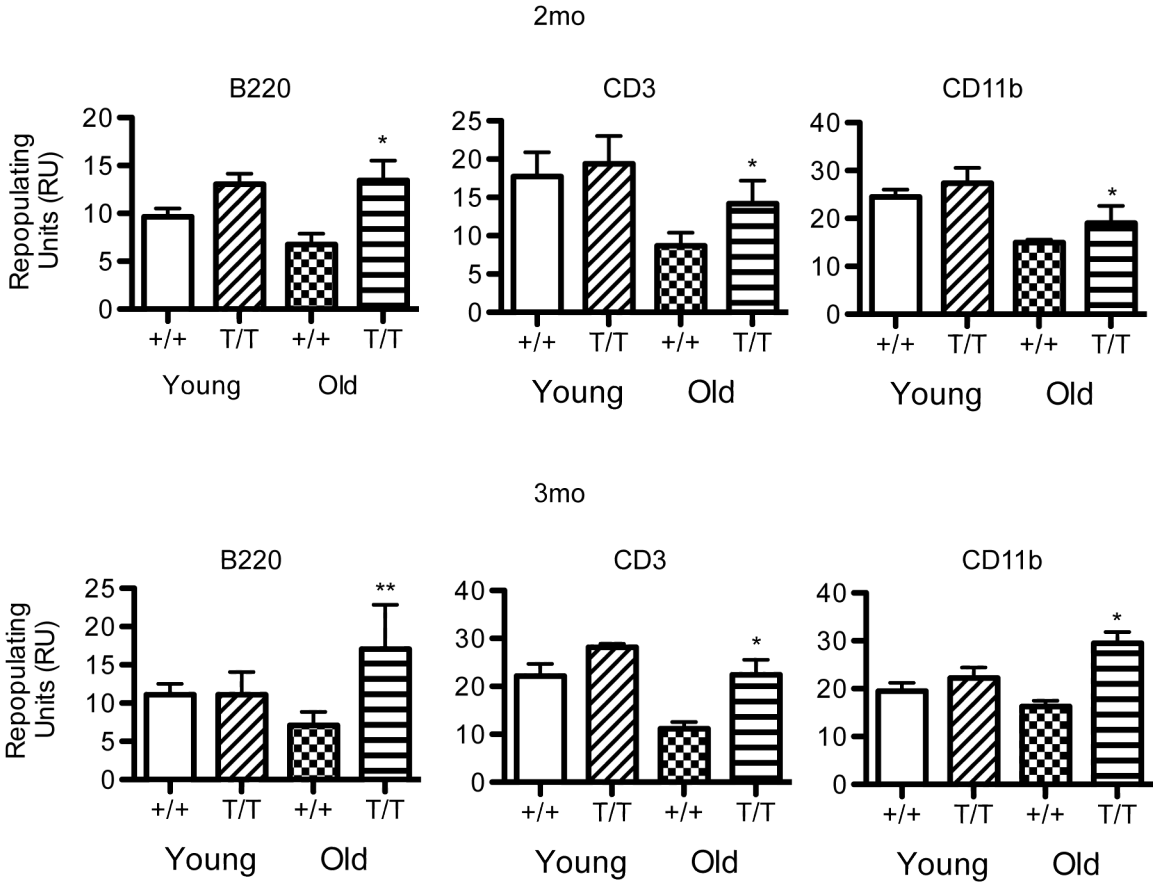
2mo
B220
CD3
CD11b
Repopulating Units (RU)
+/+ T/T +/+ T/T
Young Old
3mo
B220
CD3
CD11b
Repopulating Units (RU)
+/+ T/T +/+ T/T
Young Old

Smurf2-deficient HSCs exhibit increased proliferation and decreased quiescence and this is associated with decreased p16 expression.

In addition to the enhanced competitive repopulation ability of the aged Smurf2-deficient LT-HSCs (Fig.4.6), the young and old Smurf2-deficient LT-HSCs also have better self-renewal capacity (Figs.4.4 and 4.5). This led us to investigate the cell-cycle profiles of Smurf2-deficient HSCs to test if they proliferate better than wild-type. We stained the LSK, CD135$^-$ BM cells from both genotypes for Ki67 and DAPI. The Smurf2-deficient LT-HSCs exhibited increased numbers (1.5% in wild-type to 6% in Smurf2-deficient) of cells in the S-phase and decreased numbers of cells in the G1 phase (Fig.4.7a). We further labeled the wild-type and Smurf2-deficient mice with BrdU and found that the Smurf2-deficient LSK, CD150+ cells exhibited increased proliferation compared with wild-type (Fig.4.7b).

p16^{INK4a} deficiency in the HSC compartment attenuated the age-induced decline in proliferation and function [192], which was a phenotype that we also found in the Smurf2-deficient LT-HSCs in this study. Since the spleens and MEFs from Smurf2-deficient mice have been shown to exhibit decreased p16^{INK4a} expression, we investigated whether the BM from these mice also behaved similarly. Aged Smurf2-deficient BM exhibited lower p16^{INK4a} expression compared to wild-type by quantitative Real-time PCR (Fig.4.8a). When we compared p16^{INK4a} expression within the recipients of aged wild-type and Smurf2-deficient BM from different stages of the serial transplantation experiment, we found that the Smurf2-deficient BMs exhibited attentuated

kinetics of $p16^{INK4a}$ upregulation compared with wild-type (Fig.4.8b). This suggests that the lower levels of $p16^{INK4a}$ expression in the BM of the Smurf2-deficient mice might be responsible for a delayed senescence phenotype within the LT-HSC compartments of these mice. This could potentially be responsible for the increased proliferation phenotype exhibited by the Smurf2-deficient LT-HSCs.

Fig.4.7: *Smurf2*$^{T/T}$ HSCs display increased proliferation and decreased quiescence. (a) BMs from WT (+/+) and *Smurf2*$^{T/T}$ LT-HSCs (T/T) were stained for the HSC cocktail and then fixed and stained for Ki-67 and DAPI. The left panel represents a FACS analysis plot of WT (+/+) LSK, CD135- cells that are stained for DAPI and Ki-67. A similar panel for the *Smurf2*$^{T/T}$ LSK, CD135- cells is shown in the right panel. The *Smurf2*$^{T/T}$ HSCs exhibit increased percentage of cells in the S-phase (6% in T/T to 1% in +/+) and decreased percentage of cells in the G0 phase. **(b)** WT (+/+) and *Smurf2*$^{T/T}$ mice were injected with BrdU and sacrificed 24 hours later. BMs from WT (+/+) and *Smurf2*$^{T/T}$ LT-HSCs (T/T) were stained for the HSC cocktail and then fixed and stained for BrdU. The left panel represents a FACS analysis plot of WT (+/+) LSK, CD150+ cells that are stained for BrdU.). A similar panel for the *Smurf2*$^{T/T}$ LSK, CD150+ cells is shown in the right panel. The *Smurf2*$^{T/T}$ HSCs exhibit increased BrdU incorporation (68% to 36% in the WT).

Fig.4.7

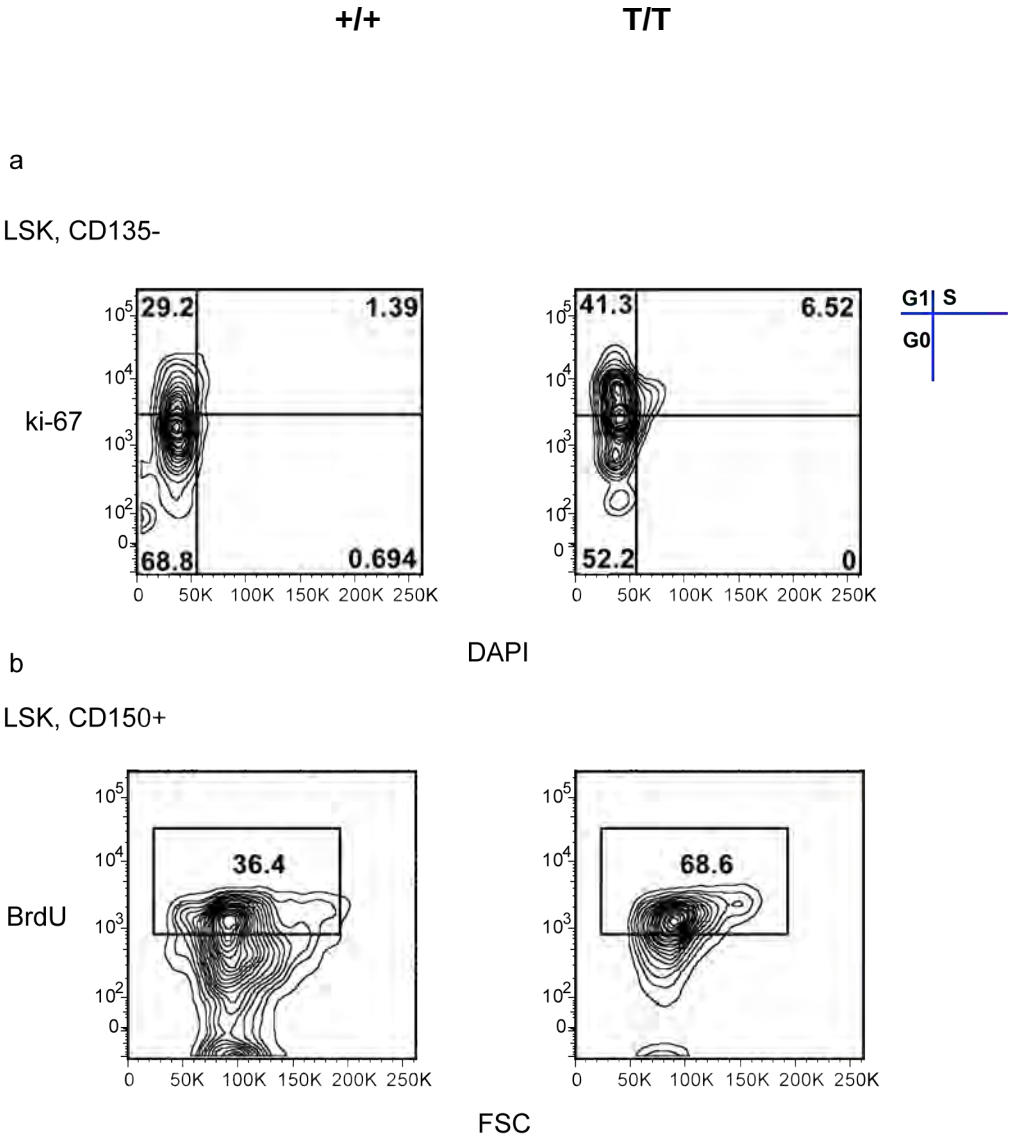
+/+
T/T
a
LSK, CD135-
ki-67
29.2
1.39
68.8
0.694
41.3
6.52
52.2
0
G1
S
G0
DAPI
b
LSK, CD150+
BrdU
36.4
68.6
FSC

Fig.4.8: Aged *Smurf2*$^{T/T}$ BM have lower p16^{INK4a} expression levels. (a) p16^{INK4a} expression in the BM of 18-month old WT (+/+) and *Smurf2*$^{T/T}$ (T/T) mice was analyzed by quantitative RT-PCR. (**b)** p16^{INK4a} expression in the BM of recipients of WT (+/+) (1st transplantation) and *Smurf2*$^{T/T}$ (T/T) (4th transplantation) BM was analyzed by quantitative RT-PCR. Relative expression in wild-type BM cells was set to be 1 after normalization with β-actin. Error bars were calculated from standard deviations of three independent experiments.

Fig.4.8

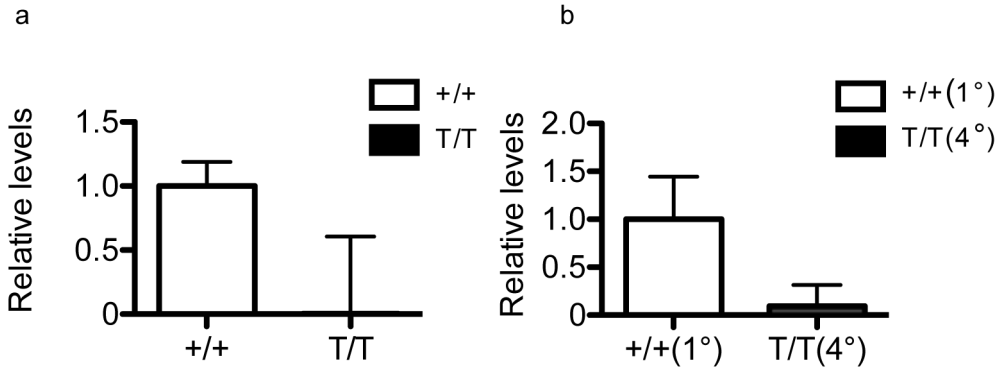
a
Relative levels
1.5
1.0
0.5
0
+/+
T/T
+/+
T/T
b
Relative levels
2.0
1.5
1.0
0.5
0
+/+(1°)
T/T(4°)
+/+(1°)
T/T(4°)

DISCUSSION

In this study we have shown that the Smurf2-deficient mice have increased BM and LT-HSC numbers. This is further associated with increased self-renewal activity of young and old Smurf2-deficient mice in a serial transplantation experiment. Further, only the old (but not the young) Smurf2-deficient mice displayed better reconstitutive capability in a competitive repopulation assay, indicating that the aged Smurf2-deficient LT-HSCs have better short-term repopulating activity than wild-type LT-HSCs. Further, cell cycle analysis of the HSCs determined that the Smurf2-deficient LT-HSCs were less quiescent and tended to proliferate more than wild-type. In addition, $p16^{INK4a}$ expression was lower in aged Smurf2-deficient BM than wild-type. Also, the kinetics of $p16^{INK4a}$ upregulation were attenuated in the recipients of Smurf2-deficient BM in the serial transplantation experiment at different cycles of transplantation. We have previously shown that spleens from the Smurf2-deficient mice exhibit increased proliferative capacity and this is associated with delayed senescence and decreased $p16^{INK4a}$ expression. Our data further show that the aged Smurf2-deficient mice partially mimic the $p16^{INK4a}$ knockout mice, behaving like the aged $p16^{INK4a}$ knockout mice in the competitive repopulation assay [192]. Work from our lab has shown that Smurf2 regulates $p16^{INK4a}$ by ubiquitinating ID1 [246]. ID1 expression is known to be enriched in the HSC compartment in mice [343]. It would be interesting to look at ID1 expression in the LT-HSCs of Smurf2-deficient mice, to test if it is increased compared to the WT-LT-HSCs, thereby providing a plausible molecular mechanism for Smurf2-mediated regulation of $p16^{INK4a}$ activity in the LT-HSC compartment.

Activation of the senescence response has not been well described in stem cell compartments. This is partially due to the fact that most stem cell compartments exhibit high levels of telomerase expression, thereby lessening the burden of telomere shortening on these cells. However, telomere shortening has been demonstrated in murine HSCs [344] during serial transplantation. Further, the phenotypes of the mTERC**−/−** mice indicate that telomere shortening plays an important role in regulating stem cell function. Since Smurf2 is known to be a critical regulator of senescence in response to telomere shortening, we hypothesize that a delayed senescence response in the Smurf2-deficient LT-HSCs, which is associated with the downregulation of $p16^{INK4a}$ in these cells, maybe responsible for the ability of these cells to proliferate better without undergoing stem-cell exhaustion. More work is necessary to ascertain if the senescence response is indeed delayed in the Smurf2-deficient LT-HSCs and if this phenotype is in fact, ID1 dependent.

MATERIALS AND METHODS:

Flow Cytometry

Mice were euthanized with isoflurane and cervical dislocation. Bone marrow was harvested from all 4 limbs of the mice using the femurs, tibiae and humerii. Cells were counted using a hemocytometer. The cells were then resuspended at $6x10^7$/ml in staining medium which consists of Biotin-, flavin and phenol red-deficient RPMI-1640 medium (Invitrogen) supplemented with 10 mM HEPES (pH 7.2), 1 mM EDTA, 2% FBS and 0.02% sodium azide. Bone marrow cells were filtered through 70 µm nylon mesh and incubated with anti-CD16/32 antibody (Bio X Cell) for 10 min on ice to block Fc receptors. Cells were incubated with primary antibodies for 20 min and washed three times. All antibiodies are from e-Bioscience unless otherwise specified. The antibodies used include the Lineage cocktail that contains biotin-conjugated Ter119 (clone TER-119), CD11b (clone M1/70), Ly-6G (Gr1, clone RB6-8C5), CD45R (B220, clone RA3-6B2), CD19 (clone 1D3) and CD3e (clone 145-2C11). Additional antibodies for HSC analysis include Ly-6A/E (Sca1)-FITC (clone D7), CD117 (c-Kit)-PE-Cy7 (clone 2B8), CD135 (Flt3)-PE (clone A2F10) and CD150-APC (clone mShad150). Cells stained with biotin-labeled antibodies (lineage cocktail) are incubated with streptavidin-eFluor 450 for 15 min on ice and washed three times with staining medium. After the final wash, cells are resuspended in 1 µg/ml propidium iodide (PI) in staining medium for the exclusion of dead cells. Flow cytometry analysis is performed on a 5-laser, 18-detector LSR II FACS machine using 405, 488, 561 and 633-nm lasers. Data are analyzed using FlowJo software (Treestar).

Complete Blood Counts

Tail veins of mice were bled into EDTA coated tubes and complete blood counts were performed using the Heska CBC-Diff Veterinary Hematology System (Heska).

Serial transplantation and Competitive Repopulation:

Young (2 mo old) and Old (24 mo old) WT and Smurf2-deficient mice were used as donors for these experiments. B6.SJL-*Ptprc*^{a} *Pepc*^{b}/BoyJ (CD45.1^{+}) aged 8-10 weeks (The Jackson Laboratory) were used as recipients. CD45.1$^{+/-}$ mice were used as the competitors for the competitive repopulation experiment. Recipient mice are treated with antibiotics in drinking water 24 hours prior to exposure to radiation. Recipient mice are exposed to a lethal dose of 10 grays (1000 Rads) whole body radiation using a Cesium-137 source. At least 5 recipient mice were used for each donor. For later (>3) cycles of transplantation, at least 10 recipient mice were used per donor. 5x10^{6} bone marrow cells (~200 HSCs) per recipient mouse were injected retro-orbitally into the recipient mice. Anti-mouse CD45.2 FITC (Clone 104) and Anti-mouse CD45.1 Pe-Cy7 (Clone A20) were used to analyze the relative contributions from the donors and recipients in the bloods and bone marrows from the reconstituted recipients.

For the competitive repopulation experiment, Repopulating Units were calculated using the formula $RU_{(D)} = RU_{(C)} \frac{\%D}{100-\%D}$ where $RU_{(C)}$ was set as 20 [345].

$RU_{(C)}$ was defined as 1 per 10^5 competitor cells where C stands for competitor and D for donor)

Cell Cycle Analysis:

Mice were injected intra-peritoneally with 1mg BrdU per mouse every 6 hours for 24 hours as described previously[346]. Bone marrow cells were stained for the LT-HSCs as described above, and fixed and permeabilized using the BrdU Flow kit (BD Biosciences) and stained for FITC-BrdU or PerCp-Cy5.5-ki-67 (Clone Sola15) for 20 minutes. Ki67 stained cells were further incubated with DAPI for 30 minutes at room temperature as described previously [347].

Quantitative PCR

Total RNA was isolated from freshly dissected tissues using Trizol (Invitrogen). RNA was reverse-transcribed using Superscript II (invitrogen). Real-time PCR was carried out on a MyiQ iCycler using a SYBR Green PCR kit (Bio-Rad). The following primers were used: β-actin (F: 5'-GCTCTTTTCCAGCCTTCCTT-3', R: 5'-GTGCTAGGAGCCAGAGCAGT-3') and p16 (5'-CGAACTCTTTCGGTCG-TACCC-3' and 5'-CGAATCTGCACCGTAGTTGAG-3').

CHAPTER V

SUMMARY & CONCLUSIONS

Cellular senescence has been postulated to function in an antagonistically pleiotropic manner, by preventing malignant transformation in young mammals but promoting aging over a lifespan, thus providing support for the Antagonistic Pleiotropy Theory of aging. Several studies have provided evidence strongly supporting the tumor suppressor function of senescence [77,83], however, the evidence supporting senescence's role in aging is as yet inconclusive. In this thesis I attempted to test the Antagonistic Pleiotropy Theory of senescence and aging. I manipulated the senescence response *in vivo*, by manipulating the expression of a key senescence regulator, Smurf2 and tested the effects of such manipulation on cancer and aging.

In Chapter II I described the generation of a Smurf2-deficient mouse model that exhibited an increased susceptibility to spontaneous tumorigenesis, indicating that Smurf2 has a tumor suppression function. Increased tumorigenesis was preceded by an impaired senescence response and associated with decreased p16 expression in pre-malignant spleens and primary fibroblasts of Smurf2-deficient mice. In Chapter III I characterized the lymphomas from the Smurf2-deficient mice as GCB-type DLBCL. Further, we showed that Smurf2 is the E3 ligase for YY1, a transcription factor known to activate c-Myc that is postulated to play a role in GC development [330]. These findings suggest that Smurf2's tumor suppressor function is not merely restricted to its regulation of the senescence response, but is also associated with its function as an E3 ligase. Smurf2-mediated ubiquitination of YY1, leading to the activation of c-Myc is one such important regulatory axis in lymphomagenesis. The Smurf2-deficient

mice also develop other kinds of tumors, including hepatocellular carcinoma, intestinal adenocarcinoma and sarcomas. There could be other potential targets of Smurf2-mediated ubiquitination that may play an important role in the development of these tumors, or they could arise as a consequence of the delayed senescence in the Smurf2-deficient mice.

The fact that Smurf2 regulates tumor suppression through multiple mechanisms adds a layer of complexity to our hypothesis that Smurf2 functions as an antagonistic pleiotropic trait by regulating senescence. Since we do not know which mechanism is more critical to Smurf2's function in tumor suppression, it would be interesting to devise ways to uncouple the 2 functions of Smurf2 in regulating senescence, and as an E3 ligase, and test if the functions on tumor suppression *in vivo* are different.

We have also found that low Smurf2 expression is associated with poor prognosis in patients with DLBCL. This correlates with a previous observation that high levels of YY1 expression correlate with poor survival prognosis in DLBCL patients [328] and suggests that the Smurf2-YY1 regulatory axis is a useful predictor of clinical outcome in DLBCL patients and a potential therapeutic target for treatment of DLBCL. Current therapies for DLBCL are not adequate, and 50% patients do relapse even after therapy [348]. While R-CHOP is more specific than CHOP therapy in that it targets B-cells, more targeted therapy is essential to ensure complete cure. Drugs that specifically target the GC B-cell are essential to the treatment of GCB-type DLBCL. We believe that the Smurf2-YY1 axis might provide an important therapeutic target in developing more

specific therapy for GCB-type DLBCL. Further, our finding that Smurf2 regulates c-Myc in GCB type DLBCL also has therapeutic value. Thus far, c-Myc has only been known to play a role in Burkitt's Lymphoma, but not the other types of DLBCL. We now provide evidence that c-Myc can also be targeted in other types of DLBCL.

After confirming that Smurf2 functions as a tumor suppressor *in vivo*, we chose to investigate the role of Smurf2 in aging in Chapter IV. We found that the Smurf2-deficient mice have enhanced LT-HSC activity, and proliferate better than wild-type HSCs. Furthermore, we found that the aged Smurf2-deficient LT-HSCs also exhibit better competitive ability *in vivo,* and this enhanced activity was associated with lower p16 expression in aged Smurf2-deficient BM. The activation of senescence in stem cell compartments is not well described. Our findings suggest that Smurf2-deficiency might potentially regulate the senescence response in the LT-HSC compartment through its regulation of p16. However, more work is necessary to conclusively determine Smurf2's function in aging.

In this thesis, I have described two opposing functions of Smurf2: as a tumor suppressor in young mice, and a negative regulator of HSC activity in aged mice. These paradoxical functions of Smurf2 suggest that by regulating the senescence response, Smurf2 functions as an antagonistic pleiotropic trait *in vivo*. Further, we have shown that Smurf2 regulates the senescence response through its regulation of p16.

p16 is an important regulator of senescence that is transcribed from the INK4a/ARF locus, along with ARF. p16 expression has been shown to increase with increasing passage number of cells in culture. In the case of MEFs, senescence in culture occurs despite their having long telomeres and high levels of telomerase, but this telomere-independent clock is attenuated in cells genetically deficient in the INK4a/ARF locus [349]. Further, the p16 null mice have been shown to be tumor prone [80]. Activation of an oncogene such as Ras leads to the activation of a tumor-protective senescence response called oncogene-induced senescence through the upregulation of p16 [350]. The expression of p16 is known to increase in rodent and human tissues with age [351,352], suggesting that is an important regulator of aging. The age-induced expression of p16INK4a in adult stem cells has been shown to be associated with impaired tissue regeneration of the pancreatic islets, hematopoietic system, and neuronal progenitors [192-194]. Complementarily, the p16 deficient mice exhibit increased regeneration potential [194,192,193]. High levels of p16 have been postulated to result in p16-induced senescence of the stem cells. Taken together, these data suggest that p16 may function as an antagonistic pleiotropic trait through its regulation of the senescence response *in vivo*. Our findings that Smurf2 functions antagonistically by regulating the senescence response through its regulation of p16, are supported by the findings that p16 functions as an antagonistic pleiotropic trait itself.

In vivo data in mammalian model systems to support the antagonistic pleiotropy theory of senescence and aging is still meager. Apart from p16 and

p53 [353], there are few examples of genes that function as senescence regulating antagonistic pleiotropic traits. A general problem in the field is that the role of senescence in aging has not been conclusively proven. Recent criticism of the antagonistic pleiotropy theory of senescence and aging suggests that the beneficial and detrimental effects of senescence might occur at any age [354]. For example, senescence might function as a tumor suppressor mechanism even in the old, while leading to aging phenotypes in the young, and it has been shown that senescent cells, once formed tend to stay in the organism for years [105,355]. However, a recent study has shown that when senescent cells marked by p16 are cleared from a progeroid mouse model, some of the aging phenotypes are delayed [356]. It might be interesting to speculate that with the help of this model as a tool, the temporal clearance of senescent cells might help to dissect the beneficial (tumor suppressive) and detrimental (acceleration of aging phenotypes) effects of senescence at different ages. This would help to conclusively prove the role of senescence as an antagonistic pleiotropic trait.

FUTURE DIRECTIONS

The function of Smurf2 in aging needs to be explored more thoroughly in order to determine that Smurf2 truly functions as an antagonistic pleiotropic trait. It would be interesting to look at other stem cell compartments in the Smurf2-deficient mice to test if their function is as enhanced as the HSC compartment of these mice. The generation of transgenic mice that overexpress either wild-type or the C716A ligase-dead Smurf2 can help in furthering our understanding of Smurf2's function in senescence and aging. If increased Smurf2 expression truly functions to enhance the aging process, we might speculate that these mice will exhibit shorter life-span than wild-type and also have other aging-associated phenotypes. It will be crucial to test the LT-HSC activity in these mice as well, to see if it is abrogated, compared to wild-type. Further the comparison between the mice that overexpress wild-type versus the C176A mutant Smurf2 will be interesting. Since we have already shown that Smurf2's role as a tumor suppressor also involves its E3 ligase function, I believe this comparison will provide some interesting differences that might enable us to tease out the different functions of Smurf2 in various processes.

Further, since we have shown that Smurf2 regulates p16 by targeting ID1 for ubiquitin-mediated degradation [246], the generation of the Smurf2, ID1 double knock-out mouse model would also be a powerful tool to test if the Smurf2-p16 axis is truly responsible for the senescence-regulated phenotypes displayed by the Smurf2 knockout mouse.

It would be interesting to investigate other targets of Smurf2-mediated ubiquitination and study their function in tumorigenesis. One method to identify new targets is to annotate all proteins that contain a PPXY motif, and have the potential to interact with Smurf2's WW domain. A thorough literature review will then identify genes from this list that play a role in tumorigenesis and are potentially important for Smurf2's function in tumor suppression, and are thus, of interest to us.

I have shown in Chapter 3, that Smurf2 regulates YY1 and this might be responsible for the lymphomagenesis in the Smurf2-deficient mice. In order to further confirm that Smurf2 regulates YY1, it is essential that the interaction between Smurf2 and YY-1 be demonstrated endogenously. Further, in order to conclusively show that Smurf2 is the E3 ligase that ubiquitinates YY1 under physiological conditions, the *in vivo* ubiquitination assay must be performed using endogenously expressed YY1 and Smurf2.

I have shown that Smurf2 regulates lymphoma cell proliferation through its regulation of YY1 in a GCB lymphoma cell line. While the role of Smurf2 in regulating lymphoma cell proliferation has been adequately demonstrated by both the overexpression and knockdown experiments, YY1 was shown to be necessary for Smurf2's effect on cell proliferation in the double knockdown experiment where both Smurf2 and YY1 were simultaneously knocked down using shRNA. In order to show that YY1 is sufficient for Smurf2's effect on cell proliferation, YY1 must be overexpressed in the cell line to see if it increases cell proliferation, akin to Smurf2 knockdown. Further, it will be interesting to test if in

the double overexpression experiment, the increased YY1 expression can partially or completely abrogate Smurf2's effect on cell proliferation. I have previously tried to overexpress YY1 in the SuDHL6 cell line and found that the cells underwent apoptosis. This is not completely unexpected, since we as well as others have shown that YY1 transactivates c-Myc. Increased levels of c-Myc might be responsible for the apoptosis. This experiment should be performed in a lymphoma cell line with a low endogenous level of YY1, since c-Myc levels are extremely critical to the downstream consequences on cell proliferation. It is known that low levels of c-Myc induce cell proliferation whereas high levels of c-Myc induce apoptosis. As YY1 levels are high in the SuDHL6 cell line, any increased overexpression might lead to the c-Myc levels crossing the critical threshold required for the induction of apoptosis.

My work has shown that the lymphomas in the Smurf2-deficient mice are germinal center derived. I have also shown that spleens from healthy, young, Smurf2-deficient mice proliferate better than WT. Characterization of the germinal centers in the Smurf2-deficient mice would provide insight into the process of lymphomagenesis in these mice. It would be interesting to test if the germinal center response was in someway enhanced in young Smurf2-deficient mice. It would also be interesting to extend this analysis further by immunizing the healthy Smurf2-deficient mice to elicit a germinal center response. If the germinal center response is enhanced in the immunized Smurf2-deficient mice, it would be interesting to observe if these immunized mice would develop

lymphomas faster than the un-immunized Smurf2-deficient mice as this would greatly decrease the latency of lymphomagenesis in this mouse model.

Bibliography:

1. Hayflick L, Moorhead PS (1961) The serial cultivation of human diploid cell strains. Exp Cell Res 25:585-621
2. Sherwood SW, Rush D, Ellsworth JL, Schimke RT (1988) Defining cellular senescence in IMR-90 cells: a flow cytometric analysis. Proc Natl Acad Sci U S A 85 (23):9086-9090
3. Cristofalo VJ, Phillips PD, Sorger T, Gerhard G (1989) Alterations in the responsiveness of senescent cells to growth factors. J Gerontol 44 (6):55-62
4. Wang E (1995) Senescent human fibroblasts resist programmed cell death, and failure to suppress bcl2 is involved. Cancer Res 55 (11):2284-2292
5. Hampel B, Wagner M, Teis D, Zwerschke W, Huber LA, Jansen-Durr P (2005) Apoptosis resistance of senescent human fibroblasts is correlated with the absence of nuclear IGFBP-3. Aging Cell 4 (6):325-330
6. Goldstein S (1990) Replicative senescence: the human fibroblast comes of age. Science 249 (4973):1129-1133
7. Dimri GP, Lee X, Basile G, Acosta M, Scott G, Roskelley C, Medrano EE, Linskens M, Rubelj I, Pereira-Smith O, et al. (1995) A biomarker that identifies senescent human cells in culture and in aging skin in vivo. Proc Natl Acad Sci U S A 92 (20):9363-9367.
8. Cristofalo VJ, Volker C, Francis MK, Tresini M (1998) Age-dependent modifications of gene expression in human fibroblasts. Crit Rev Eukaryot Gene Expr 8 (1):43-80
9. Shelton DN, Chang E, Whittier PS, Choi D, Funk WD (1999) Microarray analysis of replicative senescence. Curr Biol 9 (17):939-945.
10. Schwarze SR, DePrimo SE, Grabert LM, Fu VX, Brooks JD, Jarrard DF (2002) Novel pathways associated with bypassing cellular senescence in human prostate epithelial cells. J Biol Chem 277 (17):14877-14883
11. Zhang H, Pan KH, Cohen SN (2003) Senescence-specific gene expression fingerprints reveal cell-type-dependent physical clustering of up-regulated chromosomal loci. Proc Natl Acad Sci U S A 100 (6):3251-3256
12. Zhang H, Herbert BS, Pan KH, Shay JW, Cohen SN (2004) Disparate effects of telomere attrition on gene expression during replicative senescence of human mammary epithelial cells cultured under different conditions. Oncogene 23 (37):6193-6198
13. Harley CB, Futcher AB, Greider CW (1990) Telomeres shorten during ageing of human fibroblasts. Nature 345 (6274):458-460.
14. Harley CB (1991) Telomere loss: mitotic clock or genetic time bomb? Mutat Res 256 (2-6):271-282.
15. Holt SE, Shay JW, Wright WE (1996) Refining the telomere-telomerase hypothesis of aging and cancer. Nat Biotechnol 14 (7):836-839.
16. Blackburn EH (2001) Switching and signaling at the telomere. Cell 106 (6):661-673

17. Greider CW, Blackburn EH (1985) Identification of a specific telomere terminal transferase activity in Tetrahymena extracts. Cell 43 (2 Pt 1):405-413
18. Kim NW, Piatyszek MA, Prowse KR, Harley CB, West MD, Ho PL, Coviello GM, Wright WE, Weinrich SL, Shay JW (1994) Specific association of human telomerase activity with immortal cells and cancer. Science 266 (5193):2011-2015.
19. Shay JW, Bacchetti S (1997) A survey of telomerase activity in human cancer. Eur J Cancer 33 (5):787-791.
20. Hayflick L (1976) The cell biology of human aging. N Engl J Med 295 (23):1302-1308.
21. Goldstein S, Singal DP (1974) Senescence of cultured human fibroblasts: mitotic versus metabolic time. Exp Cell Res 88 (2):359-364
22. Vaziri H, Benchimol S (1998) Reconstitution of telomerase activity in normal human cells leads to elongation of telomeres and extended replicative life span. Curr Biol 8 (5):279-282.
23. Kiyono T, Foster SA, Koop JI, McDougall JK, Galloway DA, Klingelhutz AJ (1998) Both Rb/p16INK4a inactivation and telomerase activity are required to immortalize human epithelial cells. Nature 396 (6706):84-88.
24. Bodnar AG, Ouellette M, Frolkis M, Holt SE, Chiu CP, Morin GB, Harley CB, Shay JW, Lichtsteiner S, Wright WE (1998) Extension of life-span by introduction of telomerase into normal human cells. Science 279 (5349):349-352.
25. Hahn WC, Stewart SA, Brooks MW, York SG, Eaton E, Kurachi A, Beijersbergen RL, Knoll JH, Meyerson M, Weinberg RA (1999) Inhibition of telomerase limits the growth of human cancer cells. Nat Med 5 (10):1164-1170
26. Zhang X, Mar V, Zhou W, Harrington L, Robinson MO (1999) Telomere shortening and apoptosis in telomerase-inhibited human tumor cells. Genes Dev 13 (18):2388-2399
27. d'Adda di Fagagna F, Reaper PM, Clay-Farrace L, Fiegler H, Carr P, Von Zglinicki T, Saretzki G, Carter NP, Jackson SP (2003) A DNA damage checkpoint response in telomere-initiated senescence. Nature 426 (6963):194-198
28. Takai H, Smogorzewska A, de Lange T (2003) DNA damage foci at dysfunctional telomeres. Curr Biol 13 (17):1549-1556
29. Herbig U, Jobling WA, Chen BP, Chen DJ, Sedivy JM (2004) Telomere shortening triggers senescence of human cells through a pathway involving ATM, p53, and p21(CIP1), but not p16(INK4a). Mol Cell 14 (4):501-513
30. Serrano M, Lin AW, McCurrach ME, Beach D, Lowe SW (1997) Oncogenic ras provokes premature cell senescence associated with accumulation of p53 and p16INK4a. Cell 88 (5):593-602.
31. Zhu J, Woods D, McMahon M, Bishop JM (1998) Senescence of human fibroblasts induced by oncogenic Raf. Genes Dev 12 (19):2997-3007.
32. Lin AW, Barradas M, Stone JC, van Aelst L, Serrano M, Lowe SW (1998) Premature senescence involving p53 and p16 is activated in response to constitutive MEK/MAPK mitogenic signaling. Genes Dev 12 (19):3008-3019.
33. Robles SJ, Adami GR (1998) Agents that cause DNA double strand breaks lead to p16INK4a enrichment and the premature senescence of normal fibroblasts. Oncogene 16 (9):1113-1123.

34. Di Leonardo A, Linke SP, Clarkin K, Wahl GM (1994) DNA damage triggers a prolonged p53-dependent G1 arrest and long-term induction of Cip1 in normal human fibroblasts. Genes Dev 8 (21):2540-2551
35. Chen Q, Fischer A, Reagan JD, Yan LJ, Ames BN (1995) Oxidative DNA damage and senescence of human diploid fibroblast cells. Proc Natl Acad Sci U S A 92 (10):4337-4341.
36. von Zglinicki T, Saretzki G, Docke W, Lotze C (1995) Mild hyperoxia shortens telomeres and inhibits proliferation of fibroblasts: a model for senescence? Exp Cell Res 220 (1):186-193.
37. Parrinello S, Samper E, Krtolica A, Goldstein J, Melov S, Campisi J (2003) Oxygen sensitivity severely limits the replicative lifespan of murine fibroblasts. Nat Cell Biol 5 (8):741-747
38. Ramirez RD, Morales CP, Herbert BS, Rohde JM, Passons C, Shay JW, Wright WE (2001) Putative telomere-independent mechanisms of replicative aging reflect inadequate growth conditions. Genes Dev 15 (4):398-403
39. Sherr CJ, DePinho RA (2000) Cellular senescence: mitotic clock or culture shock? Cell 102 (4):407-410.
40. Ogryzko VV, Hirai TH, Russanova VR, Barbie DA, Howard BH (1996) Human fibroblast commitment to a senescence-like state in response to histone deacetylase inhibitors is cell cycle dependent. Mol Cell Biol 16 (9):5210-5218.
41. Villeponteau B (1997) The heterochromatin loss model of aging. Exp Gerontol 32 (4-5):383-394.
42. Howard BH (1996) Replicative senescence: considerations relating to the stability of heterochromatin domains. Exp Gerontol 31 (1-2):281-293
43. Wright WE, Shay JW (2002) Historical claims and current interpretations of replicative aging. Nat Biotechnol 20 (7):682-688
44. Wright WE, Shay JW (2001) Cellular senescence as a tumor-protection mechanism: the essential role of counting. Curr Opin Genet Dev 11 (1):98-103.
45. Wei S, Sedivy JM (1999) Expression of catalytically active telomerase does not prevent premature senescence caused by overexpression of oncogenic Ha-Ras in normal human fibroblasts. Cancer Res 59 (7):1539-1543.
46. Ben-Porath I, Weinberg RA (2005) The signals and pathways activating cellular senescence. Int J Biochem Cell Biol 37 (5):961-976
47. Afshari CA, Vojta PJ, Annab LA, Futreal PA, Willard TB, Barrett JC (1993) Investigation of the role of G1/S cell cycle mediators in cellular senescence. Exp Cell Res 209 (2):231-237
48. Atadja P, Wong H, Garkavtsev I, Veillette C, Riabowol K (1995) Increased activity of p53 in senescing fibroblasts. Proc Natl Acad Sci U S A 92 (18):8348-8352
49. Webley K, Bond JA, Jones CJ, Blaydes JP, Craig A, Hupp T, Wynford-Thomas D (2000) Posttranslational modifications of p53 in replicative senescence overlapping but distinct from those induced by DNA damage. Mol Cell Biol 20 (8):2803-2808
50. Bond J, Haughton M, Blaydes J, Gire V, Wynford-Thomas D, Wyllie F (1996) Evidence that transcriptional activation by p53 plays a direct role in the induction of cellular senescence. Oncogene 13 (10):2097-2104
51. Gire V, Roux P, Wynford-Thomas D, Brondello JM, Dulic V (2004) DNA damage checkpoint kinase Chk2 triggers replicative senescence. Embo J 23 (13):2554-2563

52. Chen QM, Bartholomew JC, Campisi J, Acosta M, Reagan JD, Ames BN (1998) Molecular analysis of H2O2-induced senescent-like growth arrest in normal human fibroblasts: p53 and Rb control G1 arrest but not cell replication. Biochem J 332 (Pt 1):43-50
53. Pearson M, Carbone R, Sebastiani C, Cioce M, Fagioli M, Saito S, Higashimoto Y, Appella E, Minucci S, Pandolfi PP, Pelicci PG (2000) PML regulates p53 acetylation and premature senescence induced by oncogenic Ras. Nature 406 (6792):207-210
54. Stott FJ, Bates S, James MC, McConnell BB, Starborg M, Brookes S, Palmero I, Ryan K, Hara E, Vousden KH, Peters G (1998) The alternative product from the human CDKN2A locus, p14(ARF), participates in a regulatory feedback loop with p53 and MDM2. Embo J 17 (17):5001-5014
55. Dirac AM, Bernards R (2003) Reversal of senescence in mouse fibroblasts through lentiviral suppression of p53. J Biol Chem 278 (14):11731-11734
56. Harvey M, Sands AT, Weiss RS, Hegi ME, Wiseman RW, Pantazis P, Giovanella BC, Tainsky MA, Bradley A, Donehower LA (1993) In vitro growth characteristics of embryo fibroblasts isolated from p53-deficient mice. Oncogene 8 (9):2457-2467
57. Kamijo T, Zindy F, Roussel MF, Quelle DE, Downing JR, Ashmun RA, Grosveld G, Sherr CJ (1997) Tumor suppression at the mouse INK4a locus mediated by the alternative reading frame product p19ARF. Cell 91 (5):649-659
58. Sherr CJ, Roberts JM (1999) CDK inhibitors: positive and negative regulators of G1-phase progression. Genes Dev 13 (12):1501-1512
59. Dulic V, Drullinger LF, Lees E, Reed SI, Stein GH (1993) Altered regulation of G1 cyclins in senescent human diploid fibroblasts: accumulation of inactive cyclin E-Cdk2 and cyclin D1-Cdk2 complexes. Proc Natl Acad Sci U S A 90 (23):11034-11038.
60. Noda A, Ning Y, Venable SF, Pereira-Smith OM, Smith JR (1994) Cloning of senescent cell-derived inhibitors of DNA synthesis using an expression screen. Exp Cell Res 211 (1):90-98
61. Tahara H, Kamada K, Sato E, Tsuyama N, Kim JK, Hara E, Oda K, Ide T (1995) Increase in expression levels of interferon-inducible genes in senescent human diploid fibroblasts and in SV40-transformed human fibroblasts with extended lifespan. Oncogene 11 (6):1125-1132.
62. Herbig U, Wei W, Dutriaux A, Jobling WA, Sedivy JM (2003) Real-time imaging of transcriptional activation in live cells reveals rapid up-regulation of the cyclin-dependent kinase inhibitor gene CDKN1A in replicative cellular senescence. Aging Cell 2 (6):295-304
63. Modestou M, Puig-Antich V, Korgaonkar C, Eapen A, Quelle DE (2001) The alternative reading frame tumor suppressor inhibits growth through p21-dependent and p21-independent pathways. Cancer Res 61 (7):3145-3150
64. Wei W, Hemmer RM, Sedivy JM (2001) Role of p14(ARF) in replicative and induced senescence of human fibroblasts. Mol Cell Biol 21 (20):6748-6757
65. McConnell BB, Starborg M, Brookes S, Peters G (1998) Inhibitors of cyclin-dependent kinases induce features of replicative senescence in early passage human diploid fibroblasts. Curr Biol 8 (6):351-354.
66. Chang BD, Watanabe K, Broude EV, Fang J, Poole JC, Kalinichenko TV, Roninson IB (2000) Effects of p21Waf1/Cip1/Sdi1 on cellular gene expression: implications

for carcinogenesis, senescence, and age-related diseases. Proc Natl Acad Sci U S A 97 (8):4291-4296
67. Brown JP, Wei W, Sedivy JM (1997) Bypass of senescence after disruption of p21CIP1/WAF1 gene in normal diploid human fibroblasts. Science 277 (5327):831-834
68. Medcalf AS, Klein-Szanto AJ, Cristofalo VJ (1996) Expression of p21 is not required for senescence of human fibroblasts. Cancer Res 56 (20):4582-4585
69. Alcorta DA, Xiong Y, Phelps D, Hannon G, Beach D, Barrett JC (1996) Involvement of the cyclin-dependent kinase inhibitor p16 (INK4a) in replicative senescence of normal human fibroblasts. Proc Natl Acad Sci U S A 93 (24):13742-13747.
70. Hara E, Smith R, Parry D, Tahara H, Stone S, Peters G (1996) Regulation of p16CDKN2 expression and its implications for cell immortalization and senescence. Mol Cell Biol 16 (3):859-867.
71. Wong H, Riabowol K (1996) Differential CDK-inhibitor gene expression in aging human diploid fibroblasts. Exp Gerontol 31 (1-2):311-325.
72. Shay JW, Pereira-Smith OM, Wright WE (1991) A role for both RB and p53 in the regulation of human cellular senescence. Exp Cell Res 196 (1):33-39
73. Smogorzewska A, de Lange T (2002) Different telomere damage signaling pathways in human and mouse cells. Embo J 21 (16):4338-4348
74. Itahana K, Zou Y, Itahana Y, Martinez JL, Beausejour C, Jacobs JJ, Van Lohuizen M, Band V, Campisi J, Dimri GP (2003) Control of the replicative life span of human fibroblasts by p16 and the polycomb protein Bmi-1. Mol Cell Biol 23 (1):389-401
75. Beausejour CM, Krtolica A, Galimi F, Narita M, Lowe SW, Yaswen P, Campisi J (2003) Reversal of human cellular senescence: roles of the p53 and p16 pathways. Embo J 22 (16):4212-4222
76. Forsyth NR, Evans AP, Shay JW, Wright WE (2003) Developmental differences in the immortalization of lung fibroblasts by telomerase. Aging Cell 2 (5):235-243
77. Kim WY, Sharpless NE (2006) The regulation of INK4/ARF in cancer and aging. Cell 127 (2):265-275
78. Jacobs JJ, Kieboom K, Marino S, DePinho RA, van Lohuizen M (1999) The oncogene and Polycomb-group gene bmi-1 regulates cell proliferation and senescence through the ink4a locus. Nature 397 (6715):164-168
79. Bracken AP, Kleine-Kohlbrecher D, Dietrich N, Pasini D, Gargiulo G, Beekman C, Theilgaard-Monch K, Minucci S, Porse BT, Marine JC, Hansen KH, Helin K (2007) The Polycomb group proteins bind throughout the INK4A-ARF locus and are disassociated in senescent cells. Genes Dev 21 (5):525-530
80. Sharpless NE, Bardeesy N, Lee KH, Carrasco D, Castrillon DH, Aguirre AJ, Wu EA, Horner JW, DePinho RA (2001) Loss of p16Ink4a with retention of p19Arf predisposes mice to tumorigenesis. Nature 413 (6851):86-91
81. Romanov SR, Kozakiewicz BK, Holst CR, Stampfer MR, Haupt LM, Tisty TD (2001) Normal human mammary epithelial cells spontaneously escape senescence and acquire genomic changes. Nature 409 (6820):633-637.
82. Vogelstein B, Kinzler KW (1993) The multistep nature of cancer. Trends Genet 9 (4):138-141
83. Campisi J (2005) Senescent cells, tumor suppression, and organismal aging: good citizens, bad neighbors. Cell 120 (4):513-522

84. Hanahan D, Weinberg RA (2000) The hallmarks of cancer. Cell 100 (1):57-70
85. Bryan TM, Englezou A, Gupta J, Bacchetti S, Reddel RR (1995) Telomere elongation in immortal human cells without detectable telomerase activity. Embo J 14 (17):4240-4248
86. Gonzalez-Suarez E, Samper E, Ramirez A, Flores JM, Martin-Caballero J, Jorcano JL, Blasco MA (2001) Increased epidermal tumors and increased skin wound healing in transgenic mice overexpressing the catalytic subunit of telomerase, mTERT, in basal keratinocytes. Embo J 20 (11):2619-2630
87. Artandi SE, Alson S, Tietze MK, Sharpless NE, Ye S, Greenberg RA, Castrillon DH, Horner JW, Weiler SR, Carrasco RD, DePinho RA (2002) Constitutive telomerase expression promotes mammary carcinomas in aging mice. Proc Natl Acad Sci U S A 99 (12):8191-8196
88. Blasco MA, Lee HW, Hande MP, Samper E, Lansdorp PM, DePinho RA, Greider CW (1997) Telomere shortening and tumor formation by mouse cells lacking telomerase RNA. Cell 91 (1):25-34
89. Khoo CM, Carrasco DR, Bosenberg MW, Paik JH, Depinho RA (2007) Ink4a/Arf tumor suppressor does not modulate the degenerative conditions or tumor spectrum of the telomerase-deficient mouse. Proc Natl Acad Sci U S A 104 (10):3931-3936
90. Greenberg RA, Chin L, Femino A, Lee KH, Gottlieb GJ, Singer RH, Greider CW, DePinho RA (1999) Short dysfunctional telomeres impair tumorigenesis in the INK4a(delta2/3) cancer-prone mouse. Cell 97 (4):515-525
91. Wong KK, Maser RS, Bachoo RM, Menon J, Carrasco DR, Gu Y, Alt FW, DePinho RA (2003) Telomere dysfunction and Atm deficiency compromises organ homeostasis and accelerates ageing. Nature 421 (6923):643-648
92. Rudolph KL, Millard M, Bosenberg MW, DePinho RA (2001) Telomere dysfunction and evolution of intestinal carcinoma in mice and humans. Nat Genet 28 (2):155-159
93. Lechel A, Holstege H, Begus Y, Schienke A, Kamino K, Lehmann U, Kubicka S, Schirmacher P, Jonkers J, Rudolph KL (2007) Telomerase deletion limits progression of p53-mutant hepatocellular carcinoma with short telomeres in chronic liver disease. Gastroenterology 132 (4):1465-1475
94. Farazi PA, Glickman J, Horner J, Depinho RA (2006) Cooperative interactions of p53 mutation, telomere dysfunction, and chronic liver damage in hepatocellular carcinoma progression. Cancer Res 66 (9):4766-4773
95. Feldser DM, Greider CW (2007) Short telomeres limit tumor progression in vivo by inducing senescence. Cancer Cell 11 (5):461-469
96. Cosme-Blanco W, Shen MF, Lazar AJ, Pathak S, Lozano G, Multani AS, Chang S (2007) Telomere dysfunction suppresses spontaneous tumorigenesis in vivo by initiating p53-dependent cellular senescence. EMBO Rep 8 (5):497-503
97. Collado M, Gil J, Efeyan A, Guerra C, Schuhmacher AJ, Barradas M, Benguria A, Zaballos A, Flores JM, Barbacid M, Beach D, Serrano M (2005) Tumour biology: senescence in premalignant tumours. Nature 436 (7051):642
98. Braig M, Lee S, Loddenkemper C, Rudolph C, Peters AH, Schlegelberger B, Stein H, Dorken B, Jenuwein T, Schmitt CA (2005) Oncogene-induced senescence as an initial barrier in lymphoma development. Nature 436 (7051):660-665

99. Sarkisian CJ, Keister BA, Stairs DB, Boxer RB, Moody SE, Chodosh LA (2007) Dose-dependent oncogene-induced senescence in vivo and its evasion during mammary tumorigenesis. Nat Cell Biol 9 (5):493-505
100. Morton JP, Timpson P, Karim SA, Ridgway RA, Athineos D, Doyle B, Jamieson NB, Oien KA, Lowy AM, Brunton VG, Frame MC, Evans TR, Sansom OJ (2010) Mutant p53 drives metastasis and overcomes growth arrest/senescence in pancreatic cancer. Proc Natl Acad Sci U S A 107 (1):246-251
101. Chen Z, Trotman LC, Shaffer D, Lin HK, Dotan ZA, Niki M, Koutcher JA, Scher HI, Ludwig T, Gerald W, Cordon-Cardo C, Pandolfi PP (2005) Crucial role of p53-dependent cellular senescence in suppression of Pten-deficient tumorigenesis. Nature 436 (7051):725-730
102. Dankort D, Filenova E, Collado M, Serrano M, Jones K, McMahon M (2007) A new mouse model to explore the initiation, progression, and therapy of BRAFV600E-induced lung tumors. Genes Dev 21 (4):379-384
103. Ha L, Ichikawa T, Anver M, Dickins R, Lowe S, Sharpless NE, Krimpenfort P, Depinho RA, Bennett DC, Sviderskaya EV, Merlino G (2007) ARF functions as a melanoma tumor suppressor by inducing p53-independent senescence. Proc Natl Acad Sci U S A 104 (26):10968-10973
104. Dhomen N, Reis-Filho JS, da Rocha Dias S, Hayward R, Savage K, Delmas V, Larue L, Pritchard C, Marais R (2009) Oncogenic Braf induces melanocyte senescence and melanoma in mice. Cancer Cell 15 (4):294-303
105. Michaloglou C, Vredeveld LC, Soengas MS, Denoyelle C, Kuilman T, van der Horst CM, Majoor DM, Shay JW, Mooi WJ, Peeper DS (2005) BRAFE600-associated senescence-like cell cycle arrest of human naevi. Nature 436 (7051):720-724
106. Bartkova J, Rezaei N, Liontos M, Karakaidos P, Kletsas D, Issaeva N, Vassiliou LV, Kolettas E, Niforou K, Zoumpourlis VC, Takaoka M, Nakagawa H, Tort F, Fugger K, Johansson F, Sehested M, Andersen CL, Dyrskjot L, Orntoft T, Lukas J, Kittas C, Helleday T, Halazonetis TD, Bartek J, Gorgoulis VG (2006) Oncogene-induced senescence is part of the tumorigenesis barrier imposed by DNA damage checkpoints. Nature 444 (7119):633-637
107. Sharpless NE, DePinho RA (2004) Telomeres, stem cells, senescence, and cancer. J Clin Invest 113 (2):160-168
108. Paradis V, Youssef N, Dargere D, Ba N, Bonvoust F, Deschatrette J, Bedossa P (2001) Replicative senescence in normal liver, chronic hepatitis C, and hepatocellular carcinomas. Hum Pathol 32 (3):327-332
109. Herbig U, Ferreira M, Condel L, Carey D, Sedivy JM (2006) Cellular senescence in aging primates. Science 311 (5765):1257
110. Going JJ, Stuart RC, Downie M, Fletcher-Monaghan AJ, Keith WN (2002) 'Senescence-associated' beta-galactosidase activity in the upper gastrointestinal tract. J Pathol 196 (4):394-400
111. Price JS, Waters JG, Darrah C, Pennington C, Edwards DR, Donell ST, Clark IM (2002) The role of chondrocyte senescence in osteoarthritis. Aging Cell 1 (1):57-65
112. Fenton M, Barker S, Kurz DJ, Erusalimsky JD (2001) Cellular senescence after single and repeated balloon catheter denudations of rabbit carotid arteries. Arterioscler Thromb Vasc Biol 21 (2):220-226

113. Matthews C, Gorenne I, Scott S, Figg N, Kirkpatrick P, Ritchie A, Goddard M, Bennett M (2006) Vascular smooth muscle cells undergo telomere-based senescence in human atherosclerosis: effects of telomerase and oxidative stress. Circ Res 99 (2):156-164
114. Wiemann SU, Satyanarayana A, Tsahuridu M, Tillmann HL, Zender L, Klempnauer J, Flemming P, Franco S, Blasco MA, Manns MP, Rudolph KL (2002) Hepatocyte telomere shortening and senescence are general markers of human liver cirrhosis. Faseb J 16 (9):935-942
115. Schneider EL, Mitsui Y (1976) The relationship between in vitro cellular aging and in vivo human age. Proc Natl Acad Sci U S A 73 (10):3584-3588
116. Rheinwald JG, Green H (1975) Serial cultivation of strains of human epidermal keratinocytes: the formation of keratinizing colonies from single cells. Cell 6 (3):331-343
117. Bierman EL (1978) The effect of donor age on the in vitro life span of cultured human arterial smooth-muscle cells. In Vitro 14 (11):951-955
118. Cristofalo VJ, Allen RG, Pignolo RJ, Martin BG, Beck JC (1998) Relationship between donor age and the replicative lifespan of human cells in culture: a reevaluation. Proc Natl Acad Sci U S A 95 (18):10614-10619
119. Goldstein S, Murano S, Benes H, Moerman EJ, Jones RA, Thweatt R, Shmookler Reis RJ, Howard BH (1989) Studies on the molecular-genetic basis of replicative senescence in Werner syndrome and normal fibroblasts. Exp Gerontol 24 (5-6):461-468
120. Nakamura K, Izumiyama-Shimomura N, Sawabe M, Arai T, Aoyagi Y, Fujiwara M, Tsuchiya E, Kobayashi Y, Kato M, Oshimura M, Sasajima K, Nakachi K, Takubo K (2002) Comparative analysis of telomere lengths and erosion with age in human epidermis and lingual epithelium. J Invest Dermatol 119 (5):1014-1019
121. Allsopp RC, Vaziri H, Patterson C, Goldstein S, Younglai EV, Futcher AB, Greider CW, Harley CB (1992) Telomere length predicts replicative capacity of human fibroblasts. Proc Natl Acad Sci U S A 89 (21):10114-10118
122. Cawthon RM, Smith KR, O'Brien E, Sivatchenko A, Kerber RA (2003) Association between telomere length in blood and mortality in people aged 60 years or older. Lancet 361 (9355):393-395
123. Hastie ND, Dempster M, Dunlop MG, Thompson AM, Green DK, Allshire RC (1990) Telomere reduction in human colorectal carcinoma and with ageing. Nature 346 (6287):866-868
124. Melk A, Ramassar V, Helms LM, Moore R, Rayner D, Solez K, Halloran PF (2000) Telomere shortening in kidneys with age. J Am Soc Nephrol 11 (3):444-453
125. Mondello C, Petropoulou C, Monti D, Gonos ES, Franceschi C, Nuzzo F (1999) Telomere length in fibroblasts and blood cells from healthy centenarians. Exp Cell Res 248 (1):234-242
126. Kitada T, Seki S, Kawakita N, Kuroki T, Monna T (1995) Telomere shortening in chronic liver diseases. Biochem Biophys Res Commun 211 (1):33-39
127. Epel ES, Blackburn EH, Lin J, Dhabhar FS, Adler NE, Morrow JD, Cawthon RM (2004) Accelerated telomere shortening in response to life stress. Proc Natl Acad Sci U S A 101 (49):17312-17315

128. Valdes AM, Andrew T, Gardner JP, Kimura M, Oelsner E, Cherkas LF, Aviv A, Spector TD (2005) Obesity, cigarette smoking, and telomere length in women. Lancet 366 (9486):662-664
129. Vulliamy T, Marrone A, Szydlo R, Walne A, Mason PJ, Dokal I (2004) Disease anticipation is associated with progressive telomere shortening in families with dyskeratosis congenita due to mutations in TERC. Nat Genet 36 (5):447-449
130. Vulliamy T, Marrone A, Goldman F, Dearlove A, Bessler M, Mason PJ, Dokal I (2001) The RNA component of telomerase is mutated in autosomal dominant dyskeratosis congenita. Nature 413 (6854):432-435
131. Yamaguchi H, Calado RT, Ly H, Kajigaya S, Baerlocher GM, Chanock SJ, Lansdorp PM, Young NS (2005) Mutations in TERT, the gene for telomerase reverse transcriptase, in aplastic anemia. N Engl J Med 352 (14):1413-1424
132. Ball SE, Gibson FM, Rizzo S, Tooze JA, Marsh JC, Gordon-Smith EC (1998) Progressive telomere shortening in aplastic anemia. Blood 91 (10):3582-3592
133. Rudolph KL, Chang S, Lee HW, Blasco M, Gottlieb GJ, Greider C, DePinho RA (1999) Longevity, stress response, and cancer in aging telomerase-deficient mice. Cell 96 (5):701-712
134. Lee HW, Blasco MA, Gottlieb GJ, Horner JW, 2nd, Greider CW, DePinho RA (1998) Essential role of mouse telomerase in highly proliferative organs. Nature 392 (6676):569-574
135. Hao LY, Armanios M, Strong MA, Karim B, Feldser DM, Huso D, Greider CW (2005) Short telomeres, even in the presence of telomerase, limit tissue renewal capacity. Cell 123 (6):1121-1131
136. Jaskelioff M, Muller FL, Paik JH, Thomas E, Jiang S, Adams AC, Sahin E, Kost-Alimova M, Protopopov A, Cadinanos J, Horner JW, Maratos-Flier E, Depinho RA (2011) Telomerase reactivation reverses tissue degeneration in aged telomerase-deficient mice. Nature 469 (7328):102-106
137. Chang S, Multani AS, Cabrera NG, Naylor ML, Laud P, Lombard D, Pathak S, Guarente L, DePinho RA (2004) Essential role of limiting telomeres in the pathogenesis of Werner syndrome. Nat Genet 36 (8):877-882
138. Du X, Shen J, Kugan N, Furth EE, Lombard DB, Cheung C, Pak S, Luo G, Pignolo RJ, DePinho RA, Guarente L, Johnson FB (2004) Telomere shortening exposes functions for the mouse Werner and Bloom syndrome genes. Mol Cell Biol 24 (19):8437-8446
139. Weissman IL (2000) Stem cells: units of development, units of regeneration, and units in evolution. Cell 100 (1):157-168
140. Li L, Clevers H (2010) Coexistence of quiescent and active adult stem cells in mammals. Science 327 (5965):542-545. doi:10.1126/science.1180794
141. Bell DR, Van Zant G (2004) Stem cells, aging, and cancer: inevitabilities and outcomes. Oncogene 23 (43):7290-7296. doi:10.1038/sj.onc.1207949
142. Dorshkind K, Montecino-Rodriguez E, Signer RA (2009) The ageing immune system: is it ever too old to become young again? Nature reviews Immunology 9 (1):57-62. doi:10.1038/nri2471
143. Jones DL, Rando TA (2011) Emerging models and paradigms for stem cell ageing. Nat Cell Biol 13 (5):506-512. doi:10.1038/ncb0511-506

144. Renault VM, Rafalski VA, Morgan AA, Salih DA, Brett JO, Webb AE, Villeda SA, Thekkat PU, Guillerey C, Denko NC, Palmer TD, Butte AJ, Brunet A (2009) FoxO3 regulates neural stem cell homeostasis. Cell Stem Cell 5 (5):527-539. doi:10.1016/j.stem.2009.09.014
145. Inomata K, Aoto T, Binh NT, Okamoto N, Tanimura S, Wakayama T, Iseki S, Hara E, Masunaga T, Shimizu H, Nishimura EK (2009) Genotoxic stress abrogates renewal of melanocyte stem cells by triggering their differentiation. Cell 137 (6):1088-1099. doi:10.1016/j.cell.2009.03.037
146. Enwere E, Shingo T, Gregg C, Fujikawa H, Ohta S, Weiss S (2004) Aging results in reduced epidermal growth factor receptor signaling, diminished olfactory neurogenesis, and deficits in fine olfactory discrimination. The Journal of neuroscience : the official journal of the Society for Neuroscience 24 (38):8354-8365. doi:10.1523/JNEUROSCI.2751-04.2004
147. Nishimura EK, Granter SR, Fisher DE (2005) Mechanisms of hair graying: incomplete melanocyte stem cell maintenance in the niche. Science 307 (5710):720-724. doi:10.1126/science.1099593
148. Wallenfang MR, Nayak R, DiNardo S (2006) Dynamics of the male germline stem cell population during aging of Drosophila melanogaster. Aging Cell 5 (4):297-304. doi:10.1111/j.1474-9726.2006.00221.x
149. Boyle M, Wong C, Rocha M, Jones DL (2007) Decline in self-renewal factors contributes to aging of the stem cell niche in the Drosophila testis. Cell Stem Cell 1 (4):470-478. doi:10.1016/j.stem.2007.08.002
150. Pan L, Chen S, Weng C, Call G, Zhu D, Tang H, Zhang N, Xie T (2007) Stem cell aging is controlled both intrinsically and extrinsically in the Drosophila ovary. Cell Stem Cell 1 (4):458-469. doi:10.1016/j.stem.2007.09.010
151. Rossi DJ, Bryder D, Zahn JM, Ahlenius H, Sonu R, Wagers AJ, Weissman IL (2005) Cell intrinsic alterations underlie hematopoietic stem cell aging. Proc Natl Acad Sci U S A 102 (26):9194-9199
152. Morrison SJ, Wandycz AM, Akashi K, Globerson A, Weissman IL (1996) The aging of hematopoietic stem cells. Nat Med 2 (9):1011-1016
153. Sudo K, Ema H, Morita Y, Nakauchi H (2000) Age-associated characteristics of murine hematopoietic stem cells. J Exp Med 192 (9):1273-1280
154. Chambers SM, Goodell MA (2007) Hematopoietic stem cell aging: wrinkles in stem cell potential. Stem cell reviews 3 (3):201-211
155. Iscove NN, Nawa K (1997) Hematopoietic stem cells expand during serial transplantation in vivo without apparent exhaustion. Curr Biol 7 (10):805-808
156. Hellman S, Mauch P (1984) Implications of a proliferative limitation on hematopoietic stem cells. Progress in clinical and biological research 148:51-58
157. Siminovitch L, Till JE, McCulloch EA (1964) Decline in Colony-Forming Ability of Marrow Cells Subjected to Serial Transplantation into Irradiated Mice. J Cell Physiol 64:23-31
158. Cudkowicz G, Upton AC, Shearer GM, Hughes WL (1964) Lymphocyte Content and Proliferative Capacity of Serially Transplanted Mouse Bone Marrow. Nature 201:165-167

159. Harrison DE, Astle CM, Delaittre JA (1978) Loss of proliferative capacity in immunohemopoietic stem cells caused by serial transplantation rather than aging. J Exp Med 147 (5):1526-1531
160. Ross EA, Anderson N, Micklem HS (1982) Serial depletion and regeneration of the murine hematopoietic system. Implications for hematopoietic organization and the study of cellular aging. J Exp Med 155 (2):432-444
161. Harrison DE, Stone M, Astle CM (1990) Effects of transplantation on the primitive immunohematopoietic stem cell. J Exp Med 172 (2):431-437
162. Chambers SM, Shaw CA, Gatza C, Fisk CJ, Donehower LA, Goodell MA (2007) Aging hematopoietic stem cells decline in function and exhibit epigenetic dysregulation. PLoS Biol 5 (8):e201
163. Conboy IM, Conboy MJ, Smythe GM, Rando TA (2003) Notch-mediated restoration of regenerative potential to aged muscle. Science 302 (5650):1575-1577
164. Brack AS, Conboy MJ, Roy S, Lee M, Kuo CJ, Keller C, Rando TA (2007) Increased Wnt signaling during aging alters muscle stem cell fate and increases fibrosis. Science 317 (5839):807-810. doi:10.1126/science.1144090
165. Gopinath SD, Rando TA (2008) Stem cell review series: aging of the skeletal muscle stem cell niche. Aging Cell 7 (4):590-598. doi:10.1111/j.1474-9726.2008.00399.x
166. Conboy IM, Rando TA (2002) The regulation of Notch signaling controls satellite cell activation and cell fate determination in postnatal myogenesis. Dev Cell 3 (3):397-409
167. Conboy IM, Conboy MJ, Wagers AJ, Girma ER, Weissman IL, Rando TA (2005) Rejuvenation of aged progenitor cells by exposure to a young systemic environment. Nature 433 (7027):760-764
168. Drummond-Barbosa D (2008) Stem cells, their niches and the systemic environment: an aging network. Genetics 180 (4):1787-1797. doi:10.1534/genetics.108.098244
169. Hsu HJ, Drummond-Barbosa D (2009) Insulin levels control female germline stem cell maintenance via the niche in Drosophila. Proc Natl Acad Sci U S A 106 (4):1117-1121. doi:10.1073/pnas.0809144106
170. LaFever L, Drummond-Barbosa D (2005) Direct control of germline stem cell division and cyst growth by neural insulin in Drosophila. Science 309 (5737):1071-1073. doi:10.1126/science.1111410
171. Sharpless NE, DePinho RA (2007) How stem cells age and why this makes us grow old. Nat Rev Mol Cell Biol 8 (9):703-713. doi:10.1038/nrm2241
172. Rossi DJ, Bryder D, Seita J, Nussenzweig A, Hoeijmakers J, Weissman IL (2007) Deficiencies in DNA damage repair limit the function of haematopoietic stem cells with age. Nature 447 (7145):725-729. doi:10.1038/nature05862
173. Rube CE, Fricke A, Widmann TA, Furst T, Madry H, Pfreundschuh M, Rube C (2011) Accumulation of DNA damage in hematopoietic stem and progenitor cells during human aging. PLoS One 6 (3):e17487. doi:10.1371/journal.pone.0017487
174. Hotta T, Hirabayashi N, Utsumi M, Murate T, Yamada H (1980) Age-related changes in the function of hemopoietic stroma in mice. Exp Hematol 8 (7):933-936
175. Mauch P, Botnick LE, Hannon EC, Obbagy J, Hellman S (1982) Decline in bone marrow proliferative capacity as a function of age. Blood 60 (1):245-252

176. Kohler A, Schmithorst V, Filippi MD, Ryan MA, Daria D, Gunzer M, Geiger H (2009) Altered cellular dynamics and endosteal location of aged early hematopoietic progenitor cells revealed by time-lapse intravital imaging in long bones. Blood 114 (2):290-298. doi:10.1182/blood-2008-12-195644
177. Liang Y, Van Zant G, Szilvassy SJ (2005) Effects of aging on the homing and engraftment of murine hematopoietic stem and progenitor cells. Blood 106 (4):1479-1487
178. Pawelec G, Hirokawa K, Fulop T (2001) Altered T cell signalling in ageing. Mech Ageing Dev 122 (14):1613-1637
179. Goronzy JJ, Lee WW, Weyand CM (2007) Aging and T-cell diversity. Exp Gerontol 42 (5):400-406. doi:10.1016/j.exger.2006.11.016
180. Franceschi C, Bonafe M, Valensin S, Olivieri F, De Luca M, Ottaviani E, De Benedictis G (2000) Inflamm-aging. An evolutionary perspective on immunosenescence. Ann N Y Acad Sci 908:244-254
181. Linton PJ, Dorshkind K (2004) Age-related changes in lymphocyte development and function. Nat Immunol 5 (2):133-139
182. Dorshkind K, Swain S (2009) Age-associated declines in immune system development and function: causes, consequences, and reversal. Curr Opin Immunol 21 (4):404-407. doi:10.1016/j.coi.2009.07.001
183. Tsaknaridis L, Spencer L, Culbertson N, Hicks K, LaTocha D, Chou YK, Whitham RH, Bakke A, Jones RE, Offner H, Bourdette DN, Vandenbark AA (2003) Functional assay for human CD4+CD25+ Treg cells reveals an age-dependent loss of suppressive activity. Journal of neuroscience research 74 (2):296-308. doi:10.1002/jnr.10766
184. Sieburg HB, Cho RH, Dykstra B, Uchida N, Eaves CJ, Muller-Sieburg CE (2006) The hematopoietic stem compartment consists of a limited number of discrete stem cell subsets. Blood 107 (6):2311-2316. doi:10.1182/blood-2005-07-2970
185. Dykstra B, Kent D, Bowie M, McCaffrey L, Hamilton M, Lyons K, Lee SJ, Brinkman R, Eaves C (2007) Long-term propagation of distinct hematopoietic differentiation programs in vivo. Cell Stem Cell 1 (2):218-229. doi:10.1016/j.stem.2007.05.015
186. Choi YJ, Hwang MS, Park JS, Bae SK, Kim YS, Yoo MA (2008) Age-related upregulation of Drosophila caudal gene via NF-kappaB in the adult posterior midgut. Biochim Biophys Acta 1780 (10):1093-1100. doi:10.1016/j.bbagen.2008.06.008
187. Biteau B, Hochmuth CE, Jasper H (2008) JNK activity in somatic stem cells causes loss of tissue homeostasis in the aging Drosophila gut. Cell Stem Cell 3 (4):442-455. doi:10.1016/j.stem.2008.07.024
188. Park JS, Kim YS, Yoo MA (2009) The role of p38b MAPK in age-related modulation of intestinal stem cell proliferation and differentiation in Drosophila. Aging 1 (7):637-651
189. Jiang H, Patel PH, Kohlmaier A, Grenley MO, McEwen DG, Edgar BA (2009) Cytokine/Jak/Stat signaling mediates regeneration and homeostasis in the Drosophila midgut. Cell 137 (7):1343-1355. doi:10.1016/j.cell.2009.05.014

190. Buchon N, Broderick NA, Chakrabarti S, Lemaitre B (2009) Invasive and indigenous microbiota impact intestinal stem cell activity through multiple pathways in Drosophila. Genes Dev 23 (19):2333-2344. doi:10.1101/gad.1827009
191. Amcheslavsky A, Jiang J, Ip YT (2009) Tissue damage-induced intestinal stem cell division in Drosophila. Cell Stem Cell 4 (1):49-61. doi:10.1016/j.stem.2008.10.016
192. Janzen V, Forkert R, Fleming HE, Saito Y, Waring MT, Dombkowski DM, Cheng T, DePinho RA, Sharpless NE, Scadden DT (2006) Stem-cell ageing modified by the cyclin-dependent kinase inhibitor p16INK4a. Nature 443 (7110):421-426
193. Krishnamurthy J, Ramsey MR, Ligon KL, Torrice C, Koh A, Bonner-Weir S, Sharpless NE (2006) p16INK4a induces an age-dependent decline in islet regenerative potential. Nature 443 (7110):453-457
194. Molofsky AV, Slutsky SG, Joseph NM, He S, Pardal R, Krishnamurthy J, Sharpless NE, Morrison SJ (2006) Increasing p16INK4a expression decreases forebrain progenitors and neurogenesis during ageing. Nature 443 (7110):448-452
195. Kuro-o M (2006) Klotho as a regulator of fibroblast growth factor signaling and phosphate/calcium metabolism. Current opinion in nephrology and hypertension 15 (4):437-441. doi:10.1097/01.mnh.0000232885.81142.83
196. Liu H, Fergusson MM, Castilho RM, Liu J, Cao L, Chen J, Malide D, Rovira, II, Schimel D, Kuo CJ, Gutkind JS, Hwang PM, Finkel T (2007) Augmented Wnt signaling in a mammalian model of accelerated aging. Science 317 (5839):803-806. doi:10.1126/science.1143578
197. Merrill BJ, Gat U, DasGupta R, Fuchs E (2001) Tcf3 and Lef1 regulate lineage differentiation of multipotent stem cells in skin. Genes Dev 15 (13):1688-1705. doi:10.1101/gad.891401
198. Andl T, Reddy ST, Gaddapara T, Millar SE (2002) WNT signals are required for the initiation of hair follicle development. Dev Cell 2 (5):643-653
199. Castilho RM, Squarize CH, Chodosh LA, Williams BO, Gutkind JS (2009) mTOR mediates Wnt-induced epidermal stem cell exhaustion and aging. Cell Stem Cell 5 (3):279-289. doi:10.1016/j.stem.2009.06.017
200. Ditadi A, de Coppi P, Picone O, Gautreau L, Smati R, Six E, Bonhomme D, Ezine S, Frydman R, Cavazzana-Calvo M, Andre-Schmutz I (2009) Human and murine amniotic fluid c-Kit+Lin- cells display hematopoietic activity. Blood 113 (17):3953-3960. doi:10.1182/blood-2008-10-182105
201. Spangrude GJ, Heimfeld S, Weissman IL (1988) Purification and characterization of mouse hematopoietic stem cells. Science 241 (4861):58-62
202. Abkowitz JL, Catlin SN, McCallie MT, Guttorp P (2002) Evidence that the number of hematopoietic stem cells per animal is conserved in mammals. Blood 100 (7):2665-2667. doi:10.1182/blood-2002-03-0822
203. Shepherd BE, Kiem HP, Lansdorp PM, Dunbar CE, Aubert G, LaRochelle A, Seggewiss R, Guttorp P, Abkowitz JL (2007) Hematopoietic stem-cell behavior in nonhuman primates. Blood 110 (6):1806-1813. doi:10.1182/blood-2007-02-075382
204. Heiss NS, Knight SW, Vulliamy TJ, Klauck SM, Wiemann S, Mason PJ, Poustka A, Dokal I (1998) X-linked dyskeratosis congenita is caused by mutations in a highly conserved gene with putative nucleolar functions. Nat Genet 19 (1):32-38

205. Mitchell JR, Wood E, Collins K (1999) A telomerase component is defective in the human disease dyskeratosis congenita. Nature 402 (6761):551-555
206. Al-Rahawan MM, Giri N, Alter BP (2006) Intensive immunosuppression therapy for aplastic anemia associated with dyskeratosis congenita. International journal of hematology 83 (3):275-276. doi:10.1532/IJH97.06030
207. Alter BP, Baerlocher GM, Savage SA, Chanock SJ, Weksler BB, Willner JP, Peters JA, Giri N, Lansdorp PM (2007) Very short telomere length by flow fluorescence in situ hybridization identifies patients with dyskeratosis congenita. Blood 110 (5):1439-1447. doi:10.1182/blood-2007-02-075598
208. Savage SA, Alter BP (2008) The role of telomere biology in bone marrow failure and other disorders. Mech Ageing Dev 129 (1-2):35-47. doi:10.1016/j.mad.2007.11.002
209. Calado RT, Young NS (2008) Telomere maintenance and human bone marrow failure. Blood 111 (9):4446-4455. doi:10.1182/blood-2007-08-019729
210. Rossi DJ, Jamieson CH, Weissman IL (2008) Stems cells and the pathways to aging and cancer. Cell 132 (4):681-696
211. Jun JI, Lau LF (2010) The matricellular protein CCN1 induces fibroblast senescence and restricts fibrosis in cutaneous wound healing. Nat Cell Biol 12 (7):676-685. doi:10.1038/ncb2070
212. Krizhanovsky V, Yon M, Dickins RA, Hearn S, Simon J, Miething C, Yee H, Zender L, Lowe SW (2008) Senescence of activated stellate cells limits liver fibrosis. Cell 134 (4):657-667. doi:10.1016/j.cell.2008.06.049
213. Medawar P (1952) An unsolved problem in Biology. London: Lewis
214. Williams GC (1957) Pleiotropy, natural selection, and the evolution of senescence. Evolution; international journal of organic evolution 11:398-411
215. Williams GC (1960) Pleiotropy, Natural Selection, and the Evolution of Senescence. . Publication of the American Institute of Biological Sciences 6:332-337
216. Rose MR, Charlesworth B (1981) Genetics of life history in Drosophila melanogaster. II. Exploratory selection experiments. Genetics 97 (1):187-196
217. Wattiaux JM (1968) Parental age effects in Drosophila pseudoobscura. Exp Gerontol 3 (1):55-61
218. Luckinbill LS, Arking R, Clare MJ, Cirocco WC, Buck SA (1984) Selection for Delayed Senescence in Drosophila-Melanogaster. Evolution; international journal of organic evolution 38 (5):996-1003
219. Rose MR (1984) Laboratory Evolution of Postponed Senescence in Drosophila-Melanogaster. Evolution; international journal of organic evolution 38 (5):1004-1010
220. Partridge L, Fowler K (1992) Direct and Correlated Responses to Selection on Age at Reproduction in Drosophila-Melanogaster. Evolution; international journal of organic evolution 46 (1):76-91
221. Partridge L, Barton NH (1993) Optimality, mutation and the evolution of ageing. Nature 362 (6418):305-311. doi:10.1038/362305a0
222. Partridge L, Mangel M (1999) Messages from mortality: the evolution of death rates in the old. Trends in ecology & evolution 14 (11):438-442

223. Zwaan B, Bijlsma R, Hoekstra RE (1995) Direct Selection on Life-Span in Drosophila-Melanogaster. Evolution; international journal of organic evolution 49 (4):649-659
224. Friedman DB, Johnson TE (1988) A mutation in the age-1 gene in Caenorhabditis elegans lengthens life and reduces hermaphrodite fertility. Genetics 118 (1):75-86
225. Kenyon C, Chang J, Gensch E, Rudner A, Tabtiang R (1993) A C. elegans mutant that lives twice as long as wild type. Nature 366 (6454):461-464. doi:10.1038/366461a0
226. Kimura KD, Tissenbaum HA, Liu Y, Ruvkun G (1997) daf-2, an insulin receptor-like gene that regulates longevity and diapause in Caenorhabditis elegans. Science 277 (5328):942-946
227. Apfeld J, Kenyon C (1998) Cell nonautonomy of C. elegans daf-2 function in the regulation of diapause and life span. Cell 95 (2):199-210
228. Apfeld J, Kenyon C (1999) Regulation of lifespan by sensory perception in Caenorhabditis elegans. Nature 402 (6763):804-809. doi:10.1038/45544
229. Klass MR (1977) Aging in the nematode Caenorhabditis elegans: major biological and environmental factors influencing life span. Mech Ageing Dev 6 (6):413-429
230. Tatar M, Kopelman A, Epstein D, Tu MP, Yin CM, Garofalo RS (2001) A mutant Drosophila insulin receptor homolog that extends life-span and impairs neuroendocrine function. Science 292 (5514):107-110. doi:10.1126/science.1057987
231. Flurkey K, Papaconstantinou J, Miller RA, Harrison DE (2001) Lifespan extension and delayed immune and collagen aging in mutant mice with defects in growth hormone production. Proc Natl Acad Sci U S A 98 (12):6736-6741. doi:10.1073/pnas.111158898
232. Srivastava S, Zou ZQ, Pirollo K, Blattner W, Chang EH (1990) Germ-line transmission of a mutated p53 gene in a cancer-prone family with Li-Fraumeni syndrome. Nature 348 (6303):747-749. doi:10.1038/348747a0
233. Donehower LA, Harvey M, Slagle BL, McArthur MJ, Montgomery CA, Jr., Butel JS, Bradley A (1992) Mice deficient for p53 are developmentally normal but susceptible to spontaneous tumours. Nature 356 (6366):215-221
234. Garcia-Cao I, Garcia-Cao M, Martin-Caballero J, Criado LM, Klatt P, Flores JM, Weill JC, Blasco MA, Serrano M (2002) "Super p53" mice exhibit enhanced DNA damage response, are tumor resistant and age normally. Embo J 21 (22):6225-6235
235. Tyner SD, Venkatachalam S, Choi J, Jones S, Ghebranious N, Igelmann H, Lu X, Soron G, Cooper B, Brayton C, Hee Park S, Thompson T, Karsenty G, Bradley A, Donehower LA (2002) p53 mutant mice that display early ageing-associated phenotypes. Nature 415 (6867):45-53
236. Gentry A, Venkatachalam S (2005) Complicating the role of p53 in aging. Aging Cell 4 (3):157-160. doi:10.1111/j.1474-9726.2005.00154.x
237. Dumble M, Moore L, Chambers SM, Geiger H, Van Zant G, Goodell MA, Donehower LA (2007) The impact of altered p53 dosage on hematopoietic stem cell dynamics during aging. Blood 109 (4):1736-1742. doi:10.1182/blood-2006-03-010413

238. Maier B, Gluba W, Bernier B, Turner T, Mohammad K, Guise T, Sutherland A, Thorner M, Scrable H (2004) Modulation of mammalian life span by the short isoform of p53. Genes Dev 18 (3):306-319
239. Matheu A, Maraver A, Klatt P, Flores I, Garcia-Cao I, Borras C, Flores JM, Vina J, Blasco MA, Serrano M (2007) Delayed ageing through damage protection by the Arf/p53 pathway. Nature 448 (7151):375-379
240. Huibregtse JM, Scheffner M, Beaudenon S, Howley PM (1995) A family of proteins structurally and functionally related to the E6-AP ubiquitin-protein ligase. Proc Natl Acad Sci U S A 92 (11):5249
241. Scheffner M, Nuber U, Huibregtse JM (1995) Protein ubiquitination involving an E1-E2-E3 enzyme ubiquitin thioester cascade. Nature 373 (6509):81-83
242. Garcia-Gonzalo FR, Rosa JL (2005) The HERC proteins: functional and evolutionary insights. Cellular and molecular life sciences : CMLS 62 (16):1826-1838. doi:10.1007/s00018-005-5119-y
243. Fukuchi M, Fukai Y, Masuda N, Miyazaki T, Nakajima M, Sohda M, Manda R, Tsukada K, Kato H, Kuwano H (2002) High-level expression of the Smad ubiquitin ligase Smurf2 correlates with poor prognosis in patients with esophageal squamous cell carcinoma. Cancer Res 62 (24):7162-7165
244. Zhu H, Kavsak P, Abdollah S, Wrana JL, Thomsen GH (1999) A SMAD ubiquitin ligase targets the BMP pathway and affects embryonic pattern formation. Nature 400 (6745):687-693
245. Zhang H, Cohen SN (2004) Smurf2 up-regulation activates telomere-dependent senescence. Genes Dev 18 (24):3028-3040
246. Kong Y, Cui H, Zhang H (2011) Smurf2-mediated ubiquitination and degradation of Id1 regulates p16 expression during senescence. Aging Cell 10 (6):1038-1046
247. Iavarone A, Garg P, Lasorella A, Hsu J, Israel MA (1994) The helix-loop-helix protein Id-2 enhances cell proliferation and binds to the retinoblastoma protein. Genes Dev 8 (11):1270-1284
248. Lyden D, Young AZ, Zagzag D, Yan W, Gerald W, O'Reilly R, Bader BL, Hynes RO, Zhuang Y, Manova K, Benezra R (1999) Id1 and Id3 are required for neurogenesis, angiogenesis and vascularization of tumour xenografts. Nature 401 (6754):670-677
249. Perk J, Iavarone A, Benezra R (2005) Id family of helix-loop-helix proteins in cancer. Nat Rev Cancer 5 (8):603-614
250. Alani RM, Young AZ, Shifflett CB (2001) Id1 regulation of cellular senescence through transcriptional repression of p16/Ink4a. Proc Natl Acad Sci U S A 98 (14):7812-7816
251. Zheng W, Wang H, Xue L, Zhang Z, Tong T (2004) Regulation of cellular senescence and p16(INK4a) expression by Id1 and E47 proteins in human diploid fibroblast. J Biol Chem 279 (30):31524-31532
252. Hara E, Uzman JA, Dimri GP, Nehlin JO, Testori A, Campisi J (1996) The helix-loop-helix protein Id-1 and a retinoblastoma protein binding mutant of SV40 T antigen synergize to reactivate DNA synthesis in senescent human fibroblasts. Dev Genet 18 (2):161-172

253. Nickoloff BJ, Chaturvedi V, Bacon P, Qin JZ, Denning MF, Diaz MO (2000) Id-1 delays senescence but does not immortalize keratinocytes. J Biol Chem 275 (36):27501-27504
254. Tang J, Gordon GM, Nickoloff BJ, Foreman KE (2002) The helix-loop-helix protein id-1 delays onset of replicative senescence in human endothelial cells. Lab Invest 82 (8):1073-1079
255. Cummings SD, Ryu B, Samuels MA, Yu X, Meeker AK, Healey MA, Alani RM (2008) Id1 delays senescence of primary human melanocytes. Mol Carcinog 47 (9):653-659
256. Suh HC, Leeanansaksiri W, Ji M, Klarmann KD, Renn K, Gooya J, Smith D, McNiece I, Lugthart S, Valk PJ, Delwel R, Keller JR (2008) Id1 immortalizes hematopoietic progenitors in vitro and promotes a myeloproliferative disease in vivo. Oncogene 27 (42):5612-5623
257. Zhang Y, Chang C, Gehling DJ, Hemmati-Brivanlou A, Derynck R (2001) Regulation of Smad degradation and activity by Smurf2, an E3 ubiquitin ligase. Proc Natl Acad Sci U S A 98 (3):974-979
258. Lin X, Liang M, Feng XH (2000) Smurf2 is a ubiquitin E3 ligase mediating proteasome-dependent degradation of Smad2 in transforming growth factor-beta signaling. J Biol Chem 275 (47):36818-36822
259. Kavsak P, Rasmussen RK, Causing CG, Bonni S, Zhu H, Thomsen GH, Wrana JL (2000) Smad7 binds to Smurf2 to form an E3 ubiquitin ligase that targets the TGF beta receptor for degradation. Mol Cell 6 (6):1365-1375
260. Di Guglielmo GM, Le Roy C, Goodfellow AF, Wrana JL (2003) Distinct endocytic pathways regulate TGF-beta receptor signalling and turnover. Nat Cell Biol 5 (5):410-421. doi:10.1038/ncb975
261. Bonni S, Wang HR, Causing CG, Kavsak P, Stroschein SL, Luo K, Wrana JL (2001) TGF-beta induces assembly of a Smad2-Smurf2 ubiquitin ligase complex that targets SnoN for degradation. Nat Cell Biol 3 (6):587-595
262. Tang LY, Yamashita M, Coussens NP, Tang Y, Wang X, Li C, Deng CX, Cheng SY, Zhang YE (2011) Ablation of Smurf2 reveals an inhibition in TGF-beta signalling through multiple mono-ubiquitination of Smad3. Embo J 30 (23):4777-4789
263. Schwamborn JC, Muller M, Becker AH, Puschel AW (2007) Ubiquitination of the GTPase Rap1B by the ubiquitin ligase Smurf2 is required for the establishment of neuronal polarity. Embo J 26 (5):1410-1422
264. Subramaniam V, Li H, Wong M, Kitching R, Attisano L, Wrana J, Zubovits J, Burger AM, Seth A (2003) The RING-H2 protein RNF11 is overexpressed in breast cancer and is a target of Smurf2 E3 ligase. Br J Cancer 89 (8):1538-1544
265. Jin YH, Jeon EJ, Li QL, Lee YH, Choi JK, Kim WJ, Lee KY, Bae SC (2004) Transforming growth factor-beta stimulates p300-dependent RUNX3 acetylation, which inhibits ubiquitination-mediated degradation. J Biol Chem 279 (28):29409-29417. doi:10.1074/jbc.M313120200
266. Kaneki H, Guo R, Chen D, Yao Z, Schwarz EM, Zhang YE, Boyce BF, Xing L (2006) Tumor necrosis factor promotes Runx2 degradation through up-regulation of Smurf1 and Smurf2 in osteoblasts. J Biol Chem 281 (7):4326-4333

267. Han G, Li AG, Liang YY, Owens P, He W, Lu S, Yoshimatsu Y, Wang D, Ten Dijke P, Lin X, Wang XJ (2006) Smad7-induced beta-catenin degradation alters epidermal appendage development. Dev Cell 11 (3):301-312
268. Kim S, Jho EH (2010) The protein stability of Axin, a negative regulator of Wnt signaling, is regulated by Smad ubiquitination regulatory factor 2 (Smurf2). J Biol Chem 285 (47):36420-36426
269. Fukunaga E, Inoue Y, Komiya S, Horiguchi K, Goto K, Saitoh M, Miyazawa K, Koinuma D, Hanyu A, Imamura T (2008) Smurf2 induces ubiquitin-dependent degradation of Smurf1 to prevent migration of breast cancer cells. J Biol Chem 283 (51):35660-35667
270. Moore FE, Osmundson EC, Koblinski J, Pugacheva E, Golemis EA, Ray D, Kiyokawa H (2010) The WW-HECT protein Smurf2 interacts with the Docking Protein NEDD9/HEF1 for Aurora A activation. Cell Div 5:22
271. Heldin CH, Landstrom M, Moustakas A (2009) Mechanism of TGF-beta signaling to growth arrest, apoptosis, and epithelial-mesenchymal transition. Curr Opin Cell Biol 21 (2):166-176. doi:10.1016/j.ceb.2009.01.021
272. Ikushima H, Miyazono K (2010) TGFbeta signalling: a complex web in cancer progression. Nat Rev Cancer 10 (6):415-424. doi:10.1038/nrc2853
273. Massague J (2008) TGFbeta in Cancer. Cell 134 (2):215-230. doi:10.1016/j.cell.2008.07.001
274. Wikstrom P, Stattin P, Franck-Lissbrant I, Damber JE, Bergh A (1998) Transforming growth factor beta1 is associated with angiogenesis, metastasis, and poor clinical outcome in prostate cancer. The Prostate 37 (1):19-29
275. Walker RA, Dearing SJ (1992) Transforming growth factor beta 1 in ductal carcinoma in situ and invasive carcinomas of the breast. Eur J Cancer 28 (2-3):641-644
276. Friedman E, Gold LI, Klimstra D, Zeng ZS, Winawer S, Cohen A (1995) High levels of transforming growth factor beta 1 correlate with disease progression in human colon cancer. Cancer epidemiology, biomarkers & prevention : a publication of the American Association for Cancer Research, cosponsored by the American Society of Preventive Oncology 4 (5):549-554
277. Dalal BI, Keown PA, Greenberg AH (1993) Immunocytochemical localization of secreted transforming growth factor-beta 1 to the advancing edges of primary tumors and to lymph node metastases of human mammary carcinoma. Am J Pathol 143 (2):381-389
278. Picon A, Gold LI, Wang J, Cohen A, Friedman E (1998) A subset of metastatic human colon cancers expresses elevated levels of transforming growth factor beta1. Cancer epidemiology, biomarkers & prevention : a publication of the American Association for Cancer Research, cosponsored by the American Society of Preventive Oncology 7 (6):497-504
279. Roberts AB, Wakefield LM (2003) The two faces of transforming growth factor beta in carcinogenesis. Proc Natl Acad Sci U S A 100 (15):8621-8623. doi:10.1073/pnas.1633291100
280. Nie J, Xie P, Liu L, Xing G, Chang Z, Yin Y, Tian C, He F, Zhang L (2010) Smad ubiquitylation regulatory factor 1/2 (Smurf1/2) promotes p53 degradation by stabilizing the E3 ligase MDM2. J Biol Chem 285 (30):22818-22830

281. Ray D, Ahsan A, Helman A, Chen G, Hegde A, Gurjar SR, Zhao L, Kiyokawa H, Beer DG, Lawrence TS, Nyati MK (2011) Regulation of EGFR protein stability by the HECT-type ubiquitin ligase SMURF2. Neoplasia 13 (7):570-578
282. Wu Q, Huang JH, Sampson ER, Kim KO, Zuscik MJ, O'Keefe RJ, Chen D, Rosier RN (2009) Smurf2 induces degradation of GSK-3beta and upregulates beta-catenin in chondrocytes: a potential mechanism for Smurf2-induced degeneration of articular cartilage. Exp Cell Res 315 (14):2386-2398
283. Narimatsu M, Bose R, Pye M, Zhang L, Miller B, Ching P, Sakuma R, Luga V, Roncari L, Attisano L, Wrana JL (2009) Regulation of planar cell polarity by Smurf ubiquitin ligases. Cell 137 (2):295-307
284. Zhang H, Teng Y, Kong Y, Kowalski PE, Cohen SN (2008) Suppression of human tumor cell proliferation by Smurf2-induced senescence. J Cell Physiol 215 (3):613-620
285. Blank M, Tang Y, Yamashita M, Burkett SS, Cheng SY, Zhang YE (2012) A tumor suppressor function of Smurf2 associated with controlling chromatin landscape and genome stability through RNF20. Nat Med 18 (2):227-234
286. Coles AH, Liang H, Zhu Z, Marfella CG, Kang J, Imbalzano AN, Jones SN (2007) Deletion of p37Ing1 in mice reveals a p53-independent role for Ing1 in the suppression of cell proliferation, apoptosis, and tumorigenesis. Cancer Res 67 (5):2054-2061
287. A clinical evaluation of the International Lymphoma Study Group classification of non-Hodgkin's lymphoma. The Non-Hodgkin's Lymphoma Classification Project (1997). Blood 89 (11):3909-3918
288. Coiffier B (2001) Diffuse large cell lymphoma. Curr Opin Oncol 13 (5):325-334
289. Alizadeh AA, Eisen MB, Davis RE, Ma C, Lossos IS, Rosenwald A, Boldrick JC, Sabet H, Tran T, Yu X, Powell JI, Yang L, Marti GE, Moore T, Hudson J, Jr., Lu L, Lewis DB, Tibshirani R, Sherlock G, Chan WC, Greiner TC, Weisenburger DD, Armitage JO, Warnke R, Levy R, Wilson W, Grever MR, Byrd JC, Botstein D, Brown PO, Staudt LM (2000) Distinct types of diffuse large B-cell lymphoma identified by gene expression profiling. Nature 403 (6769):503-511
290. Rosenwald A, Wright G, Chan WC, Connors JM, Campo E, Fisher RI, Gascoyne RD, Muller-Hermelink HK, Smeland EB, Giltnane JM, Hurt EM, Zhao H, Averett L, Yang L, Wilson WH, Jaffe ES, Simon R, Klausner RD, Powell J, Duffey PL, Longo DL, Greiner TC, Weisenburger DD, Sanger WG, Dave BJ, Lynch JC, Vose J, Armitage JO, Montserrat E, Lopez-Guillermo A, Grogan TM, Miller TP, LeBlanc M, Ott G, Kvaloy S, Delabie J, Holte H, Krajci P, Stokke T, Staudt LM (2002) The use of molecular profiling to predict survival after chemotherapy for diffuse large-B-cell lymphoma. N Engl J Med 346 (25):1937-1947
291. Wright G, Tan B, Rosenwald A, Hurt EH, Wiestner A, Staudt LM (2003) A gene expression-based method to diagnose clinically distinct subgroups of diffuse large B cell lymphoma. Proc Natl Acad Sci U S A 100 (17):9991-9996
292. Savage KJ, Monti S, Kutok JL, Cattoretti G, Neuberg D, De Leval L, Kurtin P, Dal Cin P, Ladd C, Feuerhake F, Aguiar RC, Li S, Salles G, Berger F, Jing W, Pinkus GS, Habermann T, Dalla-Favera R, Harris NL, Aster JC, Golub TR, Shipp MA (2003) The molecular signature of mediastinal large B-cell lymphoma differs from that of other

diffuse large B-cell lymphomas and shares features with classical Hodgkin lymphoma. Blood 102 (12):3871-3879. doi:10.1182/blood-2003-06-1841
293. Klein U, Dalla-Favera R (2008) Germinal centres: role in B-cell physiology and malignancy. Nature reviews Immunology 8 (1):22-33. doi:10.1038/nri2217
294. Lenz G, Staudt LM (2010) Aggressive lymphomas. N Engl J Med 362 (15):1417-1429. doi:10.1056/NEJMra0807082
295. Lenz G, Wright GW, Emre NC, Kohlhammer H, Dave SS, Davis RE, Carty S, Lam LT, Shaffer AL, Xiao W, Powell J, Rosenwald A, Ott G, Muller-Hermelink HK, Gascoyne RD, Connors JM, Campo E, Jaffe ES, Delabie J, Smeland EB, Rimsza LM, Fisher RI, Weisenburger DD, Chan WC, Staudt LM (2008) Molecular subtypes of diffuse large B-cell lymphoma arise by distinct genetic pathways. Proc Natl Acad Sci U S A 105 (36):13520-13525. doi:10.1073/pnas.0804295105
296. Compagno M, Lim WK, Grunn A, Nandula SV, Brahmachary M, Shen Q, Bertoni F, Ponzoni M, Scandurra M, Califano A, Bhagat G, Chadburn A, Dalla-Favera R, Pasqualucci L (2009) Mutations of multiple genes cause deregulation of NF-kappaB in diffuse large B-cell lymphoma. Nature 459 (7247):717-721. doi:10.1038/nature07968
297. Davis RE, Ngo VN, Lenz G, Tolar P, Young RM, Romesser PB, Kohlhammer H, Lamy L, Zhao H, Yang Y, Xu W, Shaffer AL, Wright G, Xiao W, Powell J, Jiang JK, Thomas CJ, Rosenwald A, Ott G, Muller-Hermelink HK, Gascoyne RD, Connors JM, Johnson NA, Rimsza LM, Campo E, Jaffe ES, Wilson WH, Delabie J, Smeland EB, Fisher RI, Braziel RM, Tubbs RR, Cook JR, Weisenburger DD, Chan WC, Pierce SK, Staudt LM (2010) Chronic active B-cell-receptor signalling in diffuse large B-cell lymphoma. Nature 463 (7277):88-92. doi:10.1038/nature08638
298. Ngo VN, Young RM, Schmitz R, Jhavar S, Xiao W, Lim KH, Kohlhammer H, Xu W, Yang Y, Zhao H, Shaffer AL, Romesser P, Wright G, Powell J, Rosenwald A, Muller-Hermelink HK, Ott G, Gascoyne RD, Connors JM, Rimsza LM, Campo E, Jaffe ES, Delabie J, Smeland EB, Fisher RI, Braziel RM, Tubbs RR, Cook JR, Weisenburger DD, Chan WC, Staudt LM (2011) Oncogenically active MYD88 mutations in human lymphoma. Nature 470 (7332):115-119. doi:10.1038/nature09671
299. Mandelbaum J, Bhagat G, Tang H, Mo T, Brahmachary M, Shen Q, Chadburn A, Rajewsky K, Tarakhovsky A, Pasqualucci L, Dalla-Favera R (2010) BLIMP1 is a tumor suppressor gene frequently disrupted in activated B cell-like diffuse large B cell lymphoma. Cancer Cell 18 (6):568-579. doi:10.1016/j.ccr.2010.10.030
300. Cattoretti G, Pasqualucci L, Ballon G, Tam W, Nandula SV, Shen Q, Mo T, Murty VV, Dalla-Favera R (2005) Deregulated BCL6 expression recapitulates the pathogenesis of human diffuse large B cell lymphomas in mice. Cancer Cell 7 (5):445-455. doi:10.1016/j.ccr.2005.03.037
301. Huang JZ, Sanger WG, Greiner TC, Staudt LM, Weisenburger DD, Pickering DL, Lynch JC, Armitage JO, Warnke RA, Alizadeh AA, Lossos IS, Levy R, Chan WC (2002) The t(14;18) defines a unique subset of diffuse large B-cell lymphoma with a germinal center B-cell gene expression profile. Blood 99 (7):2285-2290
302. Iqbal J, Greiner TC, Patel K, Dave BJ, Smith L, Ji J, Wright G, Sanger WG, Pickering DL, Jain S, Horsman DE, Shen Y, Fu K, Weisenburger DD, Hans CP, Campo E, Gascoyne RD, Rosenwald A, Jaffe ES, Delabie J, Rimsza L, Ott G, Muller-Hermelink HK, Connors JM, Vose JM, McKeithan T, Staudt LM, Chan WC (2007) Distinctive

patterns of BCL6 molecular alterations and their functional consequences in different subgroups of diffuse large B-cell lymphoma. Leukemia 21 (11):2332-2343. doi:10.1038/sj.leu.2404856
303. Pasqualucci L, Migliazza A, Basso K, Houldsworth J, Chaganti RS, Dalla-Favera R (2003) Mutations of the BCL6 proto-oncogene disrupt its negative autoregulation in diffuse large B-cell lymphoma. Blood 101 (8):2914-2923. doi:10.1182/blood-2002-11-3387
304. Riggs KJ, Saleque S, Wong KK, Merrell KT, Lee JS, Shi Y, Calame K (1993) Yin-yang 1 activates the c-myc promoter. Mol Cell Biol 13 (12):7487-7495
305. Shrivastava A, Yu J, Artandi S, Calame K (1996) YY1 and c-Myc associate in vivo in a manner that depends on c-Myc levels. Proc Natl Acad Sci U S A 93 (20):10638-10641
306. Ramkumar C, Kong Y, Cui H, Hao S, Jones SN, Gerstein RM, Zhang H (2012) Smurf2 regulates the senescence response and suppresses tumorigenesis in mice. Cancer Res. doi:10.1158/0008-5472.CAN-11-3773
307. Harris AW, Pinkert CA, Crawford M, Langdon WY, Brinster RL, Adams JM (1988) The E mu-myc transgenic mouse. A model for high-incidence spontaneous lymphoma and leukemia of early B cells. J Exp Med 167 (2):353-371
308. Soucek L, Whitfield J, Martins CP, Finch AJ, Murphy DJ, Sodir NM, Karnezis AN, Swigart LB, Nasi S, Evan GI (2008) Modelling Myc inhibition as a cancer therapy. Nature 455 (7213):679-683
309. Soucek L, Evan GI (2010) The ups and downs of Myc biology. Curr Opin Genet Dev 20 (1):91-95. doi:10.1016/j.gde.2009.11.001
310. Dalla-Favera R, Martinotti S, Gallo RC, Erikson J, Croce CM (1983) Translocation and rearrangements of the c-myc oncogene locus in human undifferentiated B-cell lymphomas. Science 219 (4587):963-967
311. Zeller KI, Jegga AG, Aronow BJ, O'Donnell KA, Dang CV (2003) An integrated database of genes responsive to the Myc oncogenic transcription factor: identification of direct genomic targets. Genome Biol 4 (10):R69
312. Hsu KW, Hsieh RH, Lee YH, Chao CH, Wu KJ, Tseng MJ, Yeh TS (2008) The activated Notch1 receptor cooperates with alpha-enolase and MBP-1 in modulating c-myc activity. Mol Cell Biol 28 (15):4829-4842
313. Basso K, Margolin AA, Stolovitzky G, Klein U, Dalla-Favera R, Califano A (2005) Reverse engineering of regulatory networks in human B cells. Nat Genet 37 (4):382-390
314. Hummel M, Bentink S, Berger H, Klapper W, Wessendorf S, Barth TF, Bernd HW, Cogliatti SB, Dierlamm J, Feller AC, Hansmann ML, Haralambieva E, Harder L, Hasenclever D, Kuhn M, Lenze D, Lichter P, Martin-Subero JI, Moller P, Muller-Hermelink HK, Ott G, Parwaresch RM, Pott C, Rosenwald A, Rosolowski M, Schwaenen C, Sturzenhofecker B, Szczepanowski M, Trautmann H, Wacker HH, Spang R, Loeffler M, Trumper L, Stein H, Siebert R (2006) A biologic definition of Burkitt's lymphoma from transcriptional and genomic profiling. N Engl J Med 354 (23):2419-2430
315. Lenz G, Wright G, Dave SS, Xiao W, Powell J, Zhao H, Xu W, Tan B, Goldschmidt N, Iqbal J, Vose J, Bast M, Fu K, Weisenburger DD, Greiner TC, Armitage JO, Kyle A, May L, Gascoyne RD, Connors JM, Troen G, Holte H, Kvaloy S, Dierickx D, Verhoef G,

Delabie J, Smeland EB, Jares P, Martinez A, Lopez-Guillermo A, Montserrat E, Campo E, Braziel RM, Miller TP, Rimsza LM, Cook JR, Pohlman B, Sweetenham J, Tubbs RR, Fisher RI, Hartmann E, Rosenwald A, Ott G, Muller-Hermelink HK, Wrench D, Lister TA, Jaffe ES, Wilson WH, Chan WC, Staudt LM (2008) Stromal gene signatures in large-B-cell lymphomas. N Engl J Med 359 (22):2313-2323
316. Dave SS, Wright G, Tan B, Rosenwald A, Gascoyne RD, Chan WC, Fisher RI, Braziel RM, Rimsza LM, Grogan TM, Miller TP, LeBlanc M, Greiner TC, Weisenburger DD, Lynch JC, Vose J, Armitage JO, Smeland EB, Kvaloy S, Holte H, Delabie J, Connors JM, Lansdorp PM, Ouyang Q, Lister TA, Davies AJ, Norton AJ, Muller-Hermelink HK, Ott G, Campo E, Montserrat E, Wilson WH, Jaffe ES, Simon R, Yang L, Powell J, Zhao H, Goldschmidt N, Chiorazzi M, Staudt LM (2004) Prediction of survival in follicular lymphoma based on molecular features of tumor-infiltrating immune cells. N Engl J Med 351 (21):2159-2169
317. Sehn LH, Berry B, Chhanabhai M, Fitzgerald C, Gill K, Hoskins P, Klasa R, Savage KJ, Shenkier T, Sutherland J, Gascoyne RD, Connors JM (2007) The revised International Prognostic Index (R-IPI) is a better predictor of outcome than the standard IPI for patients with diffuse large B-cell lymphoma treated with R-CHOP. Blood 109 (5):1857-1861
318. Bea S, Zettl A, Wright G, Salaverria I, Jehn P, Moreno V, Burek C, Ott G, Puig X, Yang L, Lopez-Guillermo A, Chan WC, Greiner TC, Weisenburger DD, Armitage JO, Gascoyne RD, Connors JM, Grogan TM, Braziel R, Fisher RI, Smeland EB, Kvaloy S, Holte H, Delabie J, Simon R, Powell J, Wilson WH, Jaffe ES, Montserrat E, Muller-Hermelink HK, Staudt LM, Campo E, Rosenwald A (2005) Diffuse large B-cell lymphoma subgroups have distinct genetic profiles that influence tumor biology and improve gene-expression-based survival prediction. Blood 106 (9):3183-3190
319. Salaverria I, Zettl A, Bea S, Hartmann EM, Dave SS, Wright GW, Boerma EJ, Kluin PM, Ott G, Chan WC, Weisenburger DD, Lopez-Guillermo A, Gascoyne RD, Delabie J, Rimsza LM, Braziel RM, Jaffe ES, Staudt LM, Muller-Hermelink HK, Campo E, Rosenwald A (2008) Chromosomal alterations detected by comparative genomic hybridization in subgroups of gene expression-defined Burkitt's lymphoma. Haematologica 93 (9):1327-1334
320. Scholtysik R, Kreuz M, Klapper W, Burkhardt B, Feller AC, Hummel M, Loeffler M, Rosolowski M, Schwaenen C, Spang R, Stein H, Thorns C, Trumper L, Vater I, Wessendorf S, Zenz T, Siebert R, Kuppers R (2010) Detection of genomic aberrations in molecularly defined Burkitt's lymphoma by array-based, high resolution, single nucleotide polymorphism analysis. Haematologica 95 (12):2047-2055
321. Choi YL, Tsukasaki K, O'Neill MC, Yamada Y, Onimaru Y, Matsumoto K, Ohashi J, Yamashita Y, Tsutsumi S, Kaneda R, Takada S, Aburatani H, Kamihira S, Nakamura T, Tomonaga M, Mano H (2007) A genomic analysis of adult T-cell leukemia. Oncogene 26 (8):1245-1255
322. Haslinger C, Schweifer N, Stilgenbauer S, Dohner H, Lichter P, Kraut N, Stratowa C, Abseher R (2004) Microarray gene expression profiling of B-cell chronic lymphocytic leukemia subgroups defined by genomic aberrations and VH mutation status. J Clin Oncol 22 (19):3937-3949
323. Andersson A, Ritz C, Lindgren D, Eden P, Lassen C, Heldrup J, Olofsson T, Rade J, Fontes M, Porwit-Macdonald A, Behrendtz M, Hoglund M, Johansson B, Fioretos T

(2007) Microarray-based classification of a consecutive series of 121 childhood acute leukemias: prediction of leukemic and genetic subtype as well as of minimal residual disease status. Leukemia 21 (6):1198-1203
324. Bhattacharjee A, Richards WG, Staunton J, Li C, Monti S, Vasa P, Ladd C, Beheshti J, Bueno R, Gillette M, Loda M, Weber G, Mark EJ, Lander ES, Wong W, Johnson BE, Golub TR, Sugarbaker DJ, Meyerson M (2001) Classification of human lung carcinomas by mRNA expression profiling reveals distinct adenocarcinoma subclasses. Proc Natl Acad Sci U S A 98 (24):13790-13795
325. Castellano G, Torrisi E, Ligresti G, Malaponte G, Militello L, Russo AE, McCubrey JA, Canevari S, Libra M (2009) The involvement of the transcription factor Yin Yang 1 in cancer development and progression. Cell Cycle 8 (9):1367-1372
326. Shi Y, Lee JS, Galvin KM (1997) Everything you have ever wanted to know about Yin Yang 1. Biochim Biophys Acta 1332 (2):F49-66
327. Castellano G, Torrisi E, Ligresti G, Nicoletti F, Malaponte G, Traval S, McCubrey JA, Canevari S, Libra M (2010) Yin Yang 1 overexpression in diffuse large B-cell lymphoma is associated with B-cell transformation and tumor progression. Cell Cycle 9 (3):557-563
328. Sakhinia E, Glennie C, Hoyland JA, Menasce LP, Brady G, Miller C, Radford JA, Byers RJ (2007) Clinical quantitation of diagnostic and predictive gene expression levels in follicular and diffuse large B-cell lymphoma by RT-PCR gene expression profiling. Blood 109 (9):3922-3928
329. Liu H, Schmidt-Supprian M, Shi Y, Hobeika E, Barteneva N, Jumaa H, Pelanda R, Reth M, Skok J, Rajewsky K, Shi Y (2007) Yin Yang 1 is a critical regulator of B-cell development. Genes Dev 21 (10):1179-1189. doi:10.1101/gad.1529307
330. Green MR, Monti S, Dalla-Favera R, Pasqualucci L, Walsh NC, Schmidt-Supprian M, Kutok JL, Rodig SJ, Neuberg DS, Rajewsky K, Golub TR, Alt FW, Shipp MA, Manis JP (2011) Signatures of murine B-cell development implicate Yy1 as a regulator of the germinal center-specific program. Proc Natl Acad Sci U S A 108 (7):2873-2878
331. Dang CV (2009) MYC, microRNAs and glutamine addiction in cancers. Cell Cycle 8 (20):3243-3245
332. Langdon WY, Harris AW, Cory S, Adams JM (1986) The c-myc oncogene perturbs B lymphocyte development in E-mu-myc transgenic mice. Cell 47 (1):11-18
333. Evan G, Littlewood T (1998) A matter of life and cell death. Science 281 (5381):1317-1322
334. Murphy DJ, Junttila MR, Pouyet L, Karnezis A, Shchors K, Bui DA, Brown-Swigart L, Johnson L, Evan GI (2008) Distinct thresholds govern Myc's biological output in vivo. Cancer Cell 14 (6):447-457
335. Campaner S, Doni M, Hydbring P, Verrecchia A, Bianchi L, Sardella D, Schleker T, Perna D, Tronnersjo S, Murga M, Fernandez-Capetillo O, Barbacid M, Larsson LG, Amati B (2010) Cdk2 suppresses cellular senescence induced by the c-myc oncogene. Nat Cell Biol 12 (1):54-59; sup pp 51-14
336. Muramatsu M, Kinoshita K, Fagarasan S, Yamada S, Shinkai Y, Honjo T (2000) Class switch recombination and hypermutation require activation-induced cytidine deaminase (AID), a potential RNA editing enzyme. Cell 102 (5):553-563
337. Rando TA (2006) Stem cells, ageing and the quest for immortality. Nature 441 (7097):1080-1086

338. Kiss TL, Sabry W, Lazarus HM, Lipton JH (2007) Blood and marrow transplantation in elderly acute myeloid leukaemia patients - older certainly is not better. Bone marrow transplantation 40 (5):405-416. doi:10.1038/sj.bmt.1705747
339. Beghe C, Wilson A, Ershler WB (2004) Prevalence and outcomes of anemia in geriatrics: a systematic review of the literature. The American journal of medicine 116 Suppl 7A:3S-10S. doi:10.1016/j.amjmed.2003.12.009
340. Ergen AV, Goodell MA (2010) Mechanisms of hematopoietic stem cell aging. Exp Gerontol 45 (4):286-290. doi:10.1016/j.exger.2009.12.010
341. Kim M, Moon HB, Spangrude GJ (2003) Major age-related changes of mouse hematopoietic stem/progenitor cells. Ann N Y Acad Sci 996:195-208
342. Harrison DE, Astle CM (1982) Loss of stem cell repopulating ability upon transplantation. Effects of donor age, cell number, and transplantation procedure. J Exp Med 156 (6):1767-1779
343. Perry SS, Zhao Y, Nie L, Cochrane SW, Huang Z, Sun XH (2007) Id1, but not Id3, directs long-term repopulating hematopoietic stem-cell maintenance. Blood 110 (7):2351-2360
344. Allsopp RC, Cheshier S, Weissman IL (2001) Telomere shortening accompanies increased cell cycle activity during serial transplantation of hematopoietic stem cells. J Exp Med 193 (8):917-924
345. Harrison DE, Jordan CT, Zhong RK, Astle CM (1993) Primitive hemopoietic stem cells: direct assay of most productive populations by competitive repopulation with simple binomial, correlation and covariance calculations. Exp Hematol 21 (2):206-219
346. Passegue E, Wagers AJ, Giuriato S, Anderson WC, Weissman IL (2005) Global analysis of proliferation and cell cycle gene expression in the regulation of hematopoietic stem and progenitor cell fates. J Exp Med 202 (11):1599-1611
347. Yang Q, Kardava L, St Leger A, Martincic K, Varnum-Finney B, Bernstein ID, Milcarek C, Borghesi L (2008) E47 controls the developmental integrity and cell cycle quiescence of multipotential hematopoietic progenitors. J Immunol 181 (9):5885-5894
348. Shaffer AL, 3rd, Young RM, Staudt LM (2012) Pathogenesis of human B cell lymphomas. Annual review of immunology 30:565-610. doi:10.1146/annurev-immunol-020711-075027
349. Serrano M, Lee H, Chin L, Cordon-Cardo C, Beach D, DePinho RA (1996) Role of the INK4a locus in tumor suppression and cell mortality. Cell 85 (1):27-37
350. Collado M, Serrano M (2006) The power and the promise of oncogene-induced senescence markers. Nat Rev Cancer 6 (6):472-476. doi:10.1038/nrc1884
351. Krishnamurthy J, Torrice C, Ramsey MR, Kovalev GI, Al-Regaiey K, Su L, Sharpless NE (2004) Ink4a/Arf expression is a biomarker of aging. J Clin Invest 114 (9):1299-1307
352. Ressler S, Bartkova J, Niederegger H, Bartek J, Scharffetter-Kochanek K, Jansen-Durr P, Wlaschek M (2006) p16INK4A is a robust in vivo biomarker of cellular aging in human skin. Aging Cell 5 (5):379-389
353. Ungewitter E, Scrable H (2009) Antagonistic pleiotropy and p53. Mech Ageing Dev 130 (1-2):10-17. doi:10.1016/j.mad.2008.06.002

354. Giaimo S, d'Adda di Fagagna F (2012) Is cellular senescence an example of antagonistic pleiotropy? Aging Cell 11 (3):378-383. doi:10.1111/j.1474-9726.2012.00807.x
355. Jeyapalan JC, Ferreira M, Sedivy JM, Herbig U (2007) Accumulation of senescent cells in mitotic tissue of aging primates. Mech Ageing Dev 128 (1):36-44
356. Baker DJ, Wijshake T, Tchkonia T, LeBrasseur NK, Childs BG, van de Sluis B, Kirkland JL, van Deursen JM (2011) Clearance of p16Ink4a-positive senescent cells delays ageing-associated disorders. Nature 479 (7372):232-236. doi:10.1038/nature10600